Shahid Chamran University of Ahvaz

Journal of

Applied and Computational Mechanics

Review Paper

A Scoping Review of the Thermoelectric Generator Systems Designs (Heat Exchangers and Coolers) with Locations of Application to Recover Energy from Internal Combustion Engines

Mohammed Y. Jabbar⬡, Saba Y. Ahmed⬡, Salwan Obaid Waheed Khafaji⬡

Department of Mechanical Engineering, University of Babylon, Babylon, 51002, Iraq,
Email: eng.mohammed.yousif@uobabylon.edu.iq (M.Y.J.); eng.saba.yassub@uobabylon.edu.iq (S.Y.A.); eng.salwon.obaid@uobabylon.edu.iq (S.O.W.K.)

Abstract. Currently, a significant number of automobiles are equipped with internal combustion engines. In urban areas, a significant number of transportation methods have detrimental environmental effects through the release of pollutants resulting from the combustion of fossil fuels. In addition to the emission of toxic pollutants, internal combustion engines experience significant energy losses through exhaust emissions. Advanced technological applications have the potential to recover of a portion of the waste heat from exhaust ducts. Evaluations conducted by scholars across several disciplines highlight diverse perspectives on the recycling of thermal energy from exhaust gases as a means of mitigating pollution sources. However, this review focuses on the utilization of thermoelectric generators for harvesting a fraction of the aforementioned dissipated energy. The energy harvesting system is comprised of three components: the heat exchanger, which serves as the heat source; the cooler, which functions as the heat sink; and the thermoelectric generators, which act as the heat engine sandwiched between the heat exchanger and the cooler. This review examines the diverse exterior designs of heat exchangers and coolers and categorizes them accordingly. Additionally, it identifies the optimal installation locations for harvesting systems and explores the impact of design variations, choice of metals for manufacturing, and internal topography on the generation of electrical power. The primary findings of this review emphasize the significance of prioritizing the design of heat exchangers over coolers. This is because the uniformity of the temperature distribution within the heat exchanger plays a crucial role in governing the overall performance. Moreover, the installation of the system on petrol engines was seen as more cost-effective in comparison to its installation on diesel engines, primarily due to the higher magnitude of energy emitted from the exhaust gases of the former as opposed to the latter. To the best of the author's knowledge, this review classification has never been performed before. This can be considered a brief path map and a starting point for future work by researchers and investigators in designing heat exchangers and coolers and choosing the locations of TEG system installations. Then profitable investment from the data that has been prepared and summarized.

Keywords: Thermoelectric generator, heat exchangers, heat sinks, geometry, energy conversion.

1. Introduction

The internal combustion (I.C.) engine was far from ideal in its overall performance; at best, it achieved 30–36% of the thermal efficiency of a petrol engine, while diesel achieved only 42–43% [1]. That is, the remaining fuel was almost completely burned into the exhaust. The purpose of the TEG was to recover waste heat from engine exhaust gases, provide electrical power to the vehicle, and replace the engine-driven alternator. This would reduce the required engine horsepower, leading to reduced fuel consumption and emissions.

Recently, many engineers still faced issues with this problem. Researchers tried to increase the productivity of the companies by making some modifications to cooler and HEX designs and find an alternative method to harvest the waste energy by converting it into electrical power by using TEGs, as an example.

The number of annual publications on TEGs with coolers and heat exchangers has expanded dramatically over the last ten years, from 29 to a peak of 470, according to a database search using specified keywords. The study results on TEGs with coolers and heat exchangers over time are shown in Fig. 1, which was retrieved from the database source [2] of the same author.
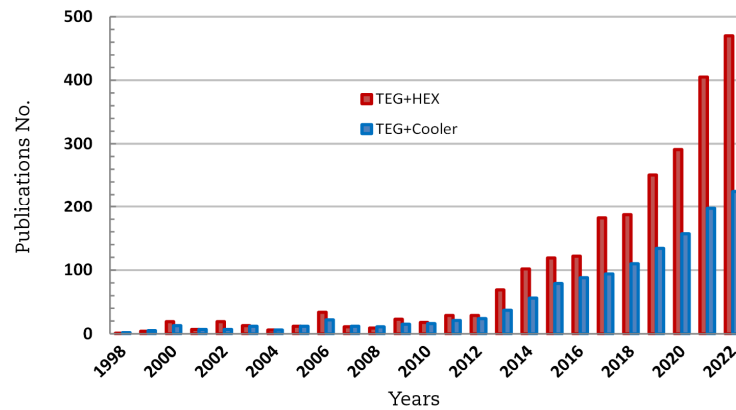
Fig. 1. Number of published works from 1998-2022 on TEG with cooler and TEG with HEX.

2. Automobile TEG Investigators' Most New or Former Works

As previously stated, two senses can be adopted initially to motivate the output energy of the TEG from the waste heat of I.C. engines: HEX and cooler construction, which play an influential role, can be produced. The thermal "HEX and Cooler" structures were critical, and they must be balanced in order to meet the objectives of the project.

The HEX shell shape, HEX internal obstruction design, and cold junction mechanism (cooler) are thoroughly explored. Various HEX designs have previously been created and explored to enhance heat recovery from exhaust gases by minimizing gas crossing thermal resistance, temperature field non-homogeneity, and weight. As a result, it was suggested that certain relevant heat transfer improvement procedures be used to boost heat transfer from heated exhaust gases to HEX surfaces and improve power output. Fins, metal foams, dimpled surfaces, waffles, vortex makers, heat pipes, and HEX exterior surface designs have all been used to promote heat transfer in the past. They improve the TEG efficiency and HEX heat transfer presentation but also create higher-pressure losses. Consequently, it is critical to achieve the correct balance between the rate of heat transfer and pressure loss when adopting a heat transfer improvement element for an HEX. In the current review, the HEX and its efficiency were mostly improved by the HEX production material, internal geometry, and external shape. An ideal HEX recovers as much heat from a hot I.C. engine exhaust as feasible while maintaining a safe pressure loss [3].

As explained previously explained, only approximately 38% of the fuel energy is used to move the vehicle or is wasted by friction and radiation. The remaining 62% was not transformed into valuable mechanical work and was rejected to the atmosphere through the exhaust pipe (33%), engine coolant cycle (24%) and friction/radiation (5%) [4]. As shown in through the exploratory review, the exhaust pipe and engine coolant cycle were two possible locations for TEG applications to be placed. In this review, construction-based classification categorizes HEXs and coolers based on their geometries. It includes types as the below flow chart.
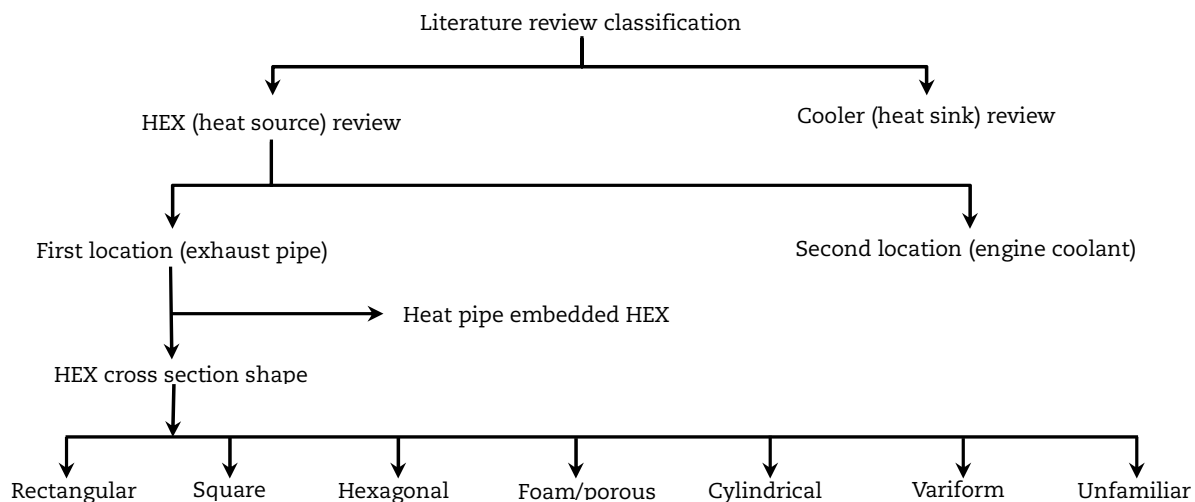
2.1. HEX (heat source) review

2.1.1. *First location TEGs installation (exhaust pipe)*

Several studies have discussed and analyzed performance of HEX. Most the studies presented effect of geometrical design on the overall performance of the HEX and TEGs. In this review, the classification will be based on the cross-sectional shapes of the HEXs.

2.1.1.1. *HEX cross section shape*

2.1.1.1.1. *Rectangular structure HEXs*

The majority of previous scholarly investigations pertaining to historical reviews have focused on rectangular cross section HEX categories. The main reason behind this phenomenon can be attributed to the convenience of the production process and the expansive surface area that can handle a considerable quantity of TEGs. Hence, in order to streamline the process of examining the extensive body of information, a tabulation was conducted and summarized in Table 1.
Note: most of the figures in Table 1 were reprinted with permission.

Table 1. Rectangular cross section HEXs categories.

| Ref No.	- Author(s) & Year - Theo. (Exp.) - Citation	TEG - Name (Mat.) - Number - Volume	(Heat source) - Int. geometries - Material - TEG system Mass - Middle part (volume/Hot area)	(Heat sink) Geometry/internal geometry - Fluid - Material	Parameters of studies	Conclusions
[5]	- Ikoma, et al., 1998 - Exp. - 255	- (Si-Ge) - 72 - (20x20x9.2) mm³	- Fins inside inner shell - SUS30 - 14.5kg - (440x180x70) mm³	- Rectangular ducts - Water - Aluminum	- Gasoline engine = 3 L - Vehicle speed = 60 km/hr & T_{inlet} = 868 K	- P_{max} = 35.6 W - R_{int} = 0.4 Ω - ΔT = 563 K - η_{sys} = 11%
[6]	- Jihad & Jamil, 2001 - Theo & Exp - 155	- (HZ-14) - 4	- Thermal spreader - Aluminum	- Water cooled heat sinks	-A ruston 3-cylinder engine air-cooled - T_{inlet} = 285°C	P_{tot} = 42.3 W ΔT = 237°C
[7]	- Hsiao, et al., 2010 - Theo & Exp - 425	- (HZ-2& TGM-127)	- Block heater	- Micro channel	- T_{inlet} = 300, 320, 340°C	- P_{max} = 51.13 W/cm² - ΔT = 290°C
[8]	- Love, et al., 2012 - Exp. - 95	- (Bi₂Te₃) - 5	- (457×51×25) mm³ with 3 mm plate thick - Aluminum & Stainless steel	- Duct with (406×51×25) mm³ with 3 mm plate thick - Mixture of water & ethylene glycol (50-50) - Aluminum	- Ducts were performed under clean stainless steel & fouled aluminum conditions <u>Exhaust gas</u> - T_{inlet} = 240 & 280°C - Flow rate = 40-150 slpm <u>Cooling water</u> - T_{inlet} = 40 & 80°C - $\dot{m}_{inlet}$= 126 g/s	Fouled HEXs degraded in performance of 5–10% matched to an un-fouled HEX of the same metal
[9]	- Chuqi, et al., 2013 - Theo. - 16	-	- Fish bones	- Figure 2	- Catalytic converter before/after HEX - Inlet velocity = 15m/s - T_{inlet} = 800 K - Out. static pressure = 0 MPa	- The HEX after the catalyst seems more practical - T_h =265.6°C - Q_{max} = 3910 W/m²
[10]	- Liu, et al., 2014 - Theo & Exp - 96	-	- Chaos shaped	- Figure 3	Catalytic converter (CC) 1-TEG between CC & muffler 2-TEG before CC & muffler 3-TEG after CC & muffler - Inlet velocity = 20 m/s - T_{inlet} = 350°C	- Case (1) uniform flow, high temp., low pressure drop
[11]	- Chuqi, et al., 2014 - Theo & Exp - 91	-	- Scatter, accordion & fish bones - Brass - (598×250) mm², (660×305) mm² & (775×365) mm²	- 12 Cuboid cooler - Aluminum, Figure 4	- T_{inlet} = 400°C - velocity inlet = 20 m/s	-
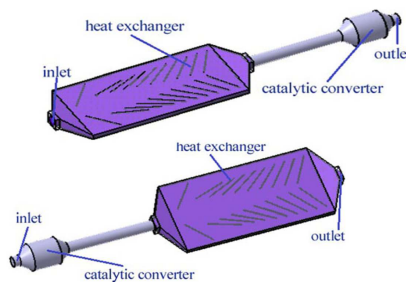
Fig. 2. Catalytic converter location [9].
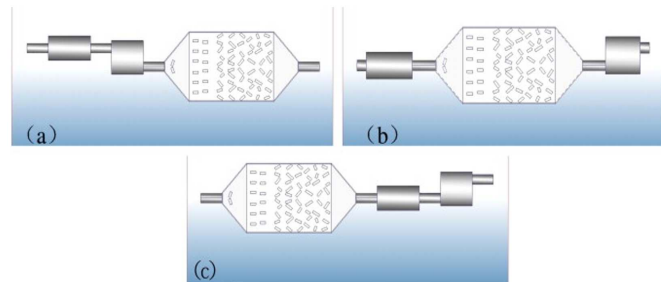
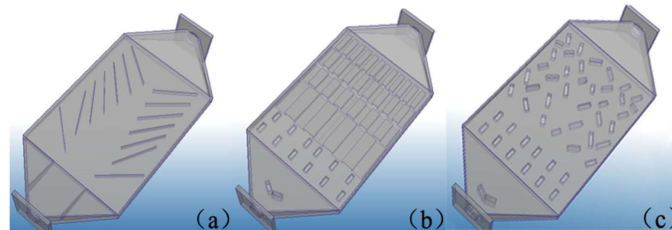Fig. 3. Catalytic converter, muffler and TEG arrangements [10].

Fig. 4. Scatter, accordion & fish bones HEXs [11].

[12]	- Zhiqiang et al., 2014 - Theo. - 137	- (Bi₂Te₃) - 20 (41×26×3.52) mm³	- Bafflers inside - Aluminum - (400×160×40) mm³	- Engine cooling water, Figure 5	- 6-cylinder diesel engine - Baffler dimensions (158×20×1) mm³ number (0-6) & angles (10-40)° <u>Hot air</u> - 3 Inlet area (30×40), (60×40), & (120×40) mm² with velocity inlet = 47.2, 22.9 & 15.3 m/s, respectively - T_{inlet} = 808.15, 792.15, 747.15, & 693.15 K <u>Cooling water</u> - T_{inlet} = 80°C - $\dot{m}_{inlet}$ = 500 g/s	- (60×40) mm² inlet area was optimal to equilibrium flow drag and TEG output - Bafflers large angle was preferred but increase pressure drop, then the variable angle was suggested
[13]	- Liu, et al., 2014 - Theo & Exp - 137	- (Bi₂Te₃) - 60 - (50×50×5) mm³	- Empty, fish bones and chaos shaped, - Brass - (400×290×18) mm³	- 12 Cuboid water tank (300×60×21) mm³ - Aluminum, Figure 6	- T_{inlet} = 350°C - Velocity inlet = 15.2 m/s	HEX with chaos and 5 mm thickness achieves perfect thermal uniformity with P_{max} = 183.24 W

| [14]	Shengqiang, et al., 2014 - Theo & Exp - 121	-	- Empty, parallel, inclined, and separate plate with holes, Serial plate and Pipes - (280×110×30) mm³	-	-1.2 L gasoline engine - T_{inlet} = 573.15, 673.15, & 873.15K - $\dot{m}_{inlet}$ = 5.7, 14.4, 80.1 g/sec	- Serial plate HEX enhanced heat transfer by 7 baffles Q_{max} = 1737 W & Δp = 9.7 kPa
[15]	- Yiping, et al., 2014 - Theo & Exp - 45	- (Bi₂Te₃) - 60	- Transverse fins - Brass - (400×310×22) mm³	- 12 Cuboid - Water tanks from engine coolant system, Figure 7	- 4-cylinder engine - T_{inlet} = 673 K - (Length, spacing between, angle, & thickness) of fins	- T_h = 260°C - Optimal design were; length = 5 mm, space = 0.05 mm, angle = 15°, thickness = 1.25 mm
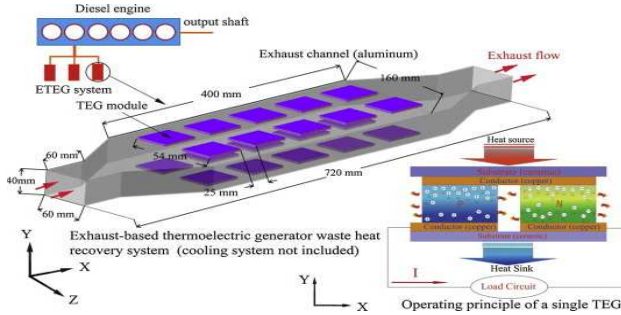
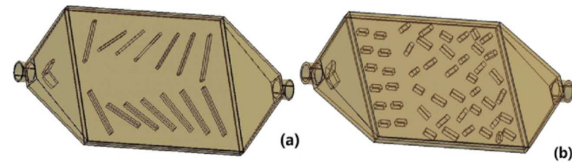**Fig. 5.** Exhaust-TEG recovery system [12].
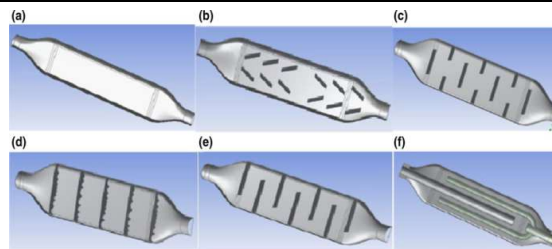

Fig. 6. (a) fishbone &(b) chaos HEXs [13].

Fig. 7. Transverse fins HEXs construction [15].

| [16]	- Liu, et al., 2015 - Theo & Exp - 228	- (Bi₂Te₃) - 240 - (50×50×5) mm³	- 4 HEXs - Brass - (400×290×18) mm³	- 48 Cuboid tanks (300×60×21) mm³ - Engine water - Aluminum	- 2.0 L engine - T_{inlet} = 340°C - Engine water temp. = 90°C	P_{max} = 944 W
[17]	- Qing, et al., 2015 - Theo. - 62	- 20	- Inclined bafflers, stainless steel 310	- Upper and lower rectangular duct (760×172×30) mm³ - Air/water - Stainless steel 310	- (Angle, number, length & location) of baffler - Co-flow & counter-flow	- Co-flow larger ΔT - Longer baffler enhances the cooling effect - P_{max} = 250 W
[18]	- Yiping, et al., 2016 - Theo & Exp - 41	- (HZ-20) - 30	- Dimples, alignment ribs conflicting ribs - Brass - (400×295×12) mm³	- Figure 8	- Dimples depth/diameter=0.2 - Rib (25×10) mm² - T_{inlet} = 600 K	P_{max} = 138 W at Re = 2500 in case of conflicting ribs
[19]	- Chuqi, et al., 2015 - Theo. - 37	- 60	- Three segments folded-shaped - (400×310×22) mm³	- 12 Cuboid tanks - Engine coolant water, Figure 9	- Length and thickness of 3 segments folded plates - T_{inlet} = 769 K - $\dot{m}_{inlet}$ = 0.03 kg/s	- The external temp. & thermal uniformity of HEX was influenced by its length, width, & height
[20]	- Tae, et al., 2016 - Theo & Exp - 150	- (Bi₂Te₃) - 40 - (44×44×3.6) mm³	- Finned structure - (253.5×372×60) mm³	- Double cuboid water tanks (253.5×372×29) mm³, finned structures Inside, Figure 10	- A turbocharged 6-cylinder diesel engine - rpm = 100, 1500, & 2000	(At 2000 rpm) - P_{max} = 119 W - $\eta_{con.}$ = 2.8% - ΔP_{max} = 1.46 kPa
[21]	- Haiyan & Miaolin, 2016 - Theo. - 0	- (TEG-127-0.4-1.6) - 20	- 2 Flat plate HEX, No.304 - Stainless steel	- 3 Cuboid tanks - Engine coolant water - No. 304 stainless steel	-	- The fuel saving ratio was 0.03 L/h and it can recover the cost in 4 years P = 40 W - ΔT_{max} = 100°C
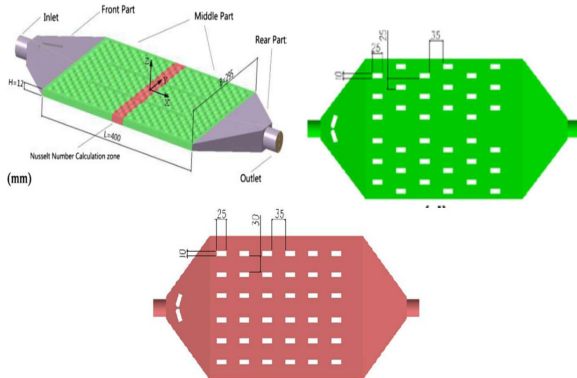
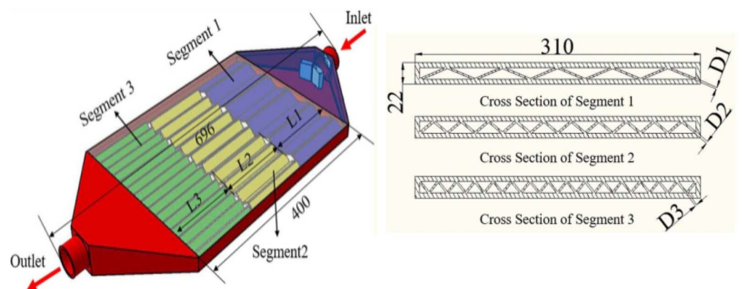**Fig. 8.** Dimples, alignment ribs conflicting ribs HEXs [18].

Fig. 9. Three segments folded shaped HEXs [19].

Fig. 10. Photos of (a) exhaust HEX, (b) perforated plate placed inside [20].

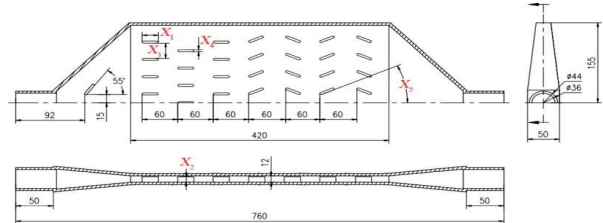| Ref	Author/Type	TEG module	Fins/Insert	Cooler	Operating conditions	Results
[22]	- Tae, et al., 2016 - Theo - 47	(Bi_2Te_3) - 40 $(44\times44\times3.6)$ mm^3	-	- 2 Cuboid coolers - Water, Figure 11	- Number & thickness of fin were optimized - Velocity inlet = 3.6 m/s	At six & 2 mm thickness the most temperature uniformity for power generation & govern the hot surface to not exceed 473 K
[23]	- Liu, et al., 2016 - Theo & Exp - 65	-	- Rectangular cross section fins - Brass - $(420\times300\times12)$ mm^3 with 5 mm plate thick	- 12 Cuboid tanks - Water, Figure 12	<u>Optimization ranges</u> - T_{inlet} = 330°C - Velocity inlet = 22 m/s - Fin length = 28-40 mm - Fin height = 6-12 mm - Interval distance = 30-36 mm - Fin thickness = 2-8 mm - Fin angle = 18-30 degree	<u>After optimization</u> Temp. difference & pressure drop significantly improved when - Length = 31.1 mm - Height = 6.8 mm - Int. dis. = 34.3 mm - Thickness = 4.5 mm - Angle = 26.7° T_h = 226.4°C
[24]	-Andrzej 2017 - Theo & Exp - 22	- (TMG- 41-1.4-1.2) - 24 $(44\times44\times3.6)$ mm^3	- A ribbing was fixed inside - Aluminum - $(400\times200\times135)$ mm^3 with 2 mm plate thick	- Figure 13	- 2 vehicles equipped with 4 cylinder, 1.2 TSI & 1.3 SDE spark & compression ignition engines, respectively - T_{inlet} = 390°C at rpm = 1800 & Torque = 60 N.m	Average value of waste energy for 1.3 SDE engine = 0.67 kW & maximum = 4.05 kW & η_{TEGs} = 0.14–1.6% The increase in the η_{TEGs} of 1.2 L SI engine with TEGs power = 0.29% & For 1.3 SDE = 0.27%
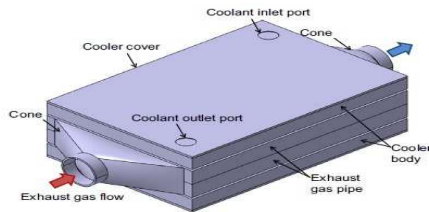
Fig. 11. Schematic illustration of TEG system [22].

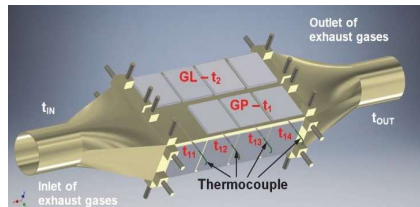

Fig. 12. Fins distribution inside rectangular HEX [23].

Fig. 13. View of TEG generator [24].

| Ref	Author/Type	TEG module	Fins/Insert	Cooler	Operating conditions	Results
[25]	- Yiping, et al., 2016 - Theo & Exp - 101	- (Bi_2Te_3) - 60 - $(55\times55\times5)$ mm^3	- Cylindrical grooves (depth/width = 0.25), random fins, smooth flat surface - Brass - $(405\times305\times22)$ mm^3 with 5 mm plate thick	- 12 Cuboid water tanks - Aluminum, Figure 14	<u>Exhaust gas</u> - T_{inlet} = 673 K - $\dot{m}_{inlet}$ = 0.033 kg/s - P_{back} = 50 mbar <u>Cooling water</u> - T_{inlet} = 313 K - Flow rate$_{inlet}$ = 12 L/s	<u>Grooves, fins vs flat</u> - Cylindrical grooves enhance power generation (P_{max} = 207.8 W) with low P_{back} = 1683 Pa - Fins enhance power generation, but with the additional P_{back}
[26]	- Wei, et al., 2017 - Theo. - 51	- (Bi_2Te_3)	- Rectangular duct - Copper	- 2 Rectangular ducts - Water engine cooling - Copper	<u>Exhaust gas</u> - T_{inlet} = 300-600°C - $\dot{m}_{inlet}$ = 46 g/s - HEX optimal height = 0.0004-0.01 m & length = 0.05-1.5 m <u>Cooling water</u> - T_{inlet} = 80°C - $\dot{m}_{inlet}$ = 500 g/s	P_{max} = 350 W at T_{inlet} = 600°C & HEX height = 0.004 m & length = 0.7m
[27]	- Éric & Rédéric, 2017 - Theo & Exp - 11	- (TEG-07025HT-SS) - 20	- Tabulated insert within channel - Aluminum	- Tabulated insert galvanized steel strips (8.66 wide×0.50 thick) mm^2 within 2 channels - Water - Aluminum, Figure 15	<u>Hot duct</u> - T_{inlet} = 85°C <u>Cold ducts</u> - T_{inlet} = 15°C - The tested linear panel densities were 0, 7.8, 15.6, 31.2, 62.5, and 125 panels/m	- Inserts raised the power from 9.5 to 25.1 W - Lower panel densities result in a less temperature difference across the system
[28]	-Xing, et al., 2017 - Theo & Exp - 82	- (TEG1-287) - 10 $(55\times55\times4)$ mm^3	- Rectangular winglet longitudinal vortex generators (20×2×5) mm^3, spacing 10 mm and angle = 45° - Stainless-steel - $(280\times75\times20)$ mm^3 with 7 mm thick	- Mini-channel (280 length × 75.5 width × 5 height) mm^3 with 21 thin plate fins inside - Aluminum, Figure 16	<u>Hot channel</u> - T_{inlet} = 523–553 K - $\dot{m}_{inlet}$ = 0.004-0.0085 kg/s - Smooth duct - Uniform winglet duct - Non uniform winglet duct <u>Water cooling chiller</u> - 7 L/min and 295 K	- The total power with uniform duct can outperform that with smooth duct by 97.5% & with non-uniform duct by 189.1%
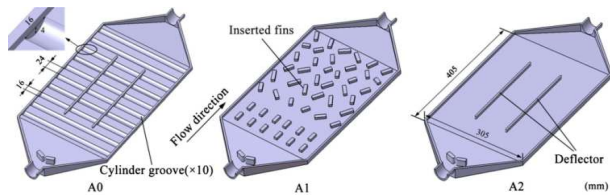
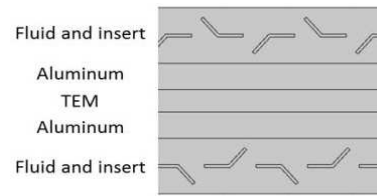**Fig. 14.** Three HEXs with different inner topologies [25].
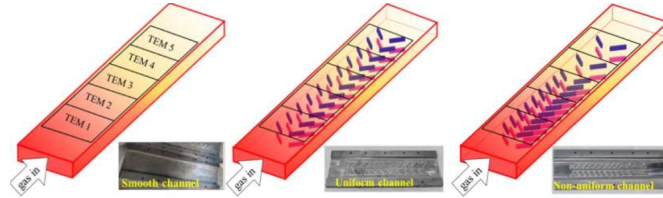

Fig. 15. Tabulated insert within HEX [27].

Fig. 16. Rectangular vortex generators distribution [28].

|					
[29]	-Simon, et al., 2018 - Theo. - 23	- 16 (40×40×5) mm³	- Stainless-steel	-	TEG recycles thermal exhaust energy directly to electricity used for TEC refrigerator of cool box (20 L) passenger car	The CC functions as thermal reservoir, facilitating the ongoing production of electricity through the exothermic reactions within its structure. Hence, the positioning of the TEG holds strategic significance
[30]	-Rui, et al., 2018 - Exp. - 38	- (Bi₂Te₃) - 60 (56×56×6) mm³	- Chaos shaped - Brass - (400×300×22) mm³ with 5 mm plate thick	- 12 Cooling boxes - Engine cooling water -Aluminum	- 2.0 L engine (PSA RFN 10LH3X) Exhaust gas - T_{inlet} = 350°C Cooling water - T_{inlet} = 90°C - Flow rate = 9.27 L/min	With conductive graphite paper (k = 3 w/mk) - P_{max} = 108.3 W Without - P_{max} = 100.1 W - Then 7.2% enhanced
[31]	-Yiping, et al., 2018 - Theo & Exp - 119	- (Bi₂Te₃) - 240 - (56×56×5) mm³	- 4 HEXs (dimple shaped inside depth/diameter = 0.28125)/ Chaos shaped - Brass - 190 kg - (305×405×22) mm³ with 5 mm plate thick	- 48 Cuboid tanks (310×60×30) mm³ - Water engine coolant (55% ethylene glycol & 45% water) - Aluminum alloy	- 3.9 L Commins 4-cylinder diesel engine Exhaust gas - T_{inlet} = 563 K - $\dot{m}_{inlet}$ = 0.0715 kg/s Cooling water - T_{inlet} = 353 K - Flow rate = 9.27 L/min	- ΔP with dimpled surface HEX reduced by 20.57% & net power output was increased by 173.60%
[32]	- Pablo, et al., 2018 - Theo & Exp - 109	- (TEG1-4199-5.3) - 80 - Square formed with 40mm sides	- Long fins, short fins and channel arranged fins - Brass	- Delta function shaped duct - Steel, Figure 17	- Nissan YD22 (2.2 L, 4-stroke, 4-cylinder diesel engine) - For optimization - Number of columns and rows - (for long fins) Inlet diffusers angle, distance of diffusers from core of HEX, distance of diffusers from symmetry axis, and fins number	- Lesser electrical creation when the number of rows & columns increases. - The diffusers angle has bigger effect on pressure drop & heat transfer near to a 40% of the other parameters
[33]	- Nour, et al., 2018 - Theo & Exp - 37	(Bi₂Te₃) & (Si80Ge20) - 6	- 3 Internal finned channels - Stainless steel - (150×31.9×14.4) mm³ with 1.2 mm plate thick for each channel	- Aluminum welded thermal spreaders, positioned around the copper tubes, Figure 18	- 4-cylinder diesel engine bench with Si80Ge20 TEG - A cylinder head and a cylinder block hot air bench with Bi2Te3 TEG	An improvement in TEG performance of actual engine test (up to 30%) compared with warm air test
[34]	- Yurong, et al., 2019 - Theo. - 12	(TMH400302055)	-	- Figure 19	- T_{inlet} = six cycles time curve - Inlet speed = 14 m/s - Accumulator (PCM) inorganic salt (LiOH) material (200×100×2) mm³ between TEGs & HEX. - Using Regenerative TEG & compared with Commercial TEG	- The oscillation of hot side temp. and output voltage reduces by 86.46-87.71% & 86.45-89.16%
[35]	- Ding, et al., 2019 - Theo. - 15	- (Bi₂Te₃) - 20	- 2 Aluminum parallel-plate fins - (200×100×40) mm³	- 2 Aluminum parallel-plate fins - From air movement comes from front of automobile, Figure 20	- Three vehicle types were considered (Heavy, Midsize & light) speed range of 10-120 km/h	- TEGs suitable to heavy-duty vehicle run at a speed lower than 100 km/h in most of time, because it was highly influenced by TEGs weight
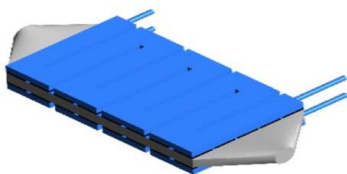
Fig. 17. HEX and cooler system [32].
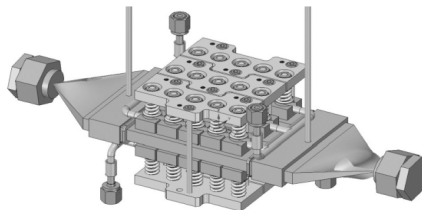
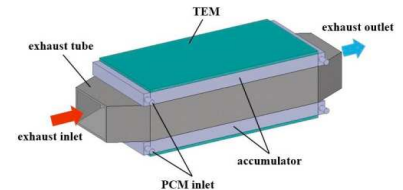**Fig. 18.** 3D model of TEG conversion device [33].

Fig. 19. The schematic structure of TEG [34].

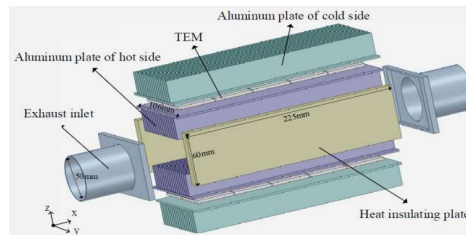**Fig. 20.** Schematic diagram of TEG system [35].

|						
[36]	- Jun, et al., 2020 - Theo. - 14	(TMH400302055) - 36 (54×52×2.8) mm³	- Empty & 27 cooper vortex rods - Aluminum - (374×176) mm²	- Cooling cycle of the engine, Figure 21	- 4-cylinder diesel engine - T$_{inlet}$ = 346, 428 & 463°C - Cold TEGs sides temp. = 95°C	- The walls temp. of HEX with vortex rods was higher and further uniform than HEX without vortex rods, but with higher P$_{back}$ about 1392 Pa
[37]	- Nor, et al., 2020 - Exp. - 0	- 2	- Empty - Aluminum - (165×165×165) mm³	- 2 heat sink screwed with two 12 V exterior fan - Air - Aluminum, Figure 22	- T$_{inlet}$ = 100, 150, 200 & 250°C	- P$_{max}$ = 183 mW at T$_{inlet}$ = 250°C
[38]	- Roozbeh, et al., 2020 - Theo & Exp - 36	- 60 - (55×55×5) mm³	- 9 HEXs with 3 different internal strategies ((size, & baffle angles at inlet), baffle arrangements in middle part & non-vertical baffle angles in a chaos-shaped figure) -(390×310×22) mm³	-	- T$_{inlet}$ = 573 K - Velocity inlet = 15.2 m/s - Cold TEGs sides temp. = 363 K	- If the space between baffle diverges from 5.2 to 16.8 mm enhance output power to 3.91%
[39]	- Kunal, et al., 2020 - Theo & Exp - 32	Skutterudite - 12 - (4×4×3.44) mm³	- 6 HEXs with different inner fin constructions - Aluminum - (220×70×34) mm³	- 4 cooling channels with (40×98×10) mm³ & 2 vertical fins inside - Water - Aluminum	<u>Hot air</u> - T$_{inlet}$ = 300, 400, 500 & 600°C - ṁ$_{inlet}$ = 0.0157 kg/s <u>Coolant water</u> - T$_{inlet}$ = 30°C - ṁ$_{inlet}$ = 0.0655 kg/s	At 600°C, HEX with inclined fins with collective fins show overall efficiencies of 1.81 & 1.88% & P$_{net}$ upper by 29and 35%, respectively, than of HEX with straight fins
[40]	- Ding, et al., 2020 - Theo & Exp - 33	- (TEG-127020) - 16	- 20 (200×20×2) mm³ longitudinal Fins, 4 mm between every 2 fins, arranged on upper & lower tilt walls of HEX - 6063 aluminum alloys	- 4 longitudinal water-cooled channels - Water - 6063 aluminum alloys, Figure 23	- Tilt angle = 0-2.5° <u>Hot air</u> - T$_{inlet}$ = 400, 450, 500, 550 K - ṁ$_{inlet}$ = 30, 60, 90 & 120 g/s <u>Cooling water</u> - T$_{inlet}$ = 300 K - ṁ$_{inlet}$ = 20.8 g/s	- The best tilt angle was 2.5°, the net power increased 20.2% at T$_{inlet}$ = 500 K & ṁ$_{inlet}$ = 30 g/s
[41]	- Farhad, et al., 2020 - Theo & Exp - 25	- 6	-	- Figure 24	- Hybrid hydroxyl (HHO) unit to reduce CO emissions about 98% by utilizing injection into intake of a petrol engine utilizing TEG to operate HHO unit	- TEG provide HHO unit energy as TEG energy between 91-169 kJ while HHO energy intake about 22.5 kJ
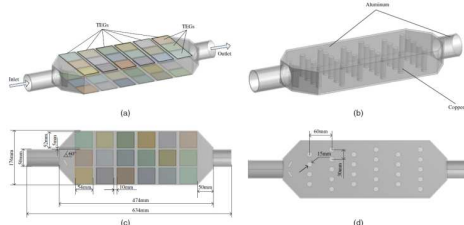
Fig. 21. Schematic diagram of heat recovery system [36].

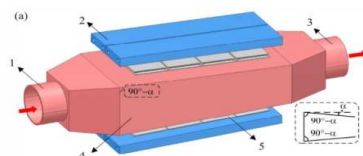**Fig. 22.** Cylindrical cross section HEX [37].

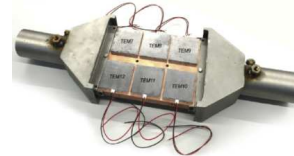**Fig. 23.** The TEG system with a tilt angle [40].

Fig. 24. TEG unit for the recovery system [41].

[42]	- Rafael, et al., 2020 - Theo & Exp - 68	- 20	- Waffle HEX shaped - Copper - (227×95) mm²	- U duct shaped - Water, Figure 25	3 fuels types used in diesel engine operation: Diesel, Biodiesel blend (B10), and Biodiesel blend (B5) <u>Hot side</u> - T$_{inlet}$ = 300°C - Velocity inlet = 20 m/s <u>Cold size</u> - The cold surface was cooled with ambient air	Results showed the power was recovered from 57.87W to 71.13W for B5, B10, and Diesel
[43]	- Krishna, et al., 2021 - Theo & Exp - 32	- (TEG1-12730) - 42 (40×40×3.4) mm³	- Set of parallel-plate fins - Steel	- 42 Cuboid tanks - Water - Aluminum, Figure 26	- Burning motor fumes (heat source) <u>Hot side</u> - T$_{inlet}$ = 80°C <u>Cold side</u> - T$_{inlet}$ = 10°C	- η$_{sys.}$ = 0.4 to 1.2% when - ΔT$_{max}$ = 25 to 70°C

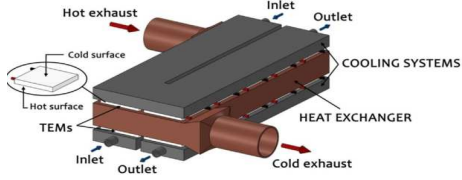| Ref	Author	Material	Hot HEX	Cold HEX	Operating conditions	Results
[44]	- Dhruv, et al., 2021 - Theo & Exp - 16	- (Bi$_2$Te$_3$) - 20 (56×56×4) mm^3	- Twisted ribs & smooth wall - Aluminum - (350×290×16) mm^3 with 3 mm plate thick	- 6 Rectangular channel (310×60×20) mm^3 - Engine cooling water - Aluminum, Figure 27	- Nissan 2.2 L 4-stroke diesel engine <u>Operating conditions</u> six different T$_{inlet}$ & ṁ$_{inlet}$ of the engine <u>Twisted tape</u> Pitch ratio, twist ratio, and tilt angle	Twist ratio of 4, pitch ratio of 8, and the tilt angle of 60° yield the highest power output P$_{max}$ = 75 W was 30% upper than smooth wall
[45]	- Jae, et al., 2021 - Theo & Exp - 31	- Skutterudite - 12 (20×20×5.44) mm^3	- 6 Straight fins (220×24×3) mm^3 - Aluminum - (220×70×34) mm^3	- 4 Coolant channels (40×98×10) mm^3 each made-up with 2 vertical fins - Water - Aluminum, Figure 28	<u>Hot air</u> - T$_{inlet}$ = 315.12, 419.26, 521.7, & 621.61°C - ṁ$_{inlet}$ = 0.0157 kg/s <u>Cooling water</u> - T$_{inlet}$ = 30°C - ṁ$_{inlet}$ = 0.0655 kg/s	- ΔT$_{max}$ = 99.72°C - ΔP = 0.175 kPa - P$_{max}$ = 45.65 W - η$_{sys.}$ = 45.43%
[46]	- Tao, et al., 2021 - Theo & Exp - 15	-	- Rectangular smooth duct - (800×68×6.8) mm^3	- Rectangular duct (800×68×3.4) mm^3 - Water	A novel of single & two stage automobile TEG <u>Hot gases</u> - T$_{inlet}$ = 673 K - ṁ$_{inlet}$ = 10 g/s <u>Cooling water</u> - T$_{inlet}$ = 300 K - ṁ$_{inlet}$ = 2.5 g/s	The two-stage could achieve the output power increments by 13.5% under the same conditions if compared to the single stage
[47]	- Wei-Hsin, et al., 2021 -Theo. - 25	- (TEC1-12706) - 1 (40×40×3.75) mm^3	- Rectangular duct with/without longitudinal aluminum fins inside (30×30×2) mm^3 - (360×200×60) mm^3	- Rectangular duct with (360×200×60) mm^3 - Air/water	- TEG was partitioned to two, four, & eight partitions - Re = 10, 100 & 1000 - Fins' number from 0-27 - HEX with/without fins	- The TEG without partition gives (0.066 W) as the TEG with 8 partitions - P$_{max}$ = 0.411 W and η$_{sys.}$ = 0.95%, with 27 fins at Re = 1000 - At 9 fins & Re = 1000 can improve P & η by 85% & 35%

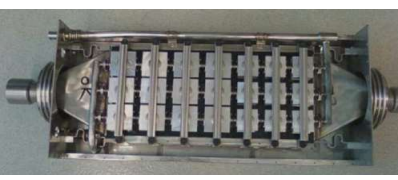**Fig. 25.** TEG device [42].

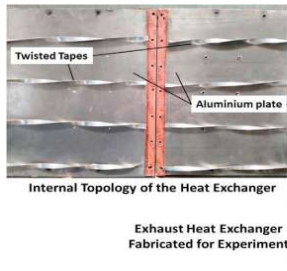**Fig. 26.** TEGs connected with exhaust HEX [43].

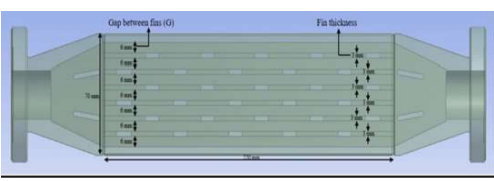**Fig. 27.** Inner and external structure of the fabricated HEX [44].

Fig. 28. Straight fins hot HEX [45].

| Ref	Author	Material	Hot HEX	Cold HEX	Operating conditions	Results
[48]	- Jie, et al., 2022 - Theo & Exp - 15	- (TEG-127020) - 16	- Rectangular duct with 4 segments of fins inside - Aluminum alloy - (200×111×75) mm^3	- 8 Rectangular duct (111×40×12) mm^3 with serpentine tube 5.5 mm diameter inside - Water - Aluminum alloy, Figure 29	<u>Hot air</u> - T$_{inlet}$ = 400, 450, 500 & 550 K - ṁ$_{inlet}$ = 10, 20, 30 & 40 g/s <u>Cooling water</u> - ṁ$_{inlet}$ = 41.67 g/s	- The output power increased 12.5% at T$_{inlet}$ = 500 K, ṁ$_{inlet}$ = 30 g/s & converging angles HEX segments 0, 2, 1 & 1.8, respectively
[49]	- Ding, et al., 2022 - Theo & Exp - 57	- (Bi$_2$Te$_3$) - 16	- 20 rectangular fins of (20×2×200) mm^3 inside HEX, & 6 mm between each two fins - Aluminum alloy - 3.35 kg - (212×111×70) mm^3	- 4 Rectangular duct (200×40×12) mm^3 with inlet/outlet tube 5.5 mm diameter - Vehicle water cooling system - Aluminum alloy, Figure 30	- Vehicle type (VEH-SUV) - Engine type) 3L FC-SI102-emis) - Vehicle speed (60, 65 & 120 km/h) <u>Hot gases</u> - T$_{inlet}$ = 544-600 K - ṁ$_{inlet}$ = 17-55 g/s <u>Engine cooling water</u> - T$_{inlet}$ = 363.15 K - Velocity$_{inlet}$ = 1 m/s	At speed of 120 km/h Pmax = 38.07 W η$_{sys.}$ = 1.53%
[50]	- Song, et al., 2022 - Theo & Exp - 17	Skutterudite - 400 (16×13×4) mm^3	- Double HEXs - Aluminum - 15 kg - (240×170×95) mm^3	- 3 Cuboid tanks - Water - Aluminum, Figure 31	- TEG installation to conventional/hybrid vehicles - 4 cylinder, 2- liters, Jaguar Land Rover gasoline engine - T$_{inlet}$ = 400 - 800 K	Electric power of auxiliary only influences performance of TEG in conventional vehicle and have little effect on that in extended-range electric vehicles
[51]	- Minghui, et al., 2022 - Exp. - 34	- (Bi$_2$Te$_3$) - TEGs Variable No. (50×50×4.2) mm^3	- Rectangular duct - Stainless steel - (545×118×18) mm^3 with 4 mm plate thickness	- Cuboid tanks - Water - Stainless steel, Figure 32	Number of TEGs groups= 4, 6, 8 & 10 Every group consists of 4 TEGs <u>Hot air</u> - Tinlet = 200, 300 & 400°C - Flow rate$_{inlet}$ = 10, 20, 30, & 40 m^3/h <u>Cooling water</u> - T$_{inlet}$ =301 K - Flow rate$_{inlet}$ = 1.4 m^3/h	- As the No. of TEGs increases, the resistance power consumption of TEGs increases - At any conditions, 40 TEGs achieved P$_{max}$ = 25.16 W & 16 TEGs give maximum η$_{sys.}$ = 1.56%
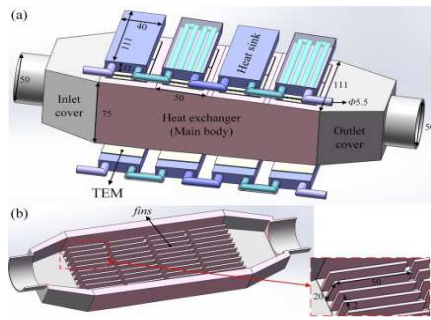
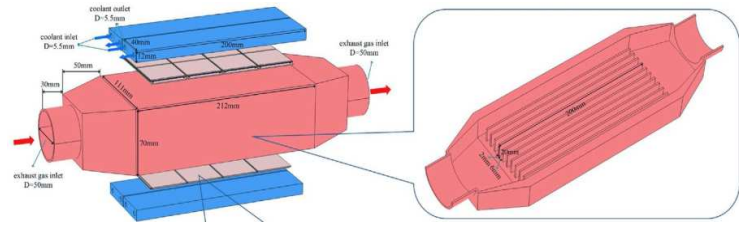**Fig. 29.** (a) 3D of TEG system, (b) Internal fins of HEX [48].

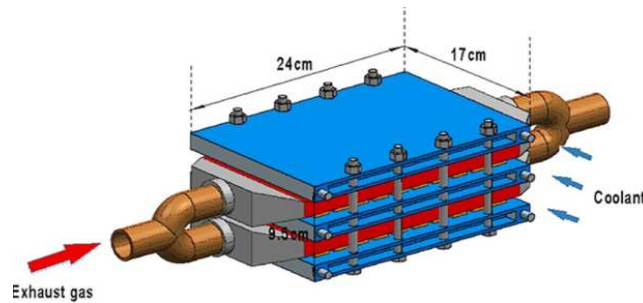**Fig. 30.** Architecture of TEG system for heat recovery [49].

Fig. 31. Structure of the TEG prototype [50].

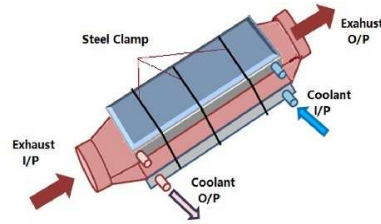|					
[52]	- Abolfazl, et al., 2022 - Theo. - 2	- 84 - (40×40×3.4) mm³	- Dual flat, C, and U shaped HEXs with simple/dimpled upper and lower internal surfaces - Cooper - (400×320×30) mm³ with 5 & 4 mm upper & lower walls thickness, dimple & simple, respectively	- Cuboid tanks - Engine water cooling - Aluminum	- Only 1/6 of exhaust gas mass flow rate & cooling water were considered <u>Hot gases</u> - T_{inlet} = 808.15- 693.15 K - $\dot{m}_{inlet}$ = 0.0496, 0.0458, 0.0431, 0.03725 & 0.02828 kg/s <u>Cooling water</u> - T_{inlet} = 366.15-363.75 K - $\dot{m}_{inlet}$ = 2.1 kg/s	- Although the highest pressure falls, a C-shaped HEX most efficient if the pressure loss was freely delivered by the engine exhaust pulse
[53]	- Rui, et al., 2022 - Theo & Exp - 10	(TEHP1-12656–0.8) - 60 (56×56×6) mm³	- 3 HEXs, Chaos shape, fishbone shape & empty - Brass - (300×400) mm² with 5 mm plate thick	- 12 Cuboid tanks (300×60×21) mm³, with 3 mm plate thickness - Engine water cooling system - 304 aluminum alloys	- PSA RFN 10LH3X (2 L) I.C. engine <u>Dry air</u> - T_{inlet} = 600 K - $Velocity_{inlet}$ = 40 m/s <u>Cooling water</u> - T_{inlet} = 90°C - Flow $rate_{inlet}$ = 0.6 m³/h	- The chaos shape HEX has the largest pressure loss at the same engine conditions - The engine without TEG system, the engine emission of CO, CO2, NOX from empty shape and others increases
[54]	- Habib, et al., 2022 - Theo & Exp - 15	- (TEG1-PB-12611-6.0) - 24 (56×56×4.95) mm³	- Labyrinth-shaped - Aluminum 6082 series - (371×127×24) mm³ with 8 mm plate thick	- Copper serpentine tubes were positioned within labyrinth tunnels of each HEX side to facilitate the efficient movement of propane mass - 50/50 mixture of ethylene glycol & water - Aluminum	- 2 Cylinder (505 cc Lombardini LGW 523 MPI) spark ignition engine cooled by water system - 8 Different engine rpm (1500-5000) with/without propane inlet gives 8 different inlet conditions of exhaust & water cooling	- TEG output power with propane was higher in the range of 11.5-12.1% without propane
[55]	- Patrick, et al., 2022 - Theo & Exp - 0	- (Bi₂Te₃) - 3	- Droplet's fin-base/parallel plate fin-base - 6063 aluminum alloys - (160×40×12) mm³	- One cuboid tanks (154.6×40×11.8) mm³ - Water - 6063 aluminum alloys, Fig. 33.	<u>Dry air</u> - T_{inlet} = 450 K - $Velocity_{inlet}$ = 4 m/s <u>Cooling water</u> - T_{inlet} = 300 K - $Velocity_{inlet}$ = 4.31 m/s	The droplets fin base HEX was more homogeneity in comparison to the parallel plate fin-base HEX
[56]	- Ding, et al., 2023 -Theo & Exp - 5	- (Bi₂Te₃) - 16 (40×40×3.4) mm³	- 20 long fins (20×2×200) mm³ were prepared on the upper & lower walls of HEX - 6063 aluminum alloys - (212×111×70) mm³	- 4 cuboid tanks (200×40×12) mm³ - Water - 6063 aluminum alloys	The numerical model encompasses both thermal and electric transient phenomena. <u>Hot gases</u> - T_{inlet}(t) & $\dot{m}_{inlet}$(t) <u>Cooling water</u> - T_{inlet} = 363.15 K - $Velocity_{inlet}$ = 1 m/s	Transient P_{max} = 45.16 W at t = 467 s & $\eta_{sys.}$ at t = 635 s touch peak values of 39.68%
[57]	- Ding, et al., 2023 - Theo & Exp - 3	- (TEG-127020) - Variable (1-36) - (40×40×3.3) mm³	- With/without fins (2 mm thickness & 4 mm spacing) - Aluminum - (Length (NL) column × Width (NW) row × Height (H) mm)	- Cuboid tanks - Aluminum	- During optimizations, H (5-30), NW (1-6), & NL (1-6) of the HEX <u>Dry air</u> - T_{inlet} = 546.73 K - $\dot{m}_{inlet}$ = 18.24 g/s <u>Cooling water</u> - T_{inlet} = 300 K - $Velocity_{inlet}$ = 1 m/s	The optimal parameters for HEX <u>With fins</u> H = 30, NW = 2, & NL = 5 <u>Without fins</u> H = 10, NW = 2, & NL = 4
[58]	- Luo, et al., 2023 - Theo & Exp - 19	-(TEG-127,020, P&N technology, China) - 16 - (40×40×3.3) mm³	- The inlet and outlet diameters of HEX = 50 mm - 20 rectangular fins of (20×2×200) mm³ inside HEX - 6063 Aluminum alloy - 3.35 kg - (212×111×70) mm³	- 4 Rectangular duct (200×40×12) mm³ with inlet/outlet tube 5.5 mm diameter - Engine water cooling system - 6063 Aluminum alloy	- Diesel engine =702 L - Equivalent exhaust data from platform of ADVISOR transient exhaust boundary. - 1/4 TEG system, with temperature dependences, topological linking of TEGs, & dynamic conditions were considered	- The mean power & efficiency of 1/4 TEGs system = 8.91 W & 3.39% which are 3.39% lower & 47.52% greater than those projected by steady-state study [47]

Ref.	Authors	TEM	HEX material	Cooler	Operating conditions	Results
[59]	- Ni, et al., 2023 - Theo & Exp - 1	- 40	- 6 baffles, lengths = 60 mm were located inside - Aluminum alloy - (304×124×20) mm³ with 2 mm plate thickness	- 3 coolers (468×124×20) mm³ with 2 mm plate thickness, 4 baffles were sited inside all cooler - Water - Aluminum alloy, Figure 34	The system consists of 2 heat collectors, 3 water coolers, <u>Hot gases</u> - T_{inlet} = 560-720 K - $Velocity_{inlet}$ = 8 m/s <u>Cooling water</u> - T_{inlet} = 300 K	The P_{max} = 15.8 W with T_{inlet} = 560 & inlet volume flow rate = 171 L/min

Fig. 32. Schematic of TEG system structure [51].

Fig. 33. Air-Water-based TEG system [55].

Fig. 34. Structure diagram of TEG device [59].

Ref.	Authors	TEM	HEX material	Cooler	Operating conditions	Results
[60]	- Ding, et al., 2023 - Theo & Exp - 0	- (Bi₂Te₃) - 1 - (40×40×3.4) mm³	- Aluminum - (85×60×60) mm³	- Rectangular duct (40×40×12) mm³ with serpentine tube 5.5 mm diameter inside - Water, Figure 35	- Dynamic performance of hybrid transient TE numerical model under various automobile driving conditions <u>Hot air</u> - $T_{inlet}(t)$ & $\dot{m}_{inlet}(t)$ <u>Cooling water</u> - T_{inlet} = 300 K - $Velocity_{inlet}$ = 1 m/s	The performance of the automotive TEG was mostly influenced by variations in exhaust heat rather than changes in vehicle speed
[61]	- Ding, et al., 2023 - Theo & Exp - 1	- (Bi₂Te₃) - 10 - (40×40×3.4) mm³	- With/without fins thickness (t), length 208 mm & spacing (d) - Aluminum alloy - (218×100×38) mm³ with 4 mm plate thick	- 4 cuboid tanks (218×40×12) mm³ - Water - Aluminum alloy, Figure 36	<u>Transient analysis</u> Fins distance (1-6) mm & thickness (0.5-3) mm & with/without fins of the HEX optimization	<u>Optimal fin dimensions</u> distance = 2 mm thickness = 0.5 mm with P_{max} = 45.02 W & η_{max} = 1.5% <u>With fins</u> P_{out}, $\eta_{conv.}$, P_{net} & η_{net} enhanced by 26.85%, 42.22%, 9.52% & 22.95%, respectively
[62]	- Abdelghany, et al., 2023 - Theo & Exp - 0	- (TEG-12708T237) - 30 - (40×40) mm²	- Steel - (350×210×60) mm³	- 2 Cooler blocks (350×200) mm² - Water - Aluminum, Figure 37	Compressed natural gas (CNG) & gasoline fuel were used for BYD-F3 4 cylinders, 4 strokes, 1600 cc - ΔT_{max} = 40% throttle= 195 & 158°C - ΔT_{max} = 80% throttle= 218 & 190°C for (CNG) & gasoline, respectively <u>Cooling water</u> - T_{inlet} = 30-45°C - $Flow_{inlet}$ = 0.08-0.13 L/s	CNG enhanced temperature uniformity P_{max} = 178.3 W but gasoline P_{max} = 164.4 W

Fig. 35. Geometry of the automobile TEG [60].

Fig. 36. Structure of the automobile TEG [61].

Fig. 37. Exhaust muffler modified with TEG [62].

[63]	- Hong, et al., 2023 - Theo & Exp - 0	- (TEHP1-1994-1.5) - 8 - (40×40) mm²	- Two model of hot HEX (rectangular & parabolic) (180×100×78) mm³ were integrated to aluminum muffler (350×90×68) mm³	- Longitudinal finned aluminum heat sink - Air cooled, Figure 38	- Optimal parabolic fin profile was calculated, to create a uniform temperature spreading on HEX's base. <u>Hot gases motor cycle engine</u> - Rpm = 4925 - T_{inlet} = 712 K - Velocity$_{inlet}$ = 1.05 m/s	- The optimal profile develops the temperature uniformity by 91.3% matched to the original profile
[64]	- Hong, et al., 2023 - Theo & Exp - 0	- (TEHP1-1994-1.5) - 8 - (40×40) mm²	- Rectangular aluminum fins, fin height = 32 to 67 mm; fins number = 15 to 23; & fin thickness = 1 to 2 mm - (180×100×10) mm³ with 4 mm plate thick	- Longitudinal finned aluminum heat sink - Air cooled - Figure 39	<u>Hot gases motor cycle engine</u> - Optimal rectangular fin is calculated T_{inlet} = 387, 584 & 712 K - Velocity$_{inlet}$ = 3.55, 10.62 & 17.71 m/s <u>Air cooled</u> - T_{inlet} = 303 K - h_{inlet} = 5 W/m²K	- At fin number = 21, fin thickness = 1 mm & fin height = 42 mm, maximum electricity power = 11.8 W
[65]	- Oh, et al., 2024 - Theo & Exp - 0	Skutterudite/Bi₂Te₃ - 40 - (50×50×7) mm³	- Rectangular HEX with flow straightener & internal 6 fins of 50 mm height & 2 mm thickness - 20 kg - (253.5×372×60) mm³ with 5 mm plate thick	- 2 cooling channels (253.5×372×29) mm³ were mounted upper & lower HEX - Internal 6 fins of 10 mm height & 5 mm lower & 4 mm upper thickness, respectively - Engine water-cooling system - Water	- Seoul city bus hydrogen engine at 1000, 1500 & 2000 rpm - TEGs series and parallel linking	- Output power of TEG varies with load resistance - Flow straighteners, enhanced uniformity of exhaust flow - Conversely, increase in pressure drop, which decline engine running
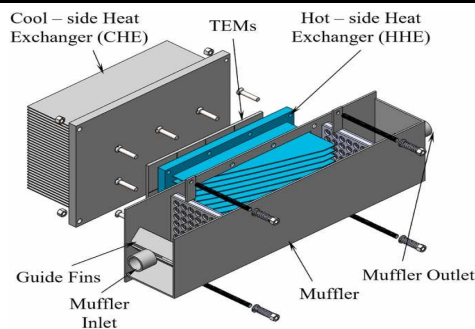
Fig. 38. Configuration of TEG [63].
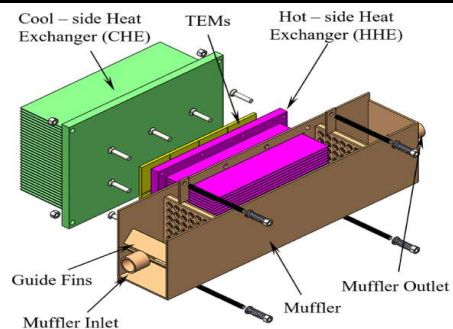
Fig. 39. Explore view of TEG [64].

2.1.1.1.2. *Square (flat) structure HEXs*

A square cross-section HEX with a (0.99x0.25x0.23) m³ size, an internal fin-like structure formed of a straight prism with a triangular base and longitudinal and transverse grooves utilizing a 48 TEGs with size a (56x56x4.45) mm³, that considerably increase the heat transfer surface was presented by Nikolay et al. [66]. The impact of the thickness and width of thermal fins and fin grooves from 0.75 to 5.0 mm and from 1.0 to 8.0 mm, respectively, on the performance of TEG for automotive I.C. engines. The inlet exhaust temperature and mass flow rate were 520ºC and 0.085 kg/s, respectively. The inlet coolant temperature and mass flow were 82ºC and 0.2 kg/s, respectively. The obtained results display the non-uniformity of the thermal field in the TEG body, which indicated irregular heating of the TEGs, decreased efficiency, overheating, and cooling fluid in an I.C. engine used as a heat source.
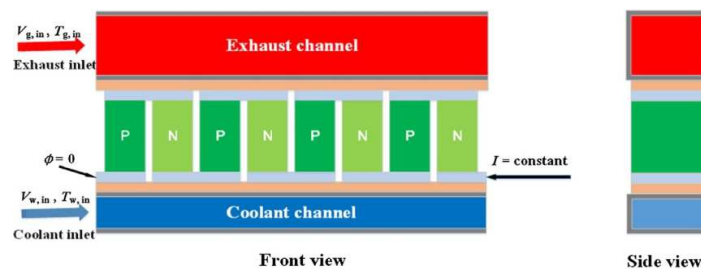

Fig. 40. Coolant, exhaust and TE unit arrangements, reprint with permission.
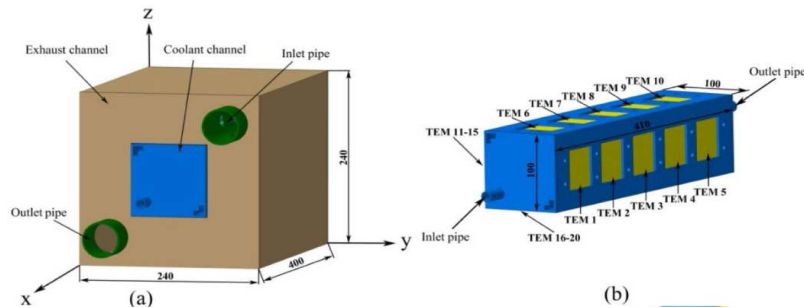
Fig. 41. 3D model of direct contact TEG (a) appearance, and (b) coolant channel, reprints with permission.

Jing-Hui et al. [67] developed a multiphysics TEG model to effectively harness the waste heat from car exhaust. The model incorporates the representation of both the water-cooling heat sink and hot exhaust source. The exhaust and coolant stream are represented as hollow rectangular aluminum pipes with a specified wall thickness. The automotive exhaust TEG system, shown in Fig. 40 was equipped with four TE units. It was worth noting that the specific number of TE units might vary within the range of six to twenty. The inlet boundary condition involved a uniform flow at the exhaust, with a velocity of 10 m/s and a temperature of 773 K. The coolant was characterized by an inlet velocity of 0.1 m/s and an inlet temperature of 300 K. The primary results indicated that the implementation of a counter-flow cooling pattern is advisable. Furthermore, it was seen that the temperature non-uniformity significantly degrades the output power.

To improve the usability and increase the scope of TEG applications, Tae et al. [68] suggested the idea of direct-contact TEGs. A 44 mm wide, 44 mm long rectangular aluminum exhaust gas duct was also created. Ten with (40x40) mm^2 apertures with flanges on either side were present in the exhaust gas channel, where 40 TEGs (44x44x3.6) mm^3 were installed. The coolant was fed into the coolant channels to eliminated heat, and a diesel engine provided a hot exhaust gas channel that acted as the heat source. The highest engine load and rotation speed conditions led to an optimal output power of 43 W and a conversion efficiency of 2.0%.

Ding et al. [69] have introduced a novel numerical model that incorporates transient fluid-thermal-electric multiphysics coupling fields. This model was experimentally validated and is the first of its kind to assess the dynamic performance of TEG systems during vehicle driving cycles. In order to mitigate the demands on computational resources and time, an investigation was conducted on one (TEG-127020) device under transient conditions representative of drive cycles. In order to enhance convective heat transmission and boost the hot-side temperature the of square HEX, certain fin structures were affixed to its inner surfaces. In addition, a cooling mechanism was positioned on the cold side of the TEG to facilitate heat dissipation. Consequently, the TEG was positioned between these components. The TEG system's steady-state numerical simulation predicts a generated electric energy of 1828.68 J, representing a 12.6% increase compared to the transient numerical simulation's prediction of 1624.07 J.

A design consisting of a solitary square exhaust channel, a square coolant channel, and a total of twenty TEGs manufactured by Fuxin was proposed by Yi-Ping et al. [70]. The TEGs were arranged into five units on each side. The dimensions of each TEG were (50x50x4) mm^3, whereas those of the aluminum cooling channel were (410x100x100) mm^3. The coolant channel shown in Fig. 41 consists of five rectangular apertures on every side, each with dimensions of (46x46) mm^2. In this novel TEG system, the TEGs were designed to have one surface in direct contact with the hot side of the automotive gas, where the other surface was in direct interaction with the cooling water. Additional examination reveals that a fluctuation of 10 K in coolant temperature will lead to a range of output power variance between 28.64% and 33.64%.

2.1.1.1.3. Hexagonal/octagon structure HEXs

Four $(L \times 48\sqrt{3} \times 2.8)$ mm^3 TEGs were coupled together in each face of the hexagon HEX, making a total of 24 TEGs that were electrically joined in series and thermally related in parallel, as studied by Chien and Mei [71]. The HEX was joined to a 62 mm-diameter exhaust pipe on both sides and was made up of a hexagonal pipe, radial fins, and a hollow center body. The 140 mm diameter circle that was etched on the hexagonal pipe, as shown in Fig. 42. The prescribed inlet boundary condition consisted of a homogeneous flow characterized by a velocity of 12 m/s and a temperature of 773 K. Zero gradients for velocity and temperature were enforced at the outlet boundary. The length of the HEX, denoted as L, ranged of values spanning from 50 mm to 240 mm. It has a divergent/convergent component that connects it to the exhaust pipe. Circumferential fins with a thickness of 1 mm, which were attached to the interior surface of the hexagonal pipe on the other end, hold the hollow center body, which consists of a circular pipe with a diameter of 100 mm and two bullet-shaped heads with a length of 90 mm. Aluminum was used to make each and every solid component. According to the computer simulation, the system produced 120 W of output with an efficiency of 5.8%.
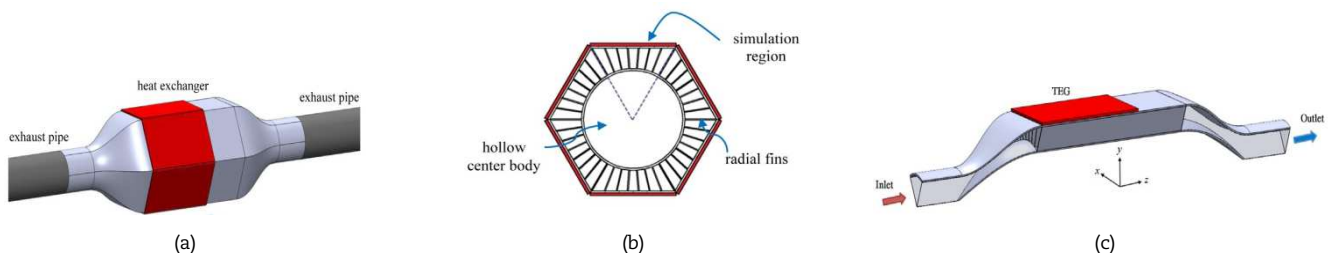

(a)   (b)   (c)

Fig. 42. 3D HEX design (a) front section (b) side section (c), reprint with permission.
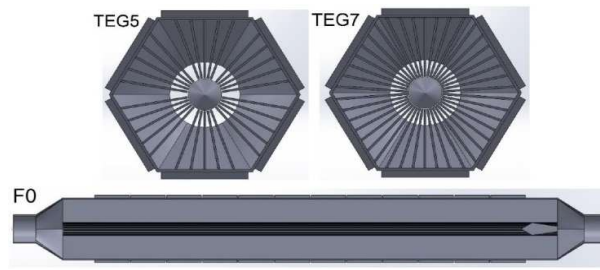
Fig. 43. Five and seven fins extended from each segment, reprint with permission.
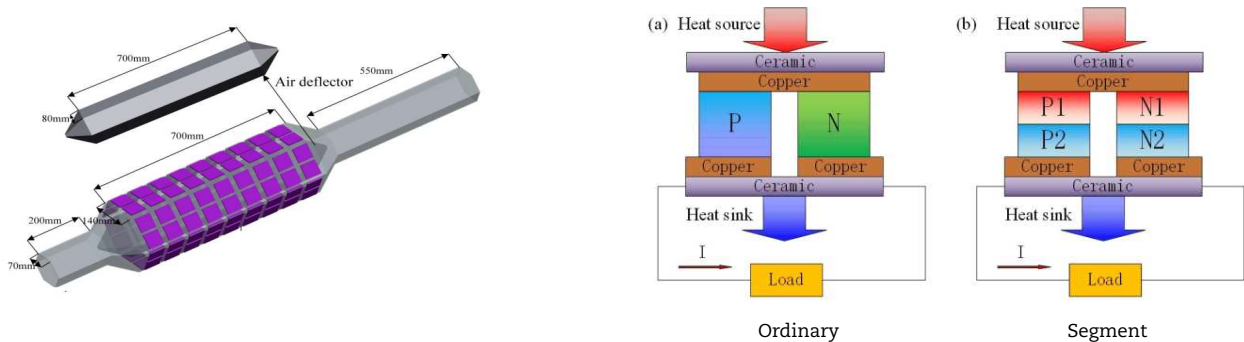

Fig. 44. HEX physical domain, ordinary, and segment structure, reprint with permission.

In order to perform better, Deng et al. [72] employed a hexagonal HEX, although the model used a couple of carriers. The distance separating the two carriers was planned to be 64 mm, with an expansion angle of 40° and a convergence angle of 70°. The mean exhaust flow rate was recorded as 15 L/s, and the temperature of the exhaust was measured at 250 °C. The temperature at which the cooling water tank inlet was configured was 67 °C. The average inlet flow rate was established at a rate of 8 L/min. The materials used for the HEX, cooling-water tank, and carriers were specified as steel with a thickness of 3 mm, aluminum with a thickness of 2 mm, and common ceramic materials, respectively. During the recycling of exhaust heat energy, an additional power of 31.93 W was produced based on the Celsius difference between both sides of the TEGs.

Utilizing a TEG to capture the waste heat energy reduces the burden placed on the engine's electric generator, improves fuel economy, and reduces pollutants. However, the placement of fins within the HEX significantly affects its function. Six TEGs were installed on a hexagonal aluminum HEX with a flat face length of 100 mm and a maximum diagonal of 134 mm. Six coolant chambers were used to cool the six TEGs, and six interior triangular fins were used in order to achieve the necessary output required for battery charging by Anand et al. [73].

Five-and-seven fins extended from each wall segment of a hexagonal warm HEX were examined by Borcuch et al. [74] to explain the impact of varying the number of fins and lengths on temperature distribution and efficiency of the HEX. The designed numerical model suggests an increase in the length of the HEX from 548 mm to 1056 mm, resulting in an expansion of the area covered by the modules from 312 mm to 880 mm. The number of TEGs situated on each side of the surface was augmented from four to twelve, see Fig. 43. The non-uniform surface temperature produced by a hot HEX with equal fin lengths along the HEX produced the highest net energy production among the other two designs.

In order to increase the effectiveness of TEG and make it more affordable and user-friendly, Kumar et al. [75] built a theoretical design and enhanced the method for installing the TEG systems in cars. To provide optimal contact between the heating source and TEG and to increase the heat transfer, the TEG was mounted over a standard octagon. Many variables, including the type of TEG material used, the temperature of exhaust gas, and the amount of heat absorbed by the coolant and the fin, were taken into consideration while determining the length of the HEX on which the TEG was being mounted.

To reduce the undesirable effects of heat gain and pressure drop, Gequn et al. [76] investigated an HEX utilizing 108 TEGs with a thin wall thickness and reasonable inlet dimensions and then compared the performance of two modes, ordinary and structured segments with various TEG configurations and topologies. Eighteen TEGs, each measuring (56x56x4) mm^3, were arranged with a spacing of 20 mm down the x axis and 9 mm over the z axis. This configuration aims to mitigate the interference of heat transfer between individual TEGs and enhance their overall performance, as shown in Fig. 44. In the single TEG mode, a segmented structure was used to compete for a significant temperature profile in the radial direction. The maximum output power increased by 13.4% in comparison to the original one.

The study conducted by Shishov [77], examined the geometries of hot hexagonal prism-shaped HEXs. This study focused on eight distinct shapes of the interior surfaces of these HEXs and aimed to evaluate their influence on the engine output during the current driving cycle. The many interior configurations of hot HEXs were indexed to oblique fins, flat walls, fins at an angle to the flow, longitudinal fins, dimpled surfaces, dimples and turbulizers, corrugation fins, and multidirectional fins, as illustrated in Fig. 45. Nevertheless, altering the internal surface of the HEX inside the exhaust system leads to an elevation in the hydraulic resistance, negatively affecting the power and efficiency of the engine. The maximum useable electrical energy generated by the sixth HEX was demonstrated with the obtained results.

Rui et al. [78] looked at the performance of an experimental TEG workbench made of stainless steel 304 hexagonal HEX with internal longitudinal peripheral fins (260x42x1.5) mm^3 and easily accessible 30 piece of Bi$_2$Te$_3$ TEGs with size (40x40x4) mm^3 and 30 aluminum cooling tank of (250x50x20) mm^3 size and 1 mm wall thickness. There were TEGs arranged along its six segments with five columns, and the hot-air inlet temperature was 260 °C, coolant initial ambient temperature was 27 °C and volume flow rate was 5000 L/hr. According to the experimental results, the HEX material, entry gas temperature, clamping pressure, and hot gas back pressure have a significant impact on the temperature profile of the hexagonal HEX. Brass HEX with lower backpressure and coolant temperature utilizing an ice-water mixture to boost the temperature difference of TEGs and improve the total output of TEG.
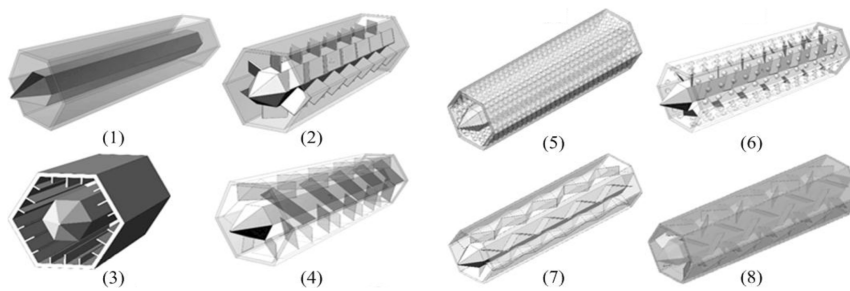
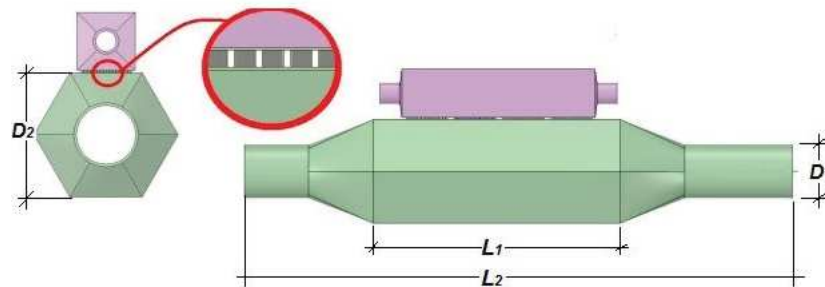**Fig. 45.** Hot HEXs internal design, reprint with permission.

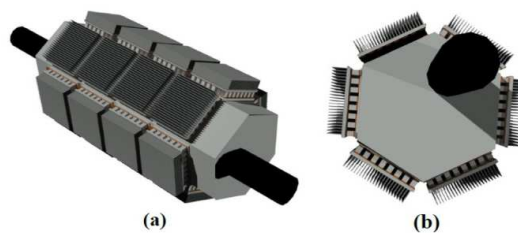**Fig. 46.** HEX and cooler design, reprint with permission.

Fig. 47. 3D HEX design (a) and side view (b) reprint with permission.

The application of TEG through experimental and numerical methods investigated by Beytullah et al. [79]. A hexagonal exhaust HEX was utilized, which was fabricated using aluminum with a thickness of 2 mm, Fig. 46. The TEG modules, specifically the TEG (GM250-127-14-10), were positioned between liquid fluid copper cooling blocks with a wall thickness of 1.2 mm and an aluminum HEX. The cooling mechanism of a single-cylinder diesel engine was utilized to cool the model. The flow rate of the fluid traveling through the coolant copper blocks was established as 1.5 liters per minute. Two types of coolant fluids were used in the experiment: pure water (100% concentration) and a (50-50% concentration) mixture of ethylene glycol and pure water. The objective of the study was to examine the impact of the coolant fluid type on the system. In instances where the fan operates continuously and a above cooling fluid mixture was utilized, an electrical power output of 10.678 W was observed at an engine speed of 1928 rpm.

Anderson et al. [80] suggest a system for recovering waste heat from TEG exhaust fumes. The muffler was constructed as a hexagonal HEX so that its functionality would not be compromised and the area could be expanded to accommodate most TEGs. There were four TEGs (TEHP-1263-1.5) with (3x3) cm^2 cross-sectional area coupled to each face, resulting in 24 TEGs, as shown in Fig. 47. These TEGs were electrically connected in series and thermally connected in parallel. Air at room temperature flowed across paired aluminum fin heat sinks on the cold side of each TEG, enhancing heat transfer and assisting in maintaining the temperature gradient. The system was able to supply 120 W of power at 5.8% efficiency using the generation obtained for a temperature gradient of 270°C.

The same hexagonal HEX of Rui et al. [78] was considered again by Rui et al. [81], but with different conclusions. The outcomes demonstrate that changing fin width, length, fin intersection angle, and fin spacing distance clearly have an impact on the heat transfer performance and back pressure of HEX.

Krzysztof et al. [82] described a hexagonal, internally finned HEX, 24 TEG converters, and 24 water-cooled tanks for performance experiments of TEGs with gas or liquid HEXs. The coolant exhibited a temperature range spanning from zero to 90°C, while the cooling flow rate ranged from 0.006 to 1.2 m^3/hr. The hot air input temperature varied between 15 and 800 °C, with a minimum inlet flow rate of 0 to 550 m^3/hr. The built-in test bed enables an accurate assessment of all the variables that can affect the TEG's conversion efficiency, as well as its net and total electrical output under various heat source and heat sink settings. Several TEGs specifically created for waste-heat recovery have been developed using the technique with success.

Zhao et al.'s study [83] examined the impact of low-speed and light-load operating conditions on the thermal heat from diesel particle filters to produce electrical energy using TEG. Every four TEMs were connected in series and connected to the load resistor at both ends, arranging 48 TEGs over a typical hexagonal HEX, as shown in Fig. 48. The exhaust gas enters the HEX via circular pipe with a diameter of 50 mm, which lead to a SiC filter with a porosity of 0.6. The diameter of the outer circular channel is 47 mm. Three low continuous regenerative temperatures (823 K, 873 K, and 923 K) and three high temperatures (1606 K, 1696 K, and 1786 K) were chosen to compare the thermoelectric conversion. The highest power output of 32.09 w/36.76 w/41.75 w of 1606 K/1696 K/1786 K, and 4.99 w/6 w/7.12 w of 823 K/873 K/923 K.
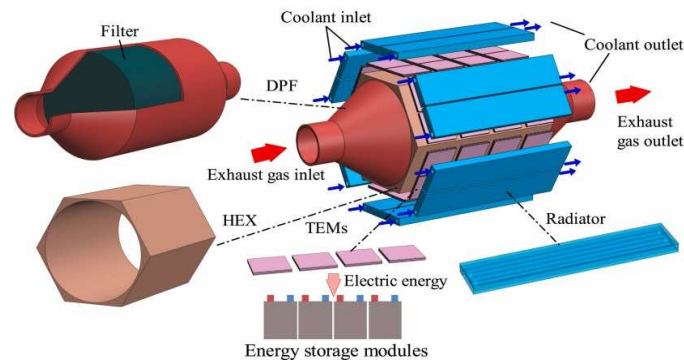
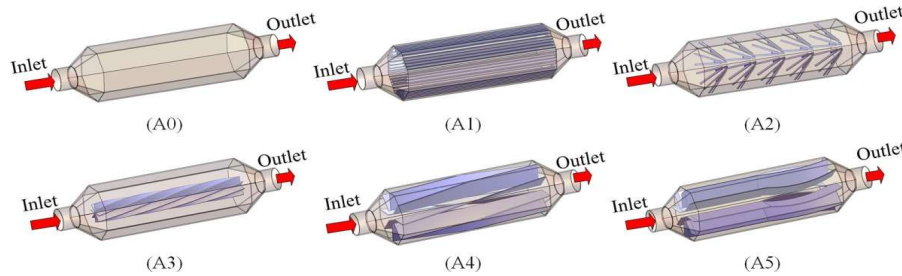**Fig. 48.** Diesel particulate filter and TEG system, reprint with permission.

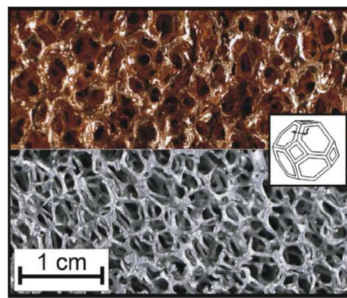**Fig. 49.** Six HEXs with different internal structure, reprint with permission.

Fig. 50. Sample from aluminum and cooper foams, reprint with permission.

Quan et al. [84] suggested a polygonal aluminum HEX with six distinct interior topologies to improve exhaust gas efficiency in TEG systems. Fig. 49 provides a detailed design of the six different interior topologies of the HEX: cavity structure (A0), inner surface flat fin structure (A1), slant-inserted V-shaped fin structure (A2), internally inserted helically twisted tape structure (A3), helical slant fin structure (A4), and sickle fin structure (A5). The HEX had a convective HEX section measuring 360 mm, a wall thickness of 2 mm, and a whole of 540 mm. The dimensions of the intake and outlet are the same, and they are seamlessly connected to the engine exhaust pipe with an inner diameter of 53 mm. Among the HEX and tanks, there are eight rows of TEGs (TEG1-127-1.4-1.6); each row consists of eight TEGs wired in series. The cooling system comprises eight hollow tanks that are 360 mm in length, 2 mm in thickness, and 5 mm in inner diameter. The outcomes showed that the TEG performance was significantly enhanced with the inserted sickle fins. However, with a greater pressure drop, the higher fins improve the output power and temperature uniformity of the system. However, longer linear fins and a wider arc fin radius lessen the pressure loss without compromising the power output. Furthermore, improving temperature uniformity with little impact on output power and pressure drop can be achieved by raising the arc's termination angle.

2.1.1.1.4. *Foam/porous internal structure HEXs*

Chi et al. [85] examined the two kinds of exhaust HEXs using 10 ppi (pores per inch) aluminum and 10, 20, 40 ppi copper foams and rectangular offset-strip fins, see Fig. 50. The metal foams provided a 60 TEG (HZ-20) with greater efficiency and total power output than a rectangular offset-strip fin. The cooling fluid HEX was constructed using aluminum and comprised of six identical rectangular flow paths with identical cross-sectional areas. Metal foams have the potential to significantly boost the TEG's overall power output from 130.32 W to 293.79 W. However, a substantial pressure drop caused by the porous (foam) media led to a low net energy production, particularly for high exhaust mass flow rates.

The impact of core flow with porous foam copper, inserted to improve heat transfer, on the productivity of TEGs (TEHP1-12656-0.3) $(55 \times 55 \times 5)$ mm^3 was studied experimentally by Yanzhe et al. [86]. An HEX with dimensions of $(350 \times 70 \times 20)$ mm^3, cooling water tanks $(300 \times 70 \times 20)$ mm^3, both with a wall thickness of 5 mm and a fill ratio of 50-75%, were used, as depicted in Fig. 51. In the experimental setup, the volumetric flow rate of the intake air was measured to be 60 m^3/hr, while the temperature at the inlet was recorded as 300 °C. The results demonstrated that 40 ppi copper foam with a 75% fill ratio had the best influence on the TEGs output power from 80% to 140%. Due to the gas side's high thermal resistance, this can reach 80%, when using a TEG with a gaseous working fluid.
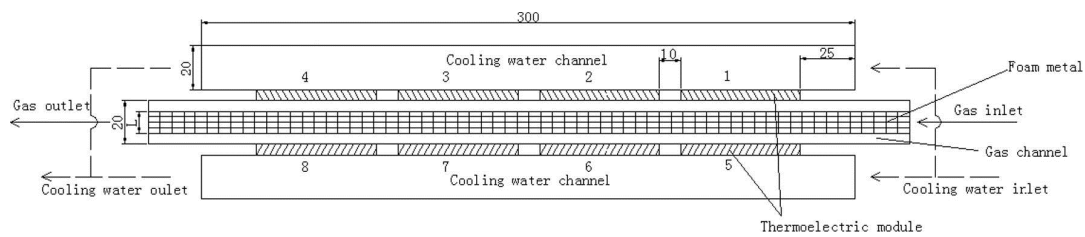
Fig. 51. Rectangular HEX occupied with metal foams, reprint with permission.
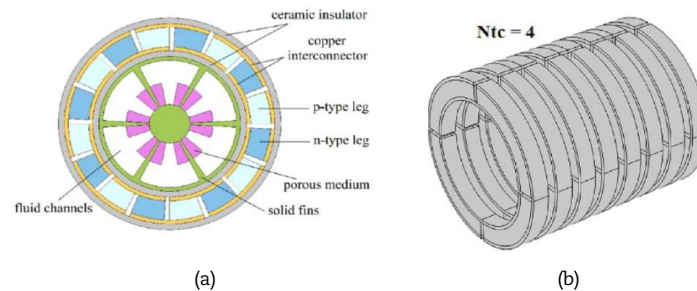

(a)   (b)

Fig. 52. (a) Pin fin porous medium inserts HEX, and (b) TEG with number of thermocouples of four, reprint with permission.
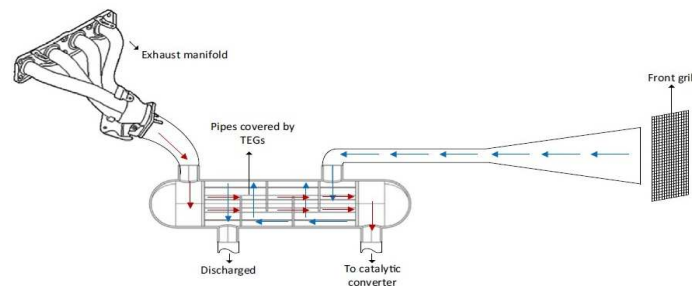

Fig. 53. Schematic TEGs system, reprint with permission.

Nithyanandam and Mahajan [87] examined the effectiveness of metal foam-based HEXs in lowering the thermal resistance of the hot side of TEGs to optimize the energy transported from the hot exhaust gas to the hot side of the TEGs. The size of the HEX length= 0.5 m, width= 0.181 m, height= 0.0744 m, and the wall thickness of the HEX was 0.003 m. The mass flow rates of the exhaust range from 20 g/s to 100 g/s, while the temperature spans from 400 °C to 700 °C. According to the findings, the highest net electricity made up of metallic foam-enhanced TEG from exhaust waste heat was 5.7 (20 ppi) to 7.8 (5 ppi) times greater than that produced by the arrangement with no metal foam.

Again Yanzhe et al. [88] increased the heat transfer performance at the hot side by inserting porous foam copper into the core flow zone of the HEX in order to utilize wasted energy by the TEG technique and address the issue of pollutants in the environment. The TEGs were in contact with the coolant water-duct walls. The HEX and cooler dimensions and boundary conditions were the same as in Yanzhe's previous work [78], but with an insertion ratio of 50% and 75% of the HEX core volume with (20 ppi) and (40 ppi). Through the results, the 75 % volume ratio and 20 ppi porous foam copper has the greatest impact on the output power.

Using external TEGs, Bernardo et al. [89] numerically investigated the impact of the thickness of aluminum foam within an exhaust gas pipe for an automobile. The exhaust gas inlet temperature is maintained at a consistent value of 723 K. The waste gas mass flow rate ranged from 20 g/s to 100 g/s. According to the study, it was possible to assess how metal foam affects TEG performance for a range of foam thicknesses, porosities, pore densities, and mass flow rates of exhaust gas in a forced convective regime with two-dimensional steady-state heat transfer. The primary conclusions indicated that as foam thickness and gas flow rate increased, the average temperature on the hot side of the TEG increased.

A fin-pin HEX with a porous insert and numerous bent TEGs (the number of thermocouples in each ring was 4, 8, 12, and 16) was contained in each TEG ring that made up a tubular TEG, as shown in Fig. 52. Sayed et al. [90] investigated this and contrasted it with a tubular TEG without a fin-pin structure or porous insert that had a smooth channel. The coaxial cylindrical geometry of the parts of the system was shared by all the parts. The pin-fin-porous tube clearly boosts the conversion efficiency while also significantly increasing the pumping power, which is one of the most noteworthy findings of this study. The greatest conversion efficiency, which was equivalent to 0.217 at Re = 200 and the number of thermocouples in each ring was 16, was achieved.

2.1.1.1.5. Cylindrical structure HEXs

To recover automotive waste heat, Murat et al. [91] suggested a shell and tube HEX, where pipes were coated with TE materials. The exhaust gas from the vehicle heated the TEG, and the air entering through the entrance grill maintained the temperature differential of the TEG. Both types of shell and tube HEX were composed of 37 tubes and 4 baffles. The tubes had a length of 1.02 m and a diameter of 3.1 cm, as shown in Fig. 53. A numerical investigation was performed using two distinct pairs of TE materials. The first TE material pair, denoted as TEG pair (1), comprised $CaMn_{0.98}Nb_{0.02}O_3$ as the n-type material and $GdCo_{0.95}Ni_{0.05}O_3$ as the p-type material. In contrast, TEG pair (2) consists of $CaMn_{0.98}-Nb_{0.02}O_3$ as the n-type material and $La_{1.98}Sr_{0.02}CuO_4$ as the p-type material. The highest power generated from waste heat was calculated to be 158 W, which corresponds to an energy efficiency of 0.51%. The TE activity of pair (1) was superior to that of pair (2).

Theoretical HEX models with double, mid, and single-finned peripheral parabolic aluminum fins were developed by Arumugam et al. in [92]. With the aid of simulation research utilizing the ANSYS Steady-State Thermal mode, the dimensions of fins were discovered in order to determine the optimal model. The base width was 0.977, 1.33, 1.737, 2.2, 2.714, 3.28, 3.91, 4.586, and 5.319 cm, and fin lengths ranged from 6 cm to 14 cm. A model of a double-finned shape with eight fins, measuring 8 cm in length and 1.737 cm in width, was found to be useful for simulating temperature profiles. The temperature distribution was uniform thanks to double-finned parabolic fins.

Soheil et al. [93] conducted a three-dimensional simulation of a single-stage and two-stage circumferential TEG to examine its thermodynamic and exergy economic performance. The heights of the p and n-type semiconductors in each stage were the same at 10 mm, and the slope between the two types of semiconductors in both stages was maintained at 20.4°. It was discovered that the economic performance of the single-stage TEG was superior to that of the two-stage TEG across all the examined heat sources. However, the conversion efficiency of the two-stage TEG surpasses that of the single-stage TEG when utilizing low-temperature and elevated temperatures materials.

Man-Wen et al. [94] examine the hollow cylindrical arrangement as a unique TEG leg construction in which the n-type and p-type legs were positioned coaxially inside one another. The azimuthal angle, slant angle, and width ratio of the cylindrical ring-shaped coaxial configuration could be varied and were all examined under various boundary conditions. Ring-shaped construction has the ability to lower thermal stress without lowering the thermal efficiency. According to the results, increasing the hot-side temperature decreased the mechanical dependability while increasing the output power and conversion efficiency of the cylindrical TEG device. Additionally, the highest Von Mises stress in the TEG legs rises with a rise in the slant inclination of the legs, improving the power produced by the cylindrical TEG.

A unique concentric annular TEG composed of annular thermocouples and concentric annular HEX was presented by Wenlong et al. [95]. Using a finite-element method, a numerical model of the concentric annular TEG was developed, and the TE performances of the proposed concentric annular TEG and standard annular TEG with a cylindrical HEX were compared. To find the best design for a concentric annular HEX, the relationship between the sizes of the HEX, how well it moves heat, and how hard it is to flow through the HEX was carefully studied. According to simulation studies, the optimal value of the inner to the outer diameters of the HEX was 0.94, with an optimal net power that was 65% greater than the standard annular TEG.

A TEC for automobiles was created and implanted by Da-hye et al. [96], along with a TEG that makes use of a cooper circular exhaust heat pipe. A thermo electric cooler was created to draw cool air from the back seat ceiling, as shown in Fig. 54. The TEG employed (TGM-199-1.4-0.8) TE modules of (40x40) mm² area. The cooler reduces the temperature of the area (the size of an adult's head) from 45 to 26 °C in less than three minutes. A TEG that may be connected to a car exhaust pipe powered the cooler. At a temperature of 90.37 °C on average, twelve TEGs generated 90.715 W of electricity.

A circular exhaust HEX, cooling water jacket, and TEG were the major parts of the vehicle exhaust annular TEG, as presented by Zu-Guo et al. [97]. An additional portion, that is, a hollow cylinder, was placed in the core of the HEX to improve the exhaust convective heat transmission capabilities. A TEG composed of n rings was maintained between the HEX and the cooling water jackets that deployed annular TEGs. Five construction parameters, cylinder diameter, HEX diameter, HEX length, leg height, and leg central angle, were studied in order to design an efficient annular TEG. The findings indicated that power develops exponentially with cylinder diameter, that net power develops with increasing HEX length, and that the maximum net power, or about 122 W, was relatively unaffected by the leg height or central angle.

The identical concentric annular TEG produced by Wenlong et al. [95] was reported once more by Wenlong et al. [98], utilizing four cooling techniques (air and water). Additionally, the effects of various exhaust variables on TEG performance were examined using the finite-element approach. The findings indicated that by employing counter-current water-cooling, an optimal net power of 432.42W was attained, with a peak net power gain of 8.9% when compared with co-current water-cooling.

The optimization of the design of automotive annular TEGs presents significant difficulties owing to the varied operating conditions of automobiles and continuously fluctuating exhaust parameters. Wen Chao et al. [99] used the finite element method to create a new non-isothermal theoretical model for annular TEGs. This was done so that they could figure out how different vehicle operating conditions affect the ideal TEG volume. Numerous ring-shape TEGs make up the annular TEG module. All thermocouples were joined in series and arranged equally. The hot endpoint (inner) and cold endpoint (outer) of the thermocouples transmit heat from the exhaust gas travelling in the axial direction to the ambient in the radial direction. The findings indicated that the ideal annular TEG setup has a single PN couple volume of 5.0625×10^{-6} m³, a total PN couple size of 2.835×10^{-4} m³, a net power of 20.85 W, and an efficiency of 3.9%.

A new hexagonal concentric tube was created. Once more, Wenlong et al. [100] proposed using a silicone polymer-based thermal conductor oil to transport heat from the exhaust to an annular TEG that follows the geometry of the exhaust pipe. The performance of the TEG was investigated using numerical simulations in relation to exhaust parameters, thermal oil parameters, and HEX structure. The results show a 19.0% increase in efficiency and a 15.2% increase in peak output power of the improved generator when compared to a traditional prior annular TEG.

Yang et al. [101] performed a numerical analysis and proposed an annular TEG with circular aluminum pin fins. Each pin fin was strategically positioned throughout the vehicle's exhaust pipe and extended axially. As shown in Fig. 55, the TEG consisted of 12 rings, each of which housed 24 pairs of annular thermocouples. Every thermocouple has a height of 4 mm, a thickness of 4 mm, a leg angle of 6°, and an angle of 1.5° between each leg. There was a 1 mm space between the rings. According to the Taguchi analysis, the mass flow rate, fin height, fin diameter, and fin number were the next most important factors influencing the thermoelectric performance after the exhaust temperature. These parameters had ideal values of 673 K, 30 g/s, 20 mm, 3 mm, and 420, respectively. The net power under the ideal design conditions is 34.11 W, which is 18.7% more than the original design.
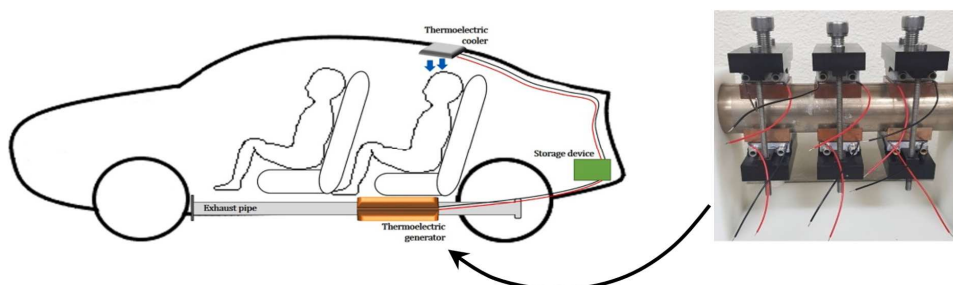

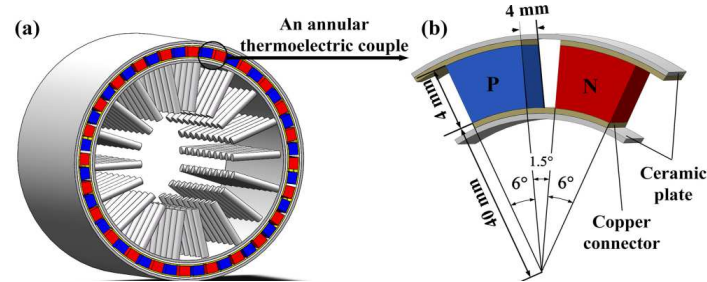**Fig. 54.** photograph TEGs' system location installation, reprint with permission.

Fig. 55. (a) All TEG system, and (b) Radial thermocouple structure, reprint with permission.

Fig. 56. Frame, aluminum hot plate, and TEGs' system, reprint with permission.
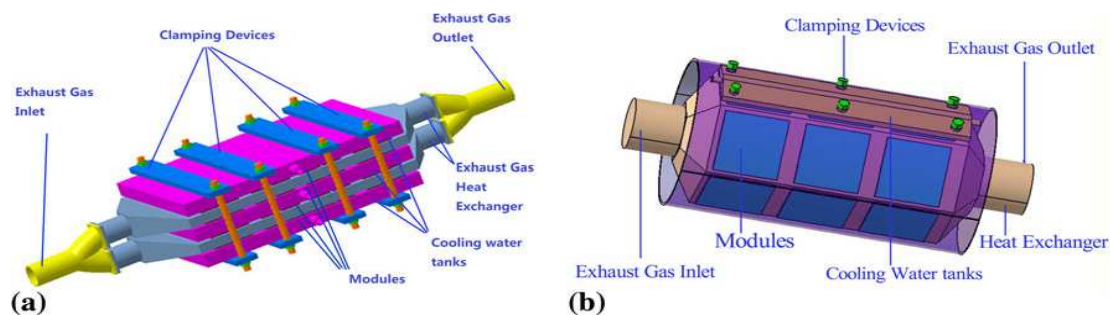

Fig. 57. Plate shape (a) Hexagonal (b) HEXs with TEGs schematic, reprint with permission.

A unique asymmetrical annular TEG with precisely balanced P and N-type leg proportions was introduced by Yang et al. [102]. subsequently created a generic formulation for optimizing the asymmetry coefficient and deduced the relationship regulating thermal-electrical impedance matching in an asymmetrical annular TEG. The effect of different temperature boundary conditions on the ideal annular leg characteristics, optimal resistance matching, and optimal asymmetrical coefficients were investigated. Our results show that the ideal load ratio is highly dependent on the thermal boundary conditions. Moreover, the suggested asymmetrical annular TEG with the optimized structure shows an astounding 16.2% increase in output power while keeping the same material volume as conventional annular TEGs.

2.1.1.1.6. Variform structure HEXs

To investigate the properties of the stream and the heat transfer, three different HEX configurations (hexagonal, triangular, and rectangular) were built using CAD and analyzed using a commercially available CFD code, as directed by Ramesh et al. [103]. The TEG comprised of three main components: an exhaust gas HEX, a counter-flow coolant cooling tank, and a series connection of 18 TEGs. The frame of the HEX was constructed using cast iron with a thickness of 5 mm. The TEGs were positioned on the upper surface of the 5 mm thick aluminum plates, while the lower surface of the plates was exposed to the exhaust. The 3 mm thick copper plate was integrated into the cooling tank and positioned above the TEGs, as depicted in Fig. 56. The overall mass of the TEGs system was recorded as 14.6 kg. The results presented that the rectangular configuration of the HEX achieved the space and mass restrictions and resulted in better outputs as compared with the other configurations.

Deng et al. [104] conducted a comprehensive study encompassing both theoretical and experimental analyses on flat plate HEXs that possess inner structures resembling fish bones, and hexagonal prisms, as visually depicted in Fig. 57. Once the gas inlet temperature exceeded 300 °C, the input flow velocity was adjusted to 20 m/s. Sixty TEGs were installed on both the hexagonal-prism-shaped HEX and plate-shaped exchanger. The volume of the hexagonal prism-shaped HEX was around 13.09 L, but the volume of the alternative design was merely 2.55 L. Consequently, the HEX, characterized by its hexagonal prism shape, exhibits an excessive volume that hinders the effective dispersion of waste gas, thereby impeding the enhancement of the hot-side temperature. Additionally, the surface areas of the two exchangers were 0.327 m^2 and 0.262 m^2, respectively. The heat loss of the hexagonal-prism-shaped HEX with a bigger surface area was comparatively higher than that of the alternative designs. After taking into account all of these aspects, it can be concluded that the plate-shaped HEX was a more appropriate choice for TEG applications.

A carbon steel heat duct with circular, triangular, and square cross-sections, as shown in Fig. 58, was modified by Banchob et al. [105] involving the utilization of a five flat TEGs (HZ-14) and bismuth telluride alloys with dimensions of (7x7) cm^2. This study also includes the design and analysis of a cooling system to facilitate power generation from waste heat. The cross-sectional areas of the three configurations were measured to be 7.07 cm^2, 43.5 cm^2, and 100 cm^2 for the circular, triangular, and square cross-sectional ducts, respectively. In summary, it can be concluded that a duct with a square cross-sectional form is the optimal configuration for power generation in TE devices. Despite the consistent decrease in temperatures across all duct forms, it was observed that the square cross-sectional duct exhibited a more uniform temperature profile compared to the other designs.
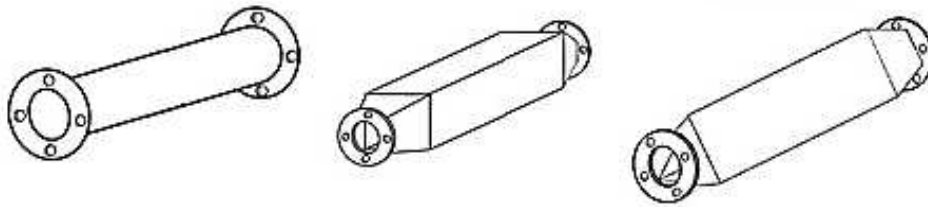
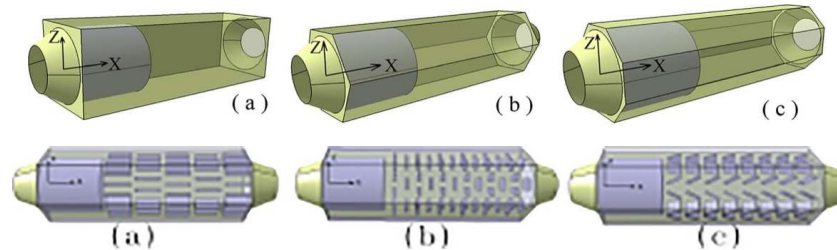**Fig. 58.** Circular, Square, and Triangular heat duct designs, reprints with permission.

Fig. 59. Cross sectional shape HEXs and interior fins arrangements, reprint with permission.
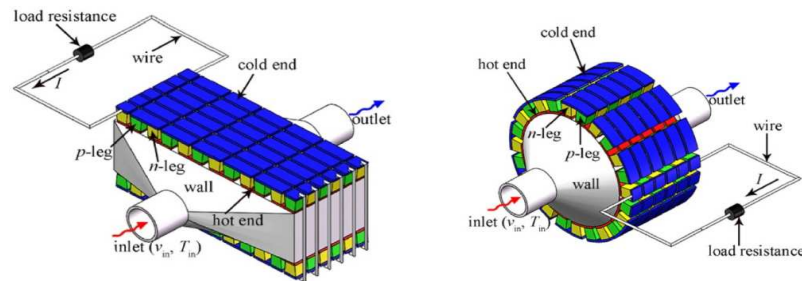

Fig. 60. 3D HEXs flat and annular constructions, reprint with permission.

Xiaohong et al. [106] modeled and compared the temperature difference and back-pressure of three HEXs with various sections (square, hexagon, and octagon). In addition, three unlike fin preparations were considered on the side: parallel, perpendicular, and skewed, as shown in Fig. 59. The mean power outputs of the TEGs with a square= 3.3124 W, hexagonal= 3.2994 W, and octagonal = 3.2774 W. Also, for parallel fin HEX, the wall temperature ranged = 258.8-267.3 °C, perpendicular = 250.7-258.1°C, and skewed = 262.2-275.8 °C. The observation may be made that the wall temperature of the HEX in skewed fins exhibited an elevated value. Finally, the findings demonstrated that the arrangement of the fins within the HEX had a significant impact on the HEX's performance but that the section shape had no discernible influence on the distribution of both pressure and temperature.

Shu-Rong et al. [107] used TEGs on the outside of a channel (square, rectangle, hexagonal, triangleular, and trapezoidal), and heated fluid was allowed to pass through the channel's interior to generate electricity. However, it has been proven that the cross-section form affects the power generator performance. Therefore, three-dimensional simulation studies were used to assess the performance of TEGs attached to canals with five different cross-sectional forms. Maximum power as a function of Reynolds number is the subject of the previous study. Regarding the outcomes, the TEG device with a rectangular-shaped canal has the highest output power. Furthermore, the Reynolds number correlates with an increase in output power.

A possible application of TEG, which may transform low-grade thermal energy into electricity, is to use the heat energy of the exhaust fumes. In terms of compatibility, it is believed that the annular TEG was significantly more practical than the flat-plate TEG for cylindrical heat sources. Mengjun et al. [108] compared the performance of annular and flat TEG by changing the velocity, temperature, and convection-heat transfer coefficient (CHTC) when a cylindrical shape-heat source was used, as shown in Fig. 60. The results showed that the conversion efficiencies and powers of both the annular and flat TEG go up when the speed of entry, the temperature, and the CHTC increased. An annular TEG always has more conversion efficiency than a flat TEG. Interest in using I.C. engine exhaust heat harvesting to cut fuel use, boost efficiency, and thus lower environmental pollution and global warming was developing.

An automobile exhaust annular TEG was primarily made up of a round-shaped exhaust HEX, annulus TEGs, and a cooling water jacket, as illustrated by Bin et al. [109]. To lessen the local pressure drop, each entrance and exit had an expansion and contraction segment. Annular TEGs wired in series and thermally connected in parallel were installed between the HEX and cooling water jacket. For the cooling medium and exhaust, two flow configurations co-current and counter-current were considered. Additionally, a flat-plate TEG for automobile exhaust is presented. For comparison, circular and flat TEGs have the same structural characteristics, including the leg number, leg height, total volume of TE material, HEX length, and cross-section area of the flowing cooling medium, as well as similar materials. Results reveal that annular TEGs perform better than flat TEGs, with the net output being on average 1.1% greater.

To determine which setup would produce the best results from these two TEGs systems, Asaduzzaman et al. [110] built two different setups out of equilateral triangular HEXs (height=12 cm, side length= 6 cm) fabricated from steel and copper, see Fig. 61. Each copper and steel HEX had six TEGs (SP1848-27145 SA) with (40x40x3.6) mm³ size, mounted on exterior surfaces that were electrically series-linked. The TEGs were covered with six rectangular aluminum water heat sinks. As a result, the power output of the TEG system constructed from copper was 48% higher than that of the TEG arrangement built from steel.
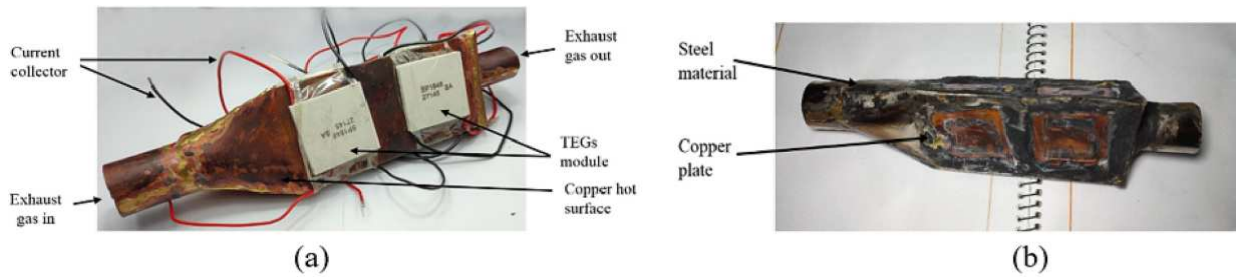
Fig. 61. Triangular HEXs (a) cooper, (b) stainless steel constructions, reprint with permission.
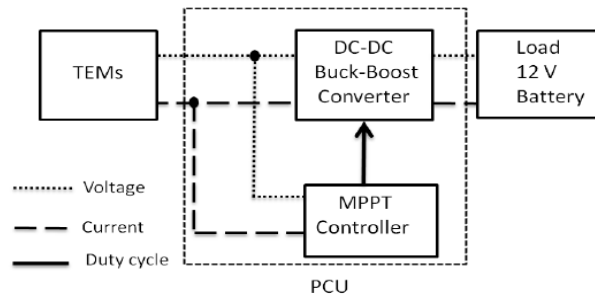

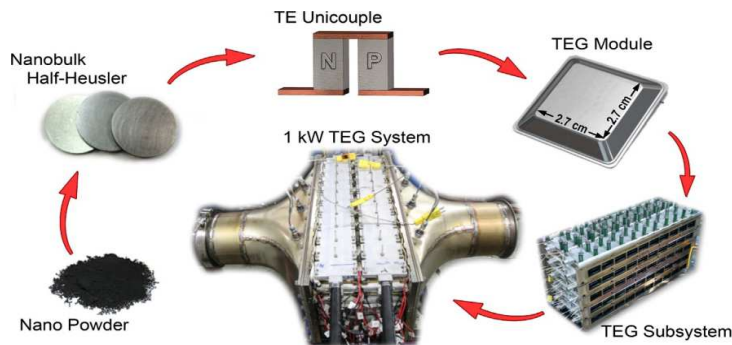**Fig. 62.** The diagram of power conditioning unit, reprint with permission.

Fig. 63. Pictures explain the stages of fabrication of high output power TEGs unit, reprint with permission.

2.1.1.1.7. Unfamiliar structure HEXs

Gequn et al. [111] proposed a novel strategy to increase engine output power and decrease fuel consumption. This approach involves the utilization of waste heat energy from engine exhaust gases through the combined use of TEGs and the organic Rankin cycle. This study specifically focuses on the theoretical analysis of this approach for a WD10D235 engine. The preheater and precooler were utilized to generate a temperature differential, with the TEGs positioned between them. The findings suggested a notable enhancement in system performance when the combination of TEGs and internal HEX was employed in conjunction with the organic Rankin cycle.

Navneesh et al. [112] introduced a tool designed to explore the utilization of TEG to recover waste energy from the exhaust of a vehicle engine. The recovered energy was then converted into electricity, which served to counter the electrical requirements of the 12V batteries. The model that was designed with three primary subsystems, namely HEX, TEGs, and the power conditioner unit, as shown in Fig. 62. The HEX mechanism facilitated the movement of thermal energy between the gaseous and liquid states, enabling the transfer of heat to and from the TEG. This process involves extracting heat from the exhaust to establish a hot side while simultaneously removing heat through the coolant cycle to establish a cold side. The TEG can produce electricity when exposed to a temperature gradient with hot and cold sides. The findings of the simulation indicated that the utilization of a power conditioning unit equipped with a buck-boost converter was appropriate for TEG systems.

A theoretical framework for a TEG device that utilizes the heat from car exhaust gases based on Fourier's law and the Seebeck effect, was developed by Yuchao et al. [113]. The model was designed to simulate the effects of many variables on power generation and efficiency. These factors included the mass flow rate of the engine exhaust, mass flow rate and temperature of various cooling fluids, CHTC, height of the PN couple, and ratio of exterior to internal resistances in the circuit. The findings indicate that altering the height of the PN couple led to the occurrence of a peak value in the output power. Furthermore, it was concluded that the peak value diminished when the TC of the PN couple decreased. Its efficiency greatly improved by altering the high-temperature side's convective heat transfer coefficient relative to the low-temperature side.

Yanliang et al. [114] were able to make a high-performance TEG device by making nanobulk half-Heuslers using a ball milling and hot press process. The HEX was constructed utilizing nickel-201 fins with thickness of 0.2 mm. These fins were arranged with a packing fraction of 15.5% to achieve equilibrium between the heat flow and pressure drop, as seen in Fig. 63. Graphite foils with 0.5 mm thickness were utilized to reduce the thermal contact resistance between the HEX and TEGs. The weight of the TEGs system was 30 kg and its dimensions were (513x232x190) mm^3. Only one special unit generated a high output power of 5.26 W/cm^2 with a temperature gradient of 500 °C between the TEG surfaces. At an exhaust temperature of 550 °C and a mass flow rate of 480 g/s, the collection of exhaust waste energy from a diesel car engine aids in the experimental demonstration of a 1002.6 W TEG system.
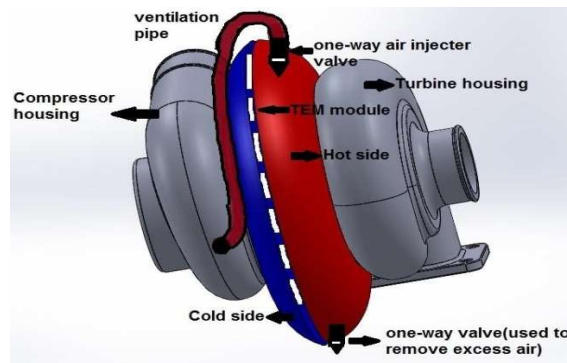
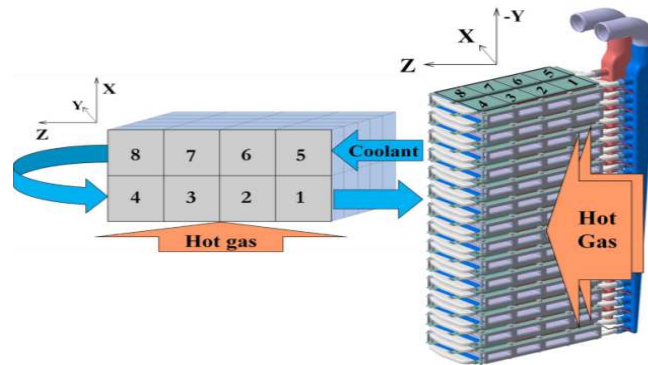**Fig. 64.** Proposed TEGs design, reprint with permission.

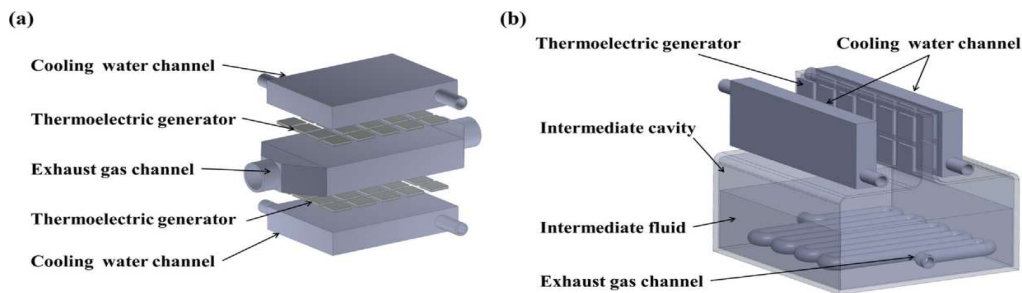**Fig. 65.** TEGs and HEX configuration, reprint with permission.

Fig. 66. (a) Known TEGs system, and (b) Intermediate liquid TEGs' system configurations, reprint with permission.

An ideal mechanism that involves the utilization of TEGSs (TE-MOD-22W7V-56) was proposed by Dhruv and Akash [115]. The objective was to install a collection of these highly efficient TEGs within the contact area of a turbocharger, specifically between the turbine housing and compressor housing, as shown in Fig. 64. This arrangement aims to exploit the thermal gradient present across the two housing units for energy generation. The installed TEGs can convert up to 6000 W of power. This conversion capacity allows for the potential elimination of the alternator in an automobile, or alternatively, the TEGs can be utilized to replenish batteries or provide tractive energy inside a hybrid system. The implementation of the proposed method has the potential to decrease the fuel consumption of a sedan automobile that was equipped with a 4-cylinder 2.2-L engine and 5-speed manual gearbox by approximately 2% to 5%.

Not enough research has been conducted to determine how the electrical equipment, converter efficiency, and layout of TEGs would work in a real world, full-scale vehicle. Hence, the TEG arrangement was depicted in Fig. 65. Arash [116] formulated a mathematical model to forecast the open-circuit voltage and internal resistance of a TEG at various temperature. A commercial TEG (TEP1-164-3.4) was selected as the most appropriate option for the anticipated temperature conditions. For the purpose at hand, eight synchronous interleaved step-down converters were designed and tested. These converters exhibited an impressive efficiency of 98% and were equipped with a perturbed and observed maximum power point tracker. The TEGs achieved a maximum electrical power recovery of 1 kW, which was subsequently communicated to the vehicle electrical system, thereby alleviating the workload of the internal combustion engine. The user's text does not provide any information to be rewritten.

Yulong et al. [117] established an intermediate-fluid TEG system that demonstrated high-power TEG conversion for vaporization and condensation of an intermediary medium (see Fig. 66. Using a computational formula for an intermediary fluid TEG system, the effects of cooling methods and the efficiency of condensed-boiling heat transfer by the intermediate fluid in the cavity were investigated on the TEG performance. It is also possible for the cooling fluid to be water- or air-cooled. Co-flow and counter-flow cooling techniques can be distinguished based on the relative flow paths of the cold fluid and the exhaust. In contrast to the conventional TEG system, the utilization of the same HEX area on the exhaust side resulted in a notable enhancement of 32.6% in the maximum energy output. Furthermore, the ideal TEG area experienced a substantial reduction of 73.8%. The maximal output power of the system was 1162 W/m^2, so it is 5.12 times greater than that of the typical TEG system.
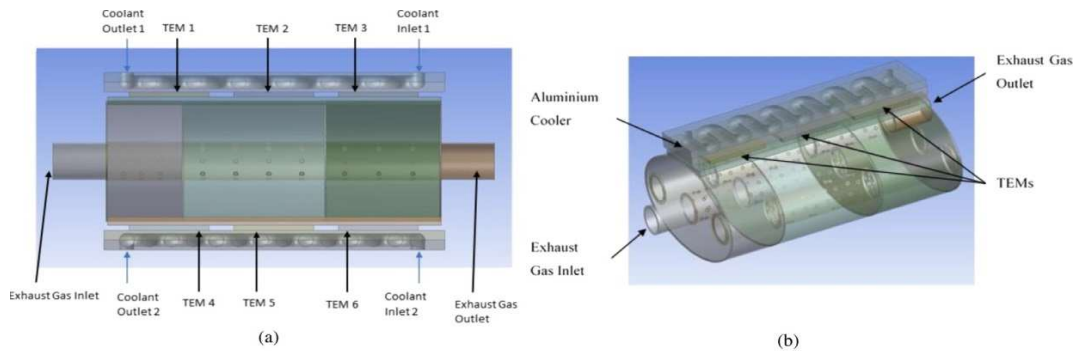
Fig. 67. (a) Cross section views of TEGs system, and (b) Isometric view of HEX and TEGs, reprint with permission.
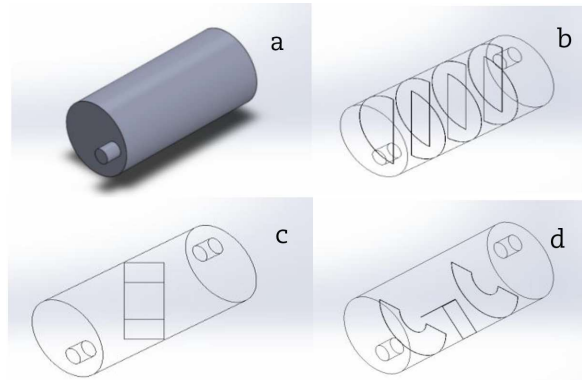

Fig. 68. Four types of mufflers; (a) Empty, (b) Serial plate, (c) Central box, and (d) Central curvature structures.
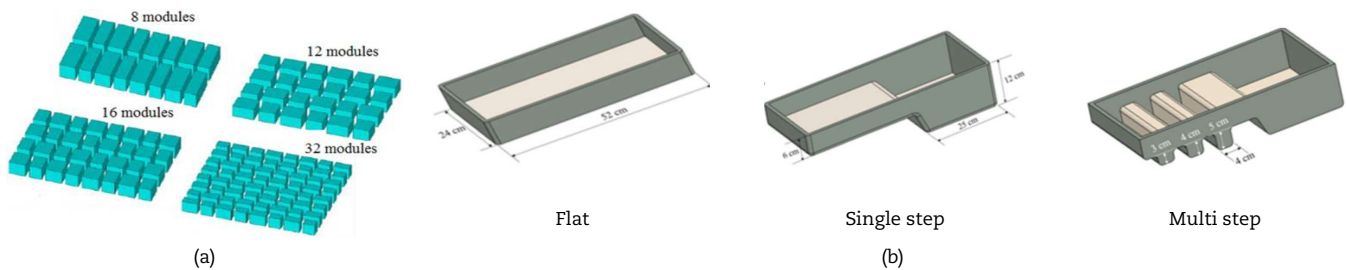

Fig. 69. (a) TE modules with different p/n number, (b) oil pan with different step partitions, reprint with permission.

The addition of additional devices reduces the overall efficiency of the engine by increasing the backpressure experienced by the exhaust system. Consequently, Hewawasam et al. [118] investigated the feasibility of incorporating a TEG into the muffler. The objective was to recover the waste heat from the engine exhaust system while ensuring that the muffler operation remained unaffected. Six (Bi$_2$Te$_3$) TEGs, each measuring (80x80x5) mm^3, were affixed to the heated muffler of a passenger car. The TEGs were evenly distributed, with three placed at the top and three at the bottom of the muffler, as seen in Fig. 67. The simulations conducted using ANSYS Fluent had an exhaust gas inlet temperature of 700 K, an inlet mass flow rate of 0.1 kg/s, a coolant inlet temperature of 280 K, and a coolant inlet mass flow rate of 0.16 kg/s. The study determined that there was a direct relationship between the exhaust mass flow rate and the increase in back pressure or pressure drop in the muffler.

Dhuha and Munther [119] executed a research investigation to investigate the thermal performance of various internal designs of mufflers. The study involved the design and analysis of four different muffler structures, namely: serial plate, central box, and central curvature, as depicted in Fig. 68. A test section consisting of a galvanized iron muffler 54 cm in length, 25 cm in width, and 0.1 cm in thickness. The dimensions of both the inlet and the outflow were 5.08 cm. The findings of this study indicated that the thermal efficiencies of the examined models, when compared to the empty cavity, were as follows: the serial plate structure exhibited a thermal efficiency of 56.11%, the center box structure showed a thermal efficiency of 52.73%, and a central curvature structure with a thermal efficiency of 29.61%. The serial plate construction exhibits the highest thermal performance compared to the other varieties.

In their study, Mutabe and Emrah [120] examined the viability of employing TEGs to recover the waste heat produced in I.C. engines, specifically focusing on their application in oil pans. The utilization of hot oil on the upper surface of the TEGs combined with air-cooling on the lower surface generates a significant temperature gradient, which facilities efficient TE conversion. The dimensions of an individual TEG volume, including the width, height, and thickness, was tuned in order to maximize the TE power output for the integrated oil pan shape. Furthermore, the design criteria for optimizing the total number of TE modules included not only the height and volume dimensions but also the surface area of the oil pan. Three different oil pan geometries, namely, flat, single-step, and multi-step oil pans, Fig. 69, were simulated. The findings from the simulations indicate that the multi-step oil pan shape can attain a maximum power density of 5.77 kW/m^2 when subjected to a temperature difference of 76 °C between the hot and cold sides.
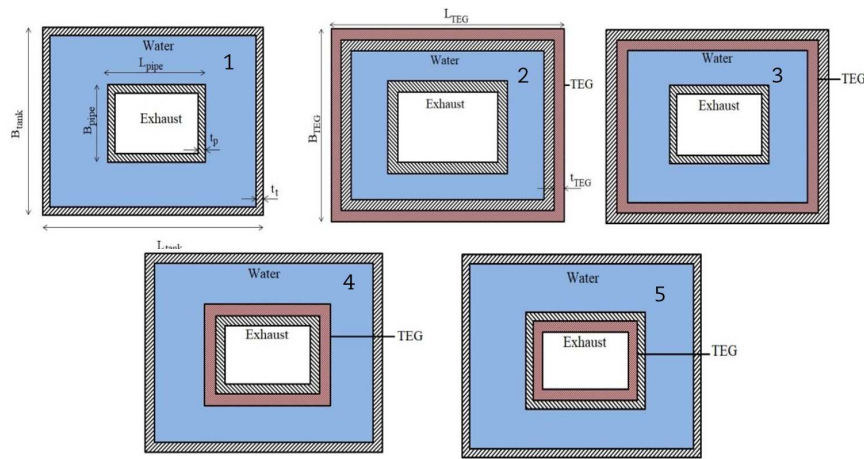
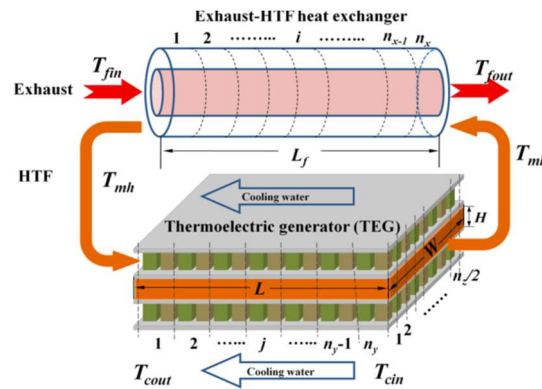**Fig. 70.** Sectional top view of five cases, reprint with permission.

Fig. 71. Schematic of the heat transfer TEG system, reprint with permission.

A home diesel electrical generator was used as the heat source. The system specifically investigated the use of a 20% blend of Mahua biodiesel. Dhruv and Rashmi [121] conducted a study in which they examined five different cases for the placement of TE generators in a rectangular cross-section exhaust manifold. These cases include (1) no TEGs, (2) TEGs positioned at the outer wall of the tank, (3) TEGs positioned at the inner wall of the tank, (4) TEGs positioned at the outer wall of the exhaust manifold, and (5) TEGs positioned at the inner wall of the exhaust manifold. The positioning of the TEGs for each case was illustrated in Fig. 70. This study examined a novel TEGs system that utilized pipe walls to transmit thermal energy from the diesel engine's exhaust to the water inside, where it eventually dissipated into the surrounding atmosphere. The comparison analysis demonstrated that in case five, the highest power output of 35 W was achieved when the TEGs were positioned along the inner wall of the rectangular exhaust design in close proximity to the heat source. The user's text does not contain any information to rewrite in an academic manner.

Yulong et al. [122] established the same intermediate-fluid TEGs system first proposed by Yulong et al. [117] to demonstrate high-power TE conversion during the vaporization and condensation of an intermediary medium. Using a computational formula for an intermediary fluid TEG system, the effects of cooling methods and the condensed-boiling heat transfer coefficient of an intermediate fluid in the cavity on TE performance were investigated. It is also possible for the cooling fluid to be water- or air-cooled. Co-flow and counter-flow cooling techniques can be distinguished based on the relative flow paths of the cold fluid and the exhaust. According to the findings, in the context of the water-cooling method, it was observed that the ideal area of the thermoelectric module decreased and the thermal behavior on both sides of the TEG was uniform. When the condensation heat transfer coefficient from the inside reached 5000 W/m^2.K, and water-cooled was considered, the generated power enhanced up to 11%.

Yulong et al. [123] recently introduced a novel TEG that incorporates a heat transfer fluid circulating system, as shown in Fig. 71. The system primarily comprises heat transfer fluids (HEX and TEG). Within the context of the heat transfer fluid HEX, it can be observed that as the exhaust interacts with the heat transfer fluid, there was a consequential decrease in the temperature of the exhaust. Simultaneously, the heat transfer fluid undergoes the absorption of heat, leading to an increase in its temperature. The high-temperature heat transfer fluid was introduced into the TEG and then into the cooling water, which served as the hot and cold sources for the TEGs, respectively. This arrangement created a temperature gradient across the two ends of the TEG, enabling the conversion of heat energy into electrical energy. The research revealed that the new generator exhibited a significant enhancement in the peak net output power, with a notable rise of 77.5% when compared to the conventional generator. Additionally, the new generator design allows for a substantial reduction in the number of modules required, with a reduction rate of 83.2%.

As demonstrated in Fig. 72, Yáñez, et al. [124] designed a system that translates the Bo-105 helicopter's (cover lifted) flight situations with the Rolls-Royce M250 turbo shaft engine, where waste energy recovery should occur to limit its influence on the engine. The exhaust gas flow temperature and exhaust duct wall temperature are the hot sources and the engine compartment air is the heat sink (cold source). The flat areas in front of the elbows and exterior of the exhaust ducts were the best places to install all TEGs. When using a non-invasive recovery technique like TEGs mounted on the wall, the baseline values of heat that can be collected from the exhaust duct walls vary from 23.6 to 31.2 kW.
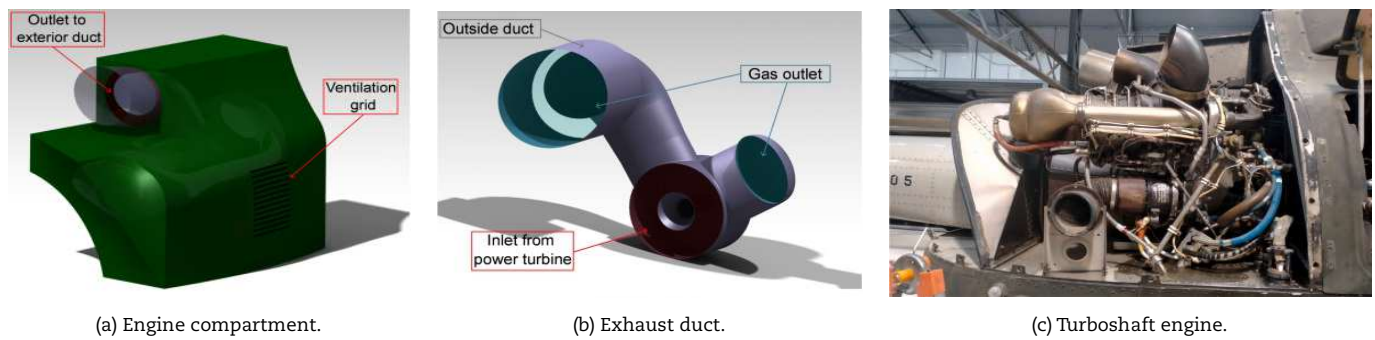
(a) Engine compartment.   (b) Exhaust duct.   (c) Turboshaft engine.

Fig. 72. (a) Engine compartment, heat sink, (b) Exhaust duct, heat source, and (c) Turboshaft engine, reprint with permission.
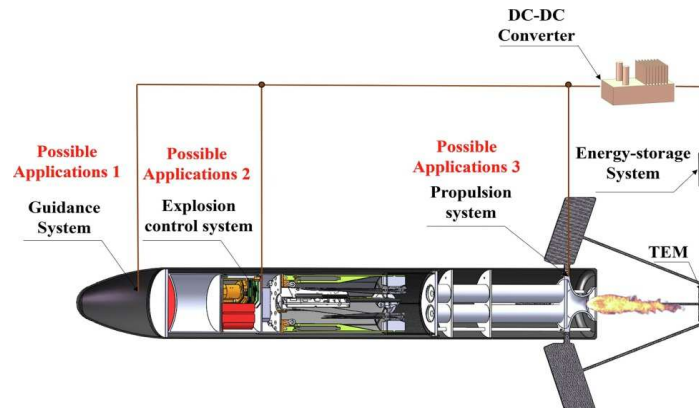

Fig. 73. Missile exhaust gases harvesting system, reprint with permission.

Fig. 74. TEGs/heat pipes system inside lab, reprint with permission.

Yue et al.'s study [125] focused on the heat waste produced by the tail flame of solid rocket motors, which are employed to increase rocket power, as shown in Fig. 73. The effects of the cooling water flow rates (0, 34, 68, and 136 L/min), jet distance (4, 6, 8, and 15 cm), and the number of PN junctions (127, 199, and 336) on the output energy were investigated numerically and experimentally. An increase in the PN junctions and the cooling water flow rate were the basis for the first increase and subsequent decrease in the output energy. Additionally, the jet distance increases the TEGs' output energy; nevertheless, if the jet distance were too short, the TEGs would not function as intended.

2.1.1.2. *Heat pipe embedded HEX*

The heat pipe is a device composed of a closed tube containing a small quantity of changing phase liquid. These devices facilitate efficient transmission of a substantial amount of heat from a heat source to a heat sink through phase-changing phenomena. The heat transfer process in this system involves the absorption of heat at the source by vaporization, which occurs in the evaporator part of the tube. Subsequently, the heat was let out at the heat sink by condensation, which takes place in the condenser part of the tube, resulting in the dissipation of heat.

The utilization of heat pipes provides more flexibility in design because it eliminates the constraint of restricting the placement of TEGs to the surface of exhaust pipes. In a study conducted by Orr et al. [126], a configuration consisting of eight TEGs with dimensions of (62x62x6) mm^3 was employed. These TEGs were placed between the exhaust pipe outlet of an automobile equipped with a 3.0 L V6 engine and the intake duct of the engine. The experimental setup and the design of the configuration are shown in Fig. 74. At an engine speed of 4000 rpm, the hot exhaust temperature reached 250 °C. The cool air duct input temperature was measured at 31 °C, while the exit temperature was recorded at 89 °C. Copper/water heat pipes with a diameter of 8 mm and thickness of 1 mm were employed. Two layers of 400 mesh wicks were employed with two heat pipes arranged in parallel on both the hot and cold sides of each TEG. Upon completion of all the testing procedures, it was determined that the system achieved a maximum power output of 38 W. This result was obtained by the utilization of eight TEGs.
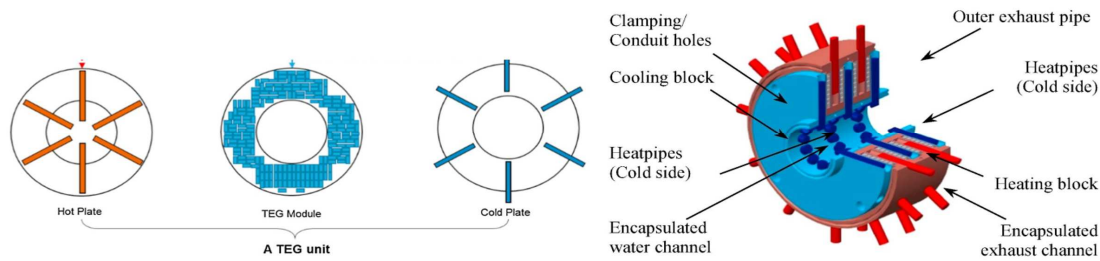
Fig. 75. A schematic of the 2D and 3D construction of TEGs and heat pipes system, reprint with permission.
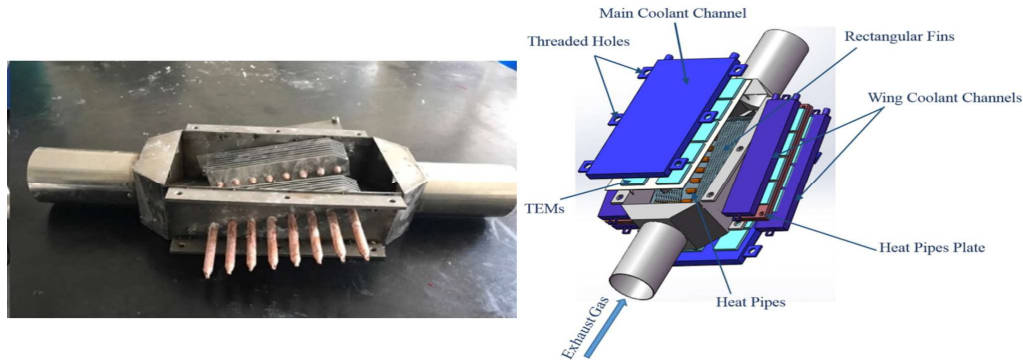

Fig. 76. A schematic and experimental photo of TEGs system utilizing cooper heat pipe, reprint with permission.
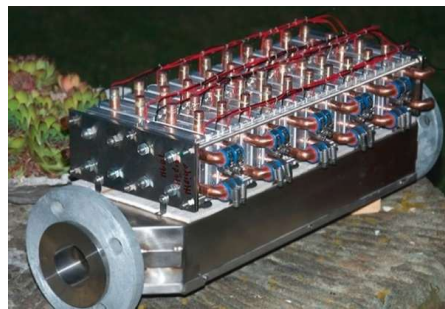

Fig. 77. Actual picture of TEGs system utilizing cooper heat pipe, reprint with permission.

Bo et al. [127] introduced a novel approach to improve the heat flow across the surface of TEG modules by including copper-water heat pipes in a radial configuration within the exhaust streams. This design featured concentric shapes to optimize the adaptation of TEG modules. The TEG system comprises a sequence of recurring units strategically positioned along the exhaust stream in order to form a functional exhaust pipe. The repeat unit consisted of four radial TEGs, three hot plates, and two cooling plates, each containing 12 heat pipes. These components are illustrated in blue and red, respectively, in Fig. 75. Furthermore, the temperature of the exhaust source was established at 823 K, while the coolant temperature was set at 323 K. It was observed that the TE material based on Bi_2Te_3 exhibits the maximum power output per unit, reaching a value of 29.8 W.

Qimin et al. [128] suggested a research study in which an experimental design was developed to determine the optimal insertion depth of copper heat pipes and the ideal angle between the heat pipe row and the path of gas flow. The study focused on the application of this prototype for car exhaust waste heat recovery, utilizing 36 TEGs, named (HP-TEG) with (40x40x4) mm^3. The dimensions of the exhaust flow duct were (240x120x60) mm^3, with a thickness of 1 mm. Four rectangular wing coolant channels (190x50x10) mm^3 were utilized, which were constructed using an aluminum alloy, as depicted in Fig. 76. Heat pipes with an external diameter of 8 mm and a length of 120 mm were equipped with a mesh wick. An aluminum alloy was chosen as the material for the rectangular fins, which were (150x30x1) mm^3, with the objective of improving the heat transmission efficiency. Two sets of heat pipes with rectangular fins were affixed to aluminum blocks. The highest voltage of the TEGs was recorded as 81.09 V. The power output and pressure drop were recorded at 13.08 W and 1657 Pa, respectively.

The inclusion of the concept of heat pipes with HEXs and TEGs was introduced by Pachecoa et al. [129]. Corrugated tubes incorporated in a matrix of cast aluminum make up the innovative exhaust HEX design, while variable conductance tubes transfer extra heat through the length of the tube. 64 TEGs were arranged over the two hot large contact areas of the HEX. Two driving cycles were considered in the simulation: driving and standard. Two types of TEGS were utilized (GM250-49-45-25) with 5.3 mm thick and (GM250-127-28-10) with a thickness of 4 mm, installed along the exhaust pipe of a vehicle with 1.6 L 118 hp gasoline engine. A 150 L/hr was the coolant water flow rate in each cooler with 27.5 W total power consumption circuits. By utilizing the TEG (GM250-49-45-25), up to 572 W and 1538 W of average and highest electrical powers over the driving cycle, and a very promising savings of 5.4% and 4.2% in fuel use through driving and standard cycles, respectively.

Electricity production and its effects on energy transfer, Seebeck voltage, and electrical currents have been taken into consideration using Olle's et al. [130] multi-physics simulation utilizing computational fluid dynamics (CFD). The heat pipes were fabricated using copper, which is known for its superior thermal conductivity (TC) compared with other metallic materials. Forty commercial (TEPH1-12680-0.15) were installed in the TEGs system and distributed into eight groups connected in parallel, as shown in Fig. 77. The tests were conducted within the controlled environment of the engine workbench labs, utilizing the exhaust gas emitted by a single-cylinder, 2.1-liter diesel-powered engine.
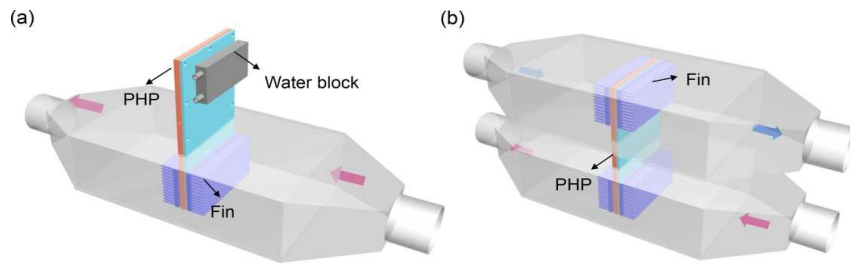
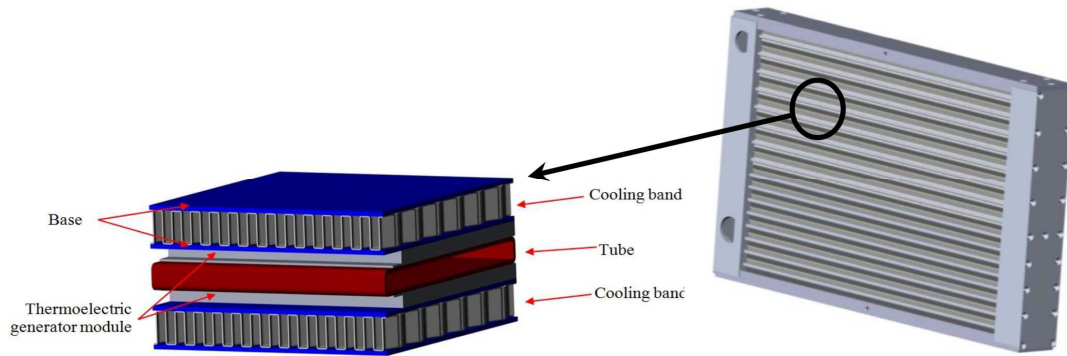**Fig. 78.** TEGs system with (a) Air-to-water mode, and (b) air-to-air mode, reprint with permission.

Fig. 79. 3D thermo cooling radiator and physical domain of TEGs system, reprint with permission.

Xu, et al. [131] investigated the performances of flat-plates with TEGs that were 3D printed and CNC machined under two recycling scenarios. Aluminum slotted fins were also mounted in the air-to-water mode on both faces of the flat-plate PHP evaporation portion (Fig. a 78), also known as mode 1. The cold surfaces of the TEGs were intimately linked to a water block, and the hot surfaces of the TEGs were placed on the condensation section of the flat-plate PHP. In air-to-air mode (Fig. b 78), also known as mode 2, two flat-plate PHPs had aluminum slotted fins fixed in their condensation and evaporation sections. The TEGs were positioned between PHP's evaporation and condensation sections of the PHP. The hot air duct is (250x150x75) mm^3 in total, with 52 mm for each air intake and output diameter. Two TEG1-199–1.4–0.5, whose external dimensions measured (40x40x3) mm^3, were chosen to create a coupling system with a flat-plate PHP for waste heat recovery from heat-to-power.

Recently, the same previous HEX built in copper heat pipes by Pachecoa et al. [129], was considered again by Carvalho et al. [132], but investigated exhaust HEX ideas that employ phase change to enable this thermal optimization under extremely varied thermal loads. Experimentally, the system question comprised of the TEGs system, with the gas flow inlet connected to the tailpipe of a 1.6 L engine TU5JP4, which was a light-duty atmospheric MPI (multi-point fuel injection) spark ignition engine. Sixteen (Hi-Z 14HV) TEGs that were specifically designed for recycling waste heat were employed. Eight attachments were present on both the lower and upper surfaces of the HEX. The employed technique allows for the optimization of converting energy without thermal dilution under small thermal loads or overheating risk under significant thermal loads. The excess heat was dispersed along the HEX via variable-conductivity heat pipes. Experimental verification of the concept's unusual heat distribution and temperature management properties indicated average fuel reductions of 4%, up to 12%, on the highway cycle.

2.1.2. Second location TEGs installation (engine coolant cycle)

A very interesting area of research was the conversion of thermal energy that was transported from the I.C. engine to the coolant into electrical power.

A low-temperature TEG using the engine's water coolant in passenger automobiles with a 2-litre engine was proposed and created by Shisho et al. [133]. According to the experimental findings, the highest calculated power delivery of the proposed TEG was 75 W and the estimated efficiency was 2.1%. At 80 km/h, the overall efficiency of TEG from the waste heat of engine coolant was 0.3%.

Without requiring extra water pumps or other requirements for the existing water cooling system, the suggested TEG can also replace traditional radiators. A TE radiator was created by Nikolay et al. [134]. For I.C. engine cooling systems, which take the engine cooling system as a whole, patented designs of TE radiators exist. The authors identified the features and components of a TE I.C. engine cooling system and created an idea based on the current designs of TE radiators for cooling systems. The created TE cooling system will increase a heat engine's energy efficiency, reduced fuel using and produce electricity within the car.

Donkyu et al. [135] proposed the first cross-layer, system-level method to increase TEG array efficiency by adding online reconfiguration of TEGs. Although waste heat energy collection may interfere with the integrity of combustion and emission control, the suggested method for capturing automobile radiator heat has no impact on the performance of the vehicle. Despite the dynamic changes in the coolant flow rate and temperature, a revolutionary TEG reconfiguration was introduced and the TEG array output was optimized, which caused a significant variance in the coolant temperature distribution throughout the radiator. Under dynamically changing vehicle-operating conditions, the suggested technique enables all TEGs to operate at or near their optimum power points. According to experimental findings, a fixed array structure, which was the norm, can be improved up to 34%.

Nikolay et al. [136] constructed a three-dimensional model of an aluminum TE cooling radiator designed for internal combustion engines, as shown in Fig. 79. This was followed by manufacturing a physical prototype of the TE radiator. The parameters of the TE cooling radiator core are as follows: height measures 436.8 mm, width was 624 mm, and tube width 60 mm. Consequently, based on the specifications of the designed TE radiator core, 168 TEG modules, specifically (H-288-14-06-L2) (52x55x3.3) mm^3 in size, were chosen. Based on the findings of first experiments, the TE radiator demonstrated an electric power output of 815.4 W, while the aerodynamic resistance of the radiator was measured to be 2374.8 Pa.
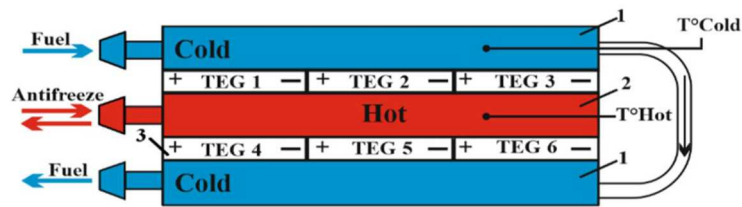
Fig. 80. Schematic diagram of the developed TEG system, reprint with permission.
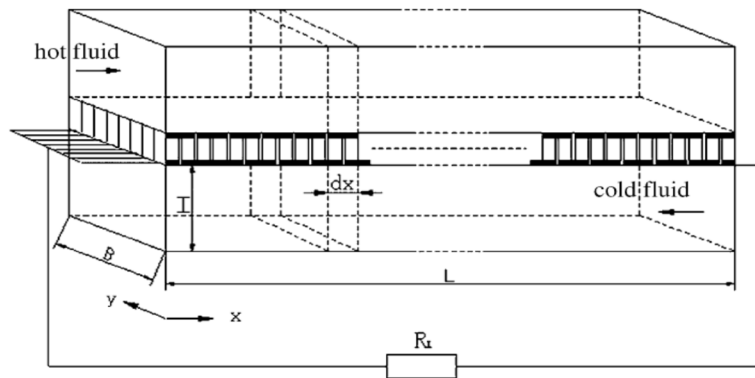

Fig. 81. Schematic layout of the model, reprint with permission.

After one year, Jaemin et al. [137] introduced the same work as Donkyu et al. [135], however, given that HEXs typically have distinct intake and outlet temperature values, the suggested method can be used to recover heat energy that has been lost in any type of TEG array. In addition, a fully developed design and implementation showcase of a reconfigurable TEG module building block was presented in this work. According to experimental findings, the proposed approach can be improved performance up to 34% when compared to the more conventional fixed array construction.

Energy from heat in automobile radiators has been used to decrease the load placed on the engine. In this experiment, Awira et al. [138] used four (TEC1-12706) TEG components on top of the TEG fixture and connected them in series with heat sinks that faced the flow of fluid. On the upper pipe radiator of an LDW1404 Lombardini diesel engine, a TEG fixture will be placed. This experiment results in an optimal voltage of 2.05 volts, a current strength of 68.4 mA, and a power of 140.22 mA, with a temperature difference of 17.8 °C between the heat source and the heat sink.

By putting the TEGs behind the engine cooling radiator to the right at the bottom, Abderezzak and Randi [139] have been tested the possibility of producing energy from recovering automotive radiator waste heat. First, the performance of a TEG in various situations was predicted using a mathematical model. But after applying direct contact to the radiator of a Renault Kangoo 1.5 DCI passenger car in a single TEG at a high radiator temperature (92-95 °C), the direct potential was then investigated. Additionally, it was discovered that the maximum power obtained was P = 1.8 W, with an efficiency of 3.85%.

Kaloyan and Anatoliy [140] developed a TE waste heat generator with six Peltier elements, specifically (TEC1–12710). The purpose of this device is to be integrated into an automobile. The generator elements were subjected to the required force as they were forced between three aluminum radiators using clamps. The dimensions of each radiator were (120x40x10) mm³. The two terminal radiators were interconnected by a copper tube, which facilitated the circulation of surplus chilled gasoline to return to the tank. This process was regulated using a pressure regulator to ensure that the temperature remained below 50 °C, as depicted in Fig. 80. The middle radiator was linked to the automobile's cooling system, which facilitated the circulation of hot antifreeze running at a maximum temperature of approximately 90 °C. The experiment was performed under actual road conditions, with the generator's maximum power output observed to be 12 W when the temperature difference (ΔT) exceeded 40°C.

2.2. Cooler (heat sink) review

In the context of HEX, the term "co-flow" refers to a situation in which a cold fluid and hot fluid flow in the same direction. Conversely, "counter-flow," describes the scenario where the cold and hot fluids flow in opposite directions.

The study conducted by Jianlin and Hua [141] introduced a numerical model that aimed to forecast the efficiency of a TEG utilizing a parallel-plate HEX. Numerical simulations were conducted to illustrate the TEG of both the parallel flow and counter-flow configurations. In the parallel flow configuration, both fluids flow in the same direction, whereas in the counter flow configuration, they flow in opposite directions. This is illustrated in Fig. 81. The flat TE modules were positioned between the hot and cold fluids and electrically interconnected in a series configuration. However, they were linked in parallel in directions orthogonal to the fluid flow. The simulation showed that the temperature of the fluids in the TEG changed in a linear way, while the temperature of fluids in a typical parallel-plate HEX changed in a logarithmic way.

Rezania et al. [142] studied the relationship between the power produced and the coolant-pumped power in the TEG during the cooling process. This study examined five different temperature variations between the hot and cold sides of a TEG. Furthermore, this study investigated the optimal coolant flow rates that lead to the highest net power output inside the system. The micro-channel heat sink under consideration was designed with twenty micro-channels, each with a rectangular cross-section. This configuration allows the creation of a lightweight and compact energy system, as depicted in Fig. 82. The heat sink features inlet and output plenums that were situated on the top cover plate. The flow of coolant traversed a U-shaped pathway within the heat sink. Consequently, the heat sink was provided and dissipates heat in a vertical orientation. The findings indicated that there was a positive correlation between the average temperature difference over the TEG and the optimal flow rate, as the latter tends to grow with the former.
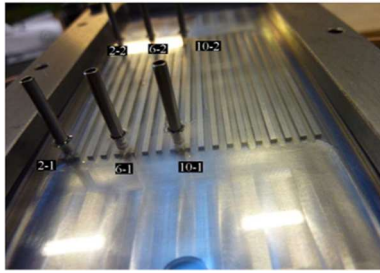
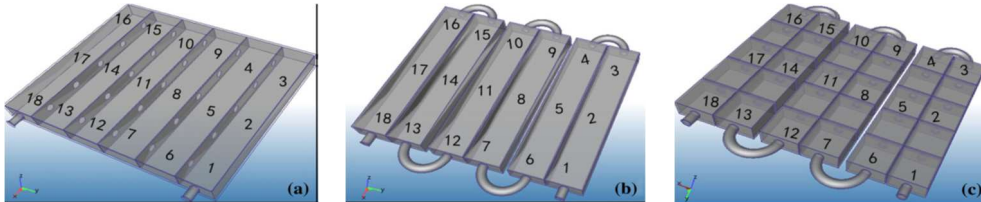**Fig. 82.** The geometrical configuration of the system, reprint with permission.

Fig. 83. TECs (a) plate (b) Stripe (c) diamond shaped in three dimensions, reprint with permission.
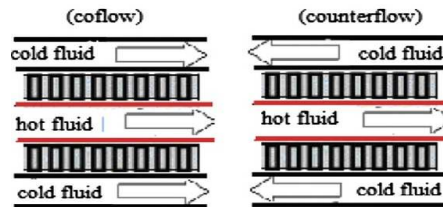

Fig. 84. TECs conceptual structure co-flow/counter-flow, reprint with permission.

Fig. 85. TECs (a) finned heat sink, and (b) heat pipe dissipater, reprint with permission.

The compatibility between the TEG cooling device and engine cooling system, focusing on the heat transfer capabilities of the TEG, was examined by Deng et al. [143]. The TEG cooling unit primarily comprised a series of 12 bar-shaped water tanks that were positioned sequentially to facilitate the flow of water. The present study involved the simulation of a novel engine-cooling system that incorporated a TEG cooling unit. The simulations were conducted under two different conditions: high power and high vehicle speed, as well as high power and low vehicle speed. The objective of these simulations is to determine the temperatures and flow rates of the essential inlets and outlets within the system. The study determined that at high speeds, the integrated cooling temperature exceeded the primary engine cooling system temperature by 5 °C, however, the coolant temperature of the TEG cooling unit remained comparatively low. However, at low speeds, the cooling temperature was increased by 20 °C. This might potentially result in a reduction of 15% in the generating capacity of the TEGs.

There are several advantages to integrating a TE cooler into the cooling channels for automotive applications, including the elimination of unnecessary mechanical parts and the preservation of space and energy. Chuqi et al. [144] constructed three alternative TE cooler designs, namely plate, stripe, and diamond shapes, based on the performance characteristics of the engine and TE units Fig. 83 and simulated various coolers and the performance of the circulating coolant. These results show that compared to TEG outputs with stripe- or plate-shaped coolers, TEG outputs with diamond-shaped coolers are able to convert more heat into electric power. As engine speed rises from 2700 to 3000 rpm, the power difference between the coolers with the diamond and stripe shapes widens, with the exception of plate configuration.

Wei et al. [145] proposed four methods to cool the TEG heat capture system, specifically the water/air co-flow and water/air counter-flow methods. These methods were suggested to demonstrate a mathematical model that examines the impact of the cooling direction and cooler type on the output power, as depicted in Fig. 84. It has been determined that the utilization of water cooling technology yields greater power production and efficiency than air cooling while considering the same module area. The counter-flow configuration often yielded a somewhat greater maximum power output, while requiring a significantly bigger module area in comparison to the co-flow approach.

Aranguren et al. [146] experimentally constructed a TEG prototype that generates 21.56 W of net electricity. On the heated side of the TEGs, some of the heat was converted into electricity. The remainder of the heat is transferred through the TEGs' cold side to the cold sink. Each of the four groups that make up the TEG has 12 TEGs (TG12-8-01L) with a total of 48 TEGs, and is equipped with an aluminum cold-side heat sink with a finned dissipater, or heat pipe, as shown in Fig. 85. The stainless steel rounded chimney pipe that carried gases with 1000 °C transferred to a rectangular flat duct with (0.25x0.25) m^2 cross sectional area. The heat pipes beat finned dissipaters in terms of heat dissipation; 43% greater net power was achieved if it was compared with the finned dissipater.
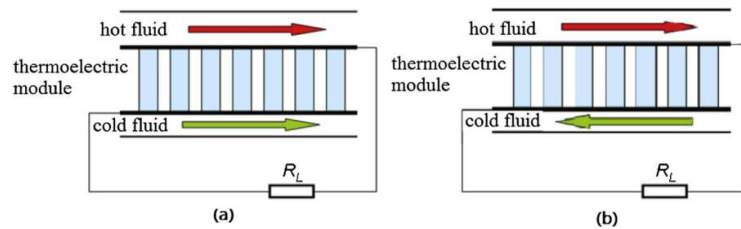
Fig. 86. TECs (a) co-flow (b) counter-flow arrangements, reprint with permission.
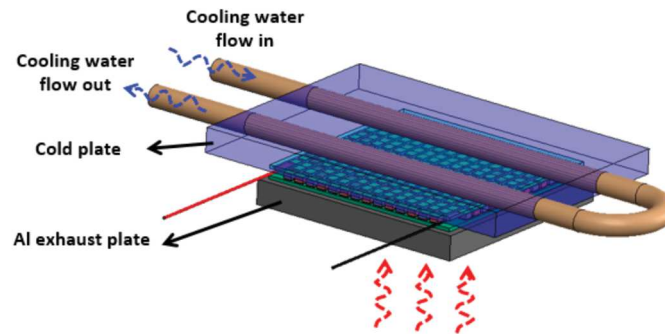

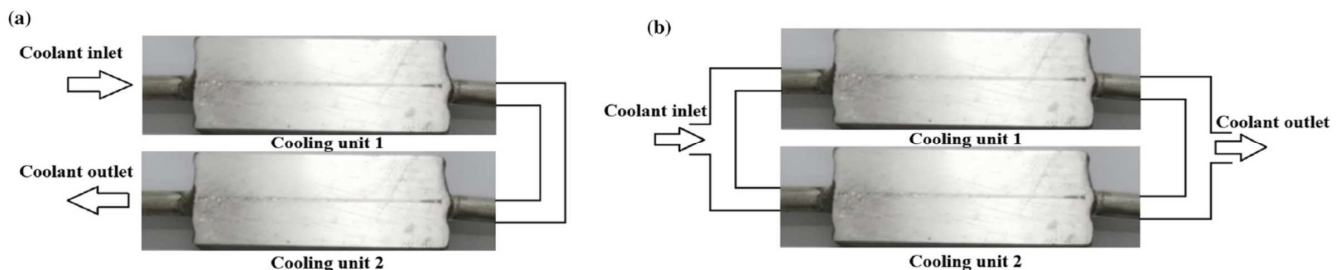**Fig. 87.** TE cooler plate arrangements, reprint with permission.

Fig. 88. Cooling units in series connection (a) and parallel connection (b), reprint with permission.

Drawing from the same underlying premise of co/counter flow idea, Wei et al. [147] again investigated both layouts of HEXs, as explained in Fig. 86. The temperature exhibited fluctuations within the range of 250-550 °C, whilst the mass flow rate experienced fluctuations within the range of 5-50 g/s. Hence, the impact of these variations in exhaust gas characteristics on the ideal TE performance was examined with the aim of maximizing the total power production using the FORTRAN programming language. The results indicated that the ideal design areas for the co-flow and counter-flow were 0.22 m^2 and 0.3 m^2, respectively. The counter-flow configuration was suggested because to its ability to minimize the departure from the maximum power output compared to a co-flow arrangement.

Qiang et al. [148] optimized the TEG cold wall temperature and the cooler obstruction distribution on its interior faces to improve the cooling parts' performance for car TEGs. Based on experimental data and simulation studies, a response surface model of different interior constructions was developed to investigate the heat transfer and pressure loss properties of the flowing fluid in the cooling part. For the fin distributions, five distinct parameters were considered: height, length, thickness, space, and separation from the boundaries. An experimental study design utilizing the central combined design approach was necessary to assess the impact of fin distributions on the temperature distribution and pressure loss in the cooling components. It demonstrated that the variations in temperature across the three experimental designs. It showed that the temperature disparities in the three designs of experiment strategies were all greater for fins oriented transversely than for fins positioned longitudinally.

There has been significant scholarly attention towards investigating the prospect of utilizing the waste heat extracted by TEG systems for marine applications. This interest arises from the substantial volume of engine exhaust, various scenarios where prolonged high temperatures are encountered, and the significant cooling capacity offered by seawater. Liping and Alessandro [149] conducted experimental and numerical modeling optimizations to investigate the cooling technique for a TE module balancing device. The open-circuit voltage of a device with a typical cooling plate design and tubed water-cooling plate is shown in Fig. 87 was determined using TE simulations. The newly introduced cold plate features an integrated flat groove, which enhances the cooling efficiency compared with the traditional tubed plate design. The enhanced cooling system demonstrates a 2.7% increase in maximum output power, rising from 7.435 to 7.63 W, as compared to conventional tubes operating at a temperature of 225 °C. The marginal improvement in performance at the module level has the potential to significantly influence the entire output of the system.

The majority of the collaboration in [145] resurfaced later to investigate the effects on the automotive exhaust TEG of coolant flow rate, coolant flow sense, and cooling unit configuration. Chuqi et al. [150] constructed a TEG model, "strip-shaped" water cooler, and a matching test bench, arranged in Fig. 88 with series and parallel connections. Inconsistent surface temperature of the heat source indicates that the coolant flow direction affects the TEG's output power. Because the cooling unit's temperature uniformity can be improved by adjusting the coolant's volumetric flow rate, multiple modules connected in series or parallel can have their output power increased.
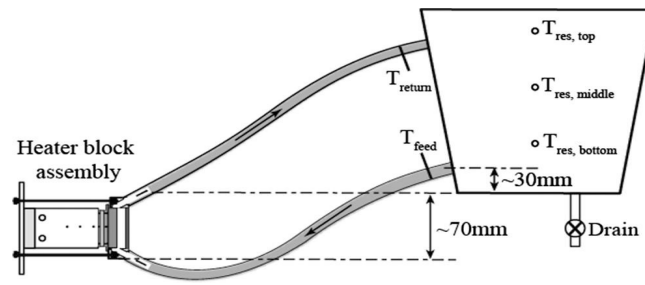
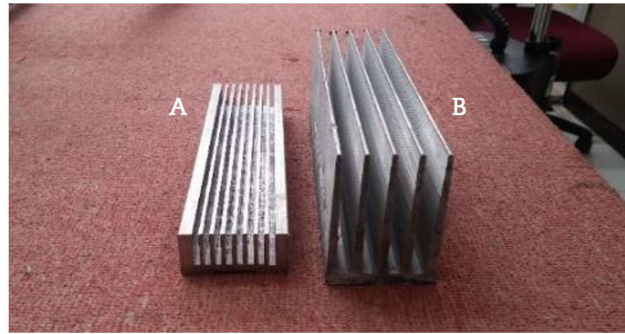**Fig. 89.** Schematic of experimental setup, reprint with permission.

Fig. 90. The profiles A and B of rectangular geometry heat sinks, reprint with permission.
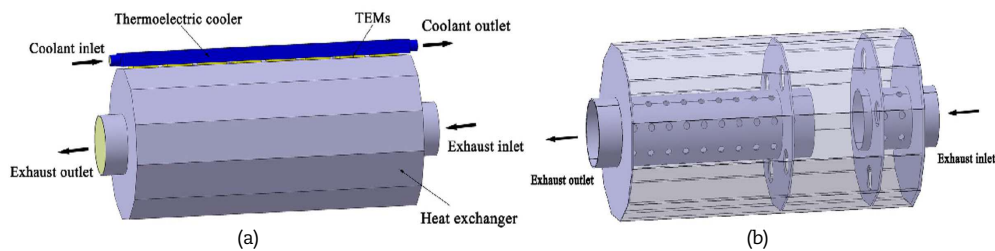

Fig. 91. (a) 3D model of TEC, (b) HEX internal structure, reprint with permission.

Both theoretical and experimental calculations indicate that when the cooling units are connected in series rather than in parallel, the cooling system with two cooling parts has a higher maximum output power. The study conducted by Deasy et al. [151] investigated the design of a passive cooling system for a single TEG using computational simulations and practical testing. This system utilizes the natural buoyant circulation of water between a controlled heat source and an open water reservoir. As thermal energy is transferred to the water, density variations arise, resulting in the upward movement of the warmer fluid towards the upper region of the reservoir. The circulation loop shown in Fig. 89 demonstrates the movement of cold fluid from the lower portion of the reservoir to the heated zone, thereby maintaining mass conservation and facilitating the transfer of heat between the heat source and the reservoir. This paper presents the implementation of a simulation-driven design methodology for the development of a structure for a single TEG. It also includes the experimental validation of the simulation outcomes and the assessment of the TEG's performance characteristics when integrated with the newly designed cooling system.

The effective cooling of the heat discharge surfaces plays a crucial role in optimizing the performance of TEGs. Rectangular geometry fins are a type of structural element that is characterized by its rectangular shape and is commonly used in various engineering applications. Akif and Haluk [152] used two different sizes and different aluminum alloys of heat sinks (A and B profiles), Fig. 90, to cool a TEG (TG-12-8-01L) with (44x40x3.6) mm^3 in the waste heat recapture system. Under a constant boundary condition of (T_h = 250 °C, ΔT = 20 °C), while different electronic load tester of 5 Ω and 55 Ω, the "B" profile achieved a maximum voltage of 12.5 V, current of 0.46 A and the "A" profile achieved a maximum voltage of 10.27 V, current of 8.92 A, respectively.

A methodology that integrates numerical modeling and experimental design to investigate the optimal coolant flow rate to minimize pump energy use and maximize output power was employed by Xing et al. [153]. The energy use of the TE cooler system can be determined by the following equation:

$$p = \frac{Qgh}{3.6\eta} = \frac{QP}{3.6\eta\rho} \tag{1}$$

The topic of interest pertains to the consumption of power by W_P, where the coolant flow rate (Q), gravity acceleration (g), hydraulic head (h), efficiency (η, typically ranging from 0.75 to 0.85), pressure differential (P), and coolant density (ρ). Eight TEGs were uniformly distributed over the outside surface of the dodecagon-shaped HEX, which was covered by a strip-shaped TEC. The dimensions of the TE coolers were (584x60x24) mm^3. The HEX, which functions as a muffler, consists of many perforated pipes and perforated plates, as depicted in Fig. 91. The pipes were equipped with uniformly distributed holes, each with a diameter of 10 mm. Similarly, the plates had four similarly distributed holes, each with a diameter of 40 mm. Ultimately, the module's highest net output power was disclosed, and a proposed correlation between the coolant flow rate and the average temperature of the TEGs' hot end was presented. This correlation can potentially serve as a theoretical foundation for managing the cooling water flow rate in the TEG system.
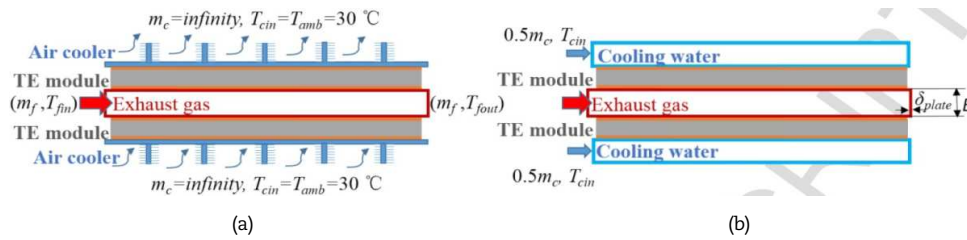
Fig. 92. Configuration of TEGs system with (a) air cooler, (b) water cooler, reprint with permission.
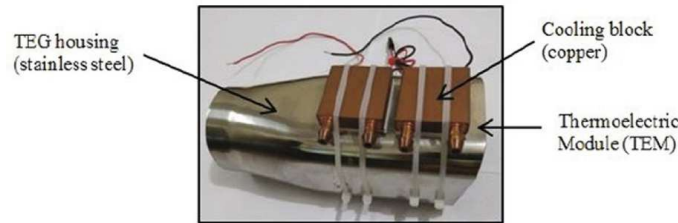

Fig. 93. The physical domain of TEGs system, reprint with permission.

There are two prevalent categories of cooling systems utilized in exhaust TEG systems. One configuration used ambient air as the cold fluid for the TEG, whereas the other configuration employs engine-cooling water. The authors Wei et al. [154] conducted a numerical simulation to depict the standard configuration of sandwich plate-type single TEG systems. A schematic representation of these systems, including an air cooler and a water cooler, is illustrated in Fig. 92. In addition, this study encompasses various work conditions encompassing a range of exhaust parameters ($\dot{m}_f$=10-50 g/s and T_{fin}= 300-600 °C), as well as the heat transfer processes of the coolers. The findings suggested that regardless of the specific work conditions, the best height remained consistent. Specifically, the optimum overall HEX height (B) was determined to be 7.0 mm and 4.0 mm for the air-cooling and water-cooling methods, respectively.

In order to enhance the operational effectiveness of TEGs, researchers Mohd et al. [155] used a Nano-fluid, especially titanium oxide (TiO_2), as a forced convection-cooling medium to facilitate heat dissipation from the cold sides of the TEGs. The investigation involved examining the performance of the TEG by manipulating the speed of the car engine within the range of 700 - 1500 rpm. The experimental setup involved the placement of two TEGs measuring (40x40) mm^2. These TEGs were positioned between a stainless steel connector and copper cooling blocks, as depicted in Fig. 93. The introduction of a titanium oxide (TiO_2) Nano fluid resulted in a maximum peak current of 14.43 mA and a maximum power generation of 27.9 mW. This was a significant enhancement of more than 4% compared to water-cooling at 1500 rpm.

Poornima and Vivekanandan [156] conducted a comparison of an air-cooled and water-cooled TEG systems. In their study, a Suzuki Max 100R two-stroke air-cooled petrol engine was employed as the heat source for experimental evaluation. The experimental setup utilized an (SP1848-27145) TEG with dimensions of (40x40) mm^2. The device exhibited an operational temperature span of 0 - 120 °C and a voltage of 4.8 volts when no electrical connection was connected. The phenomenon of the temperature difference separating the hot and cool sides of the TEG decreasing was noted when water was employed as a coolant. This decrease in temperature difference leads to a significant reduction in the power output of the TEG in comparison to an air-cooled system.

3. Summary

During the aforementioned exploratory review, it was observed that the HEX design exhibits a greater degree of effectiveness in generating output power than the TEG. Consequently, the majority of researchers directed their investigations towards the proposition of diverse cross-sectional designs and geometric configurations, as well as fins of varying shapes, sizes, and angles, to be positioned within the core of the HEX. Various metals were selected for the production of HEXs in order to accommodate the specific boundary requirements, the weight of the TEGs system, and the installation site. Subsequently, an investigation was conducted to analyze the impact of the internal geometry on the distribution of temperature uniformity, and its influence on the collected power was examined. The power obtained from the system was directly proportional to the uniformity of the temperature distribution, and conversely, the power decreases as the distribution becomes less uniform. Additionally, the losses in the pressure drop were taken into consideration. The heat sources under consideration were hot exhaust gases emitted by I.C. engines, a heat gun, and a combustor. In numerous studies, exhaust gases have commonly been regarded as hot air, as the outcomes did not exhibit any substantial disparities when engine exhausts were considered as such.

Furthermore, the impact of TEC has often been overlooked in numerous studies because the improvement in design does not result in an inlet-to-exit temperature difference above 6°C. Hence, it was postulated that the temperature of the TEGs' cold surface would remain constant at 90°C, corresponding to the engine water cooling system temperature. Alternatively, a boundary condition was enforced, wherein heat transfer occurred through convection with a coefficient that did not exceed 60 W/m^2.K.

Multiple TEGs sourced from various manufacturers and firms were employed. The selection of these TEGs was based on the temperature threshold achievable by the HEX, considering the prevailing conditions at the intake and the design specifications of the HEX. The terminals of TEGs can be interconnected either in series or in parallel. Subsequently, the positive and negative terminals were linked to a power analyzer, electronic load tester, or potentiometer. This connection facilitates the assessment of the maximum total power achievable by connecting the external variable resistance. In certain instances, the regulation of electricity produced by the TEGs system is achieved using a DC-to-DC inverter circuit. The energy produced was allocated towards various purposes within the automobile system, such as powering electronic circuits, recharging batteries, operating a compact air conditioning system, and occasionally replacing or eliminating the alternator. This result in fuel savings by reducing the overall weight of the automobile.

4. Principal Goals of the Project

The primary goal of this study was to use the thermal energy generated from engine exhaust because it transports the majority of the energy emitted as heat (up to 40 %) and uses TEG technology transforms it into useful electrical energy. This lowers chemical and thermal emissions while also using less fuel.

5. Name the Primary Limitations

1. The exhaust gases temperature that enters HEX must not be higher than the temperature that the TEG's manufacturer has set for the hot surface that comes into contact with HEX.
2. To prevent a large drop in pressure, a gap that matches the quantity of exhaust gases passing through the HEX core must be left. If care was not taken in the manufacturing, this drop in pressure may cause the TEGs system to collapse and the application to fail.

6. Conclusions and Recommendations

In light of the relatively low CHTC exhibited by exhaust gases produced through the combustion of fossil fuels in I.C. engines, scholars have endeavored to enhance this coefficient by augmenting the contact area between the exhaust and HEX surfaces or by inducing turbulence in the flow. These measures impede the progression of the flow into the HEX, thereby allowing ample time for effective heat transfer to occur. The aforementioned objective may be attained through the implementation of fins or various geometric configurations protruding from the inside surfaces of HEXs. Therefore, through the above review, the following were concluded:

1. A body of research has observed divergent findings regarding the comparative efficacy of water-based cooling and air-based cooling. Variations in the density or viscosity cannot be the sole cause of this phenomenon, nor can there be significant differences between the characteristics of water and air. The cause can be ascribed to the cooler's design and the exterior or interior heat transfer coefficient, respectively.

2. The metals used in the manufacture of HEXs and coolers have a significant impact on the uniformity of the thermal distribution of the HEX surfaces, and thus, greatly affect the amount of energy produced. This is because of the thermal conductivity coefficient of each metal. Therefore, industries must be geared towards metals that have a large conduction coefficient.

3. The weight of the TEGs system must be taken into account, which will increase the weight of the automobile, and if it exceeds the specified limit, it will result in an increase in fuel consumption instead of saving it. It was possible to develop a catalytic converter or muffler to replace the heat exchanger, as it was manufactured in a form that enabled easy installation of TEGs on its outer surface. Through this idea, part of the additional weight from installing the system will be eliminated.

4. The porous media that was placed inside the HEX was considered one of the best barriers that could be used because it provided the best uniform distribution of temperatures on the surfaces of the HEX, even better than the best type of other internal geometric shapes. However, because of the narrow passages and the bifurcation of the exhaust gas passage paths, which, over time and due to deposits, will close; therefore, from this point of view, this application was not recommended for passing exhaust gases from I.C. engines, but it was possible to benefit from this application in other areas where the heat sources were clean. There will also be a high-pressure drop resulting from this application, which increases the backpressure on the engine and thus increases fuel consumption instead of saving it.

5. In the case of the water coolers, it was observed that the difference between the temperature of the outlet and the inlet water did not exceed 6°C, regardless of the different external or internal designs. However, in HEXs with various internal or external designs, the difference between the inlet and outlet temperatures ranges between 20 and 40 °C. It was concluded that HEXs, not coolers, play the most important role in harvesting the most energy. So more focus and attention must be paid to the designers to take care of the HEX designs more than the coolers.

6. The energy released from the exhaust in I.C. engines that run on gasoline fuel (40%) was greater than that of those that run on diesel fuel (33%); therefore, installing the TEGs system on the exhaust pipe of gasoline engines was more economically feasible than installing it on diesel engines. This principle also applies to TEG systems installed on the water engine cooling system.

7. If the system was installed in low-saloon cars (high SUV cars were excluded from this), and to protect the TEGs system from bruises while the automobile was driving and thus damage, TEGs systems with a HEX of a rectangular cross-section were preferred because of their flatness and low heights.

8. TEGs systems sandwiching solid-state flat TEGs were more reliable than those TEGs systems sandwiching flexible-state TEGs, due to the high-temperature resistivity of solid-state materials versus the low silicon resistivity of flexible-state materials.

9. A new method is proposed to improve the heat gain of HEX outside the use of known fixed obstacles or internal fin. This method involves the installation of moving or rotating blades inside a HEX core at different angles and locations, such as the concept clarified by [157]. These blades can generate more vortices and disperse flow in several directions. The result is to harvest as much energy as possible and perhaps with less pressure drop.

Author Contributions

The concept of the review paper was proposed by Mohammed Y. Jabbar, developed edited and reviewed by my supervisors Saba Y. Ahmed and Salwan Obaid Waheed Khafaji. All authors participated in a thorough classification, the composition of the sections, goal of the project, and conclusions and recommendations.

Acknowledgments

Conflict of Interest

The authors declared no potential conflicts of interest concerning the research, authorship, and publication of this article.

Funding

Data Availability Statements

The datasets generated and/or analyzed during the current study are available within the paper.

Nomenclature

LATIN SYMBOLS			T	Temperature ($^{\circ}$C)
AC	Alternating current		TE	Thermoelectric
Bi$_2$Te$_3$	Bismuth telluride		TEG	Thermoelectric Generator
CC	Catalytic converter		TEC	Thermoelectric Cooler
CHTC	Convection heat transfer coefficient		Theo.	Theoretical
Citat.	Citation		x	Horizontal coordinate (m)
DC	Direct current		y	Vertical coordinate (m)
Exp.	Experimental		z	Normal coordinate (m)
HEX	Heat exchanger		GREEK SYMBOLS	
I.C.	Internal combustion		η	Efficiency
$\dot{m}$	Mass flow rate (kg.s^{-1})		Δ	Difference
P	Power (W)		Ω	Ohm
p	Pressure (pas)		SUBSCRIPT	
Q	Specific heat released (W)		inlet	Inlet
R	Electrical resistance (Ω)		max.	Maximum
Re	Reynolds number		sys.	System
SUV	Sport utility vehicle		f	Fluid
rpm	Revolution per minute		fin	Fin

References

[1] Dahham, R.Y., Wei, H., Pan, J., Improving thermal efficiency of internal combustion engines: recent progress and remaining challenges, *Energies*, 15(17), 2022, 1-60.

[2] Jabbar, M.Y., Ahmed, S.Y., Exploratory review of the heat exchanger and cooler geometrical effect on energy harvesting from automobile exhaust using thermoelectric generators, *Journal of Thermal Analysis and Calorimetry*, 148, 2023, 6607-6644.

[3] Sivaprahasam, D., Harish, S., Gopalan, R., Sundararajan, G., Automotive waste heat recovery by thermoelectric generator technology, *Bringing Thermoelectricity into Reality*, 11, 2018, 163-182.

[4] Madaro, F., Mehdipour, I., Caricato, A., Guido, F., Rizzi, F., Carlucci, A.P., De Vittorio, M., Available energy in cars' exhaust system for IoT remote exhaust gas sensor and piezoelectric harvesting, *Energies*, 13(16), 2020, 1-15.

[5] Ikoma, K., Munekiyo, M., Furuya, K., Kobayashi, M.A.K.M., Izumi, T.A.I.T., Shinohara, K.A.S.K., Thermoelectric module and generator for gasoline engine vehicles, *In Seventeenth International Conference on Thermoelectrics*, Proceedings ICT98 (Cat. No. 8TH8365) (pp. 464-467), IEEE, 1998.

[6] Haidar, J.G., Ghojel, J.I., Waste heat recovery from the exhaust of low-power diesel engine using thermoelectric generators, In *Proceedings ICT2001, 20 International Conference on Thermoelectrics* (Cat. No. 01TH8589) (pp. 413-418), IEEE, 2001.

[7] Hsiao, Y.Y., Chang, W.C., Chen, S.L., A mathematic model of thermoelectric module with applications on waste heat recovery from automobile engine, *Energy*, 35(3), 2010, 1447-1454.

[8] Love, N.D., Szybist, J.P., Sluder, C.S., Effect of heat exchanger material and fouling on thermoelectric exhaust heat recovery, *Applied Energy*, 89(1), 2012, 322-328.

[9] Su, C., Tong, N., Xu, Y., Chen, S., Liu, X., Effect of the sequence of the thermoelectric generator and the three-way catalytic converter on exhaust gas conversion efficiency, *Journal of Electronic Materials*, 42, 2013, 1877-1881.

[10] Liu, X., Deng, Y.D., Chen, S., Wang, W.S., Xu, Y., Su, C.Q., A case study on compatibility of automotive exhaust thermoelectric generation system, catalytic converter and muffler, *Case Studies in Thermal Engineering*, 2, 2014, 62-66.

[11] Su, C.Q., Wang, W.S., Liu, X., Deng, Y.D., Simulation and experimental study on thermal optimization of the heat exchanger for automotive exhaust-based thermoelectric generators, *Case Studies in Thermal Engineering*, 4, 2014, 85-91.

[12] Niu, Z., Diao, H., Yu, S., Jiao, K., Du, Q., Shu, G., Investigation and design optimization of exhaust-based thermoelectric generator system for internal combustion engine, *Energy Conversion and Management*, 85, 2014, 85-101.

[13] Liu, X., Deng, Y.D., Zhang, K., Xu, M., Xu, Y., Su, C.Q., Experiments and simulations on heat exchangers in thermoelectric generator for automotive application, *Applied Thermal Engineering*, 71(1), 2014, 364-370.

[14] Bai, S., Lu, H., Wu, T., Yin, X., Shi, X., & Chen, L., Numerical and experimental analysis for exhaust heat exchangers in automobile thermoelectric generators, *Case Studies in Thermal Engineering*, 4, 2014, 99-112.

[15] Wang, Y., Wu, C., Tang, Z., Yang, X., Deng, Y., Su, C., Optimization of fin distribution to improve the temperature uniformity of a heat exchanger in a thermoelectric generator, *Journal of Electronic Materials*, 44, 2015, 1724-1732.

[16] Liu, X., Deng, Y.D., Li, Z., Su, C.Q., Performance analysis of a waste heat recovery thermoelectric generation system for automotive application, *Energy Conversion and Management*, 90, 2015, 121-127.

[17] Du, Q., Diao, H., Niu, Z., Zhang, G., Shu, G., Jiao, K., Effect of cooling design on the characteristics and performance of thermoelectric generator used for internal combustion engine, *Energy Conversion and Management*, 101, 2015, 9-18.

[18] Wang, Y., Li, S., Yang, X., Deng, Y., Su, C., Numerical and experimental investigation for heat transfer enhancement by dimpled surface heat exchanger in thermoelectric generator, *Journal of Electronic Materials*, 45, 2016, 1792-1802.

[19] Su, C.Q., Huang, C., Deng, Y.D., Wang, Y.P., Chu, P.Q., Zheng, S.J., Simulation and optimization of the heat exchanger for automotive exhaust-based thermoelectric generators, *Journal of Electronic Materials*, 45, 2016, 1464-1472.

[20] Kim, T.Y., Negash, A.A., Cho, G., Waste heat recovery of a diesel engine using a thermoelectric generator equipped with customized thermoelectric modules, *Energy Conversion and Management*, 124, 2016, 280-286.

[21] Dai, H., Li, M., Design of Thermoelectric Power Generation Based on Engine Exhaust gas, *4th International Conference on Mechanical Materials and Manufacturing Engineering,* (pp. 537-541), Atlantis Press, 2016.

[22] Kim, T.Y., Lee, S., Lee, J., Fabrication of thermoelectric modules and heat transfer analysis on internal plate fin structures of a thermoelectric generator, *Energy Conversion and Management*, 124, 2016, 470-479.

[23] Liu, C., Deng, Y.D., Wang, X.Y., Liu, X., Wang, Y.P., Su, C.Q., Multi-objective optimization of heat exchanger in an automotive exhaust thermoelectric generator, *Applied Thermal Engineering*, 108, 2016, 916-926.

[24] Ziolkowski, A., Automotive Thermoelectric Generator impact on the efficiency of a drive system with a combustion engine, In *MATEC Web of Conferences,* (Vol. 118, p. 00024), EDP Sciences, 2017.

[25] Wang, Y., Li, S., Zhang, Y., Yang, X., Deng, Y., Su, C., The influence of inner topology of exhaust heat exchanger and thermoelectric module distribution on the performance of automotive thermoelectric generator, *Energy Conversion and Management*, 126, 2016, 266-277.

[26] He, W., Wang, S., Yue, L., High net power output analysis with changes in exhaust temperature in a thermoelectric generator system, *Applied Energy*, 196, 2017, 259-267.

[27] Sempels, É.V., Lesage, F.J., Optimal thermal conditions for maximum power generation when operating thermoelectric liquid-to-liquid generators, *IEEE Transactions on Components, Packaging and Manufacturing Technology*, 7(6), 2017, 872-881.

[28] Lu, X., Yu, X., Qu, Z., Wang, Q., Ma, T., Experimental investigation on thermoelectric generator with non-uniform hot-side heat exchanger for waste heat recovery, *Energy Conversion and Management*, 150, 2017, 403-414.

[29] Chinguwa, S., Musora, C., Mushiri, T., The design of portable automobile refrigerator powered by exhaust heat using thermoelectric, *Procedia Manufacturing*, 21, 2018, 741-748.

[30] Quan, R., Liu, G., Wang, C., Zhou, W., Huang, L., Deng, Y., Performance investigation of an exhaust thermoelectric generator for military SUV application, *Coatings*, 8(1), 2018, 45.

[31] Wang, Y., Li, S., Xie, X., Deng, Y., Liu, X., Su, C., Performance evaluation of an automotive thermoelectric generator with inserted fins or dimpled-surface hot heat exchanger, *Applied Energy*, 218, 2018, 391-401.

[32] Fernández-Yañez, P., Armas, O., Capetillo, A., Martínez-Martínez, S., Thermal analysis of a thermoelectric generator for light-duty diesel engines, *Applied Energy*, 226, 2018, 690-702.

[33] Eddine, A.N., Chalet, D., Faure, X., Aixala, L., Chessé, P., Effect of engine exhaust gas pulsations on the performance of a thermoelectric generator for wasted heat recovery: An experimental and analytical investigation, *Energy*, 162, 2018, 715-727.

[34] Yang, Y., Wang, S., He, W., Simulation study on regenerative thermoelectric generators for dynamic waste heat recovery, *Energy Procedia*, 158, 2019, 571-576.

[35] Luo, D., Wang, R., Yu, W., Sun, Z., Meng, X., Theoretical analysis of energy recovery potential for different types of conventional vehicles with a thermoelectric generator, *Energy Procedia*, 158, 2019, 142-147.

[36] Wang, J., Song, X., Li, Y., Zhang, C., Zhao, C., Zhu, L., Modeling and analysis of thermoelectric generators for diesel engine exhaust heat recovery system, *Journal of Energy Engineering*, 146(2), 2020, 04020002.

[37] Singh, B.S.B., Noh, N.A.S.M., Remeli, M.F., Oberoi, A., Experimental Study on Waste Heat Recovery from an Internal Combustion Engine Using Thermoelectric Generator, *Journal of Advanced Research in Applied Mechanics*, 72(1), 2020, 25-36.

[38] Sheikh, R., Gholampour, S., Fallahsohi, H., Goodarzi, M., Mohammad Taheri, M., Bagheri, M., Improving the efficiency of an exhaust thermoelectric generator based on changes in the baffle distribution of the heat exchanger, *Journal of Thermal Analysis and Calorimetry*, 143, 2021, 523-533.

[39] Garud, K.S., Seo, J.H., Patil, M.S., Bang, Y.M., Pyo, Y.D., Cho, C.P., Lee, M.Y., Thermal–electrical–structural performances of hot heat exchanger with different internal fins of thermoelectric generator for low power generation application, *Journal of Thermal Analysis and Calorimetry*, 143, 2021, 387-419.

[40] Luo, D., Wang, R., Yu, W., Zhou, W., Performance optimization of a converging thermoelectric generator system via multiphysics simulations, *Energy*, 204, 2020, 117974.

[41] Salek, F., Zamen, M., Hosseini, S.V., Babaie, M., Novel hybrid system of pulsed HHO generator/TEG waste heat recovery for CO reduction of a gasoline engine, *International Journal of Hydrogen Energy*, 45(43), 2020, 23576-23586.

[42] Ramírez, R., Gutiérrez, A.S., Eras, J.J.C., Valencia, K., Hernández, B., Forero, J.D., Evaluation of the energy recovery potential of thermoelectric generators in diesel engines, *Journal of Cleaner Production*, 241, 2019, 118412.

[43] Kumar, T.K., Kumar, S.A., Ram, K.K., Goli, K.R., Prasad, V.S., Analysis of thermo electric generators in automobile applications, *Materials Today: Proceedings*, 45, 2021, 5835-5839.

[44] Karana, D.R., Sahoo, R.R., Performance assessment of the automotive heat exchanger with twisted tape for thermoelectric based waste heat recovery, *Journal of Cleaner Production*, 283, 2021, 124631.

[45] Seo, J.H., Garud, K.S., Lee, M.Y., Grey relational based Taguchi analysis on thermal and electrical performances of thermoelectric generator system with inclined fins hot heat exchanger, *Applied Thermal Engineering*, 184, 2021, 116279.

[46] Yin, T., Li, Z.M., Peng, P., Liu, W., Shao, Y.Y., He, Z.Z., Performance analysis of a novel Two-stage automobile thermoelectric generator with the Temperature-dependent materials, *Applied Thermal Engineering*, 195, 2021, 117249.

[47] Chen, W.H., Chiou, Y.B., Chein, R.Y., Uan, J.Y., Wang, X.D., Power generation of thermoelectric generator with plate fins for recovering low-temperature waste heat, *Applied Energy*, 306, 2022, 118012.

[48] Chen, J., Wang, R., Luo, D., Zhou, W., Performance optimization of a segmented converging thermoelectric generator for waste heat recovery, *Applied Thermal Engineering*, 202, 2022, 117843.

[49] Luo, D., Sun, Z., Wang, R., Performance investigation of a thermoelectric generator system applied in automobile exhaust waste heat recovery, *Energy*, 238, 2022, 121816.

[50] Lan, S., Stobart, R., Chen, R., Performance comparison of a thermoelectric generator applied in conventional vehicles and extended-range electric vehicles, *Energy Conversion and Management*, 266, 2022, 115791.

[51] Ge, M., Li, Z., Zhao, Y., Xuan, Z., Li, Y., Zhao, Y., Experimental study of thermoelectric generator with different numbers of modules for waste heat recovery, *Applied Energy*, 322, 2022, 119523.

[52] Fini, A.T., Hashemi, S.A., Fattahi, A., On the efficient topology of the exhaust heat exchangers equipped with thermoelectric generators for an internal combustion engine, *Energy Conversion and Management*, 268, 2022, 115966.

[53] Quan, R., Liang, W., Quan, S., Huang, Z., Liu, Z., Chang, Y., Tan, B., Performance interaction assessment of automobile exhaust thermoelectric generator and engine under different operating conditions, *Applied Thermal Engineering*, 216, 2022, 119055.

[54] Gürbüz, H., Akçay, H., & Topalcı, Ü., Experimental investigation of a novel thermoelectric generator design for exhaust waste heat recovery in a gas-fueled SI engine, *Applied Thermal Engineering*, 216, 2022, 119122.

[55] Cuyubamba, P., Asto-Evangelista, J., Almerco-Ataucusi, J.R., Valenzuela-Lino, Y.S., Huamanchahua, D., Moggiano, N., Design and Performance Study of the Heat Exchanger of a Fin-Based Thermoelectric Generator via Numerical Simulations, *11th International Conference on Power Science and Engineering (ICPSE)* (pp. 34-39), IEEE, 2022.

[56] Luo, D., Yan, Y., Li, Y., Wang, R., Cheng, S., Yang, X., Ji, D., A hybrid transient CFD-thermoelectric numerical model for automobile thermoelectric generator system, *Applied Energy*, 332, 2023, 120502.

[57] Luo, D., Wu, Z., Yan, Y., Ji, D., Cheng, Z., Wang, R., Yang, X., Optimal design of a heat exchanger for automotive thermoelectric generator systems applied to a passenger car, *Applied Thermal Engineering*, 227, 2023, 120360.

[58] Luo, D., Yan, Y., Chen, W.H., Yang, X., Chen, H., Cao, B., Zhao, Y., A comprehensive hybrid transient CFD-thermal resistance model for automobile thermoelectric generators, *International Journal of Heat and Mass Transfer*, 211, 2023, 124203.

[59] Ni, P., Hua, R., Lv, Z., Wang, X., Zhang, X., Li, X., Performance analysis of compact thermoelectric generation device for harvesting waste heat, *Energy Conversion and Management*, 291, 2023, 117333.

[60] Luo, D., Yan, Y., Li, Y., Chen, W.H., Yang, X., Wang, X., Cao, B., Dynamic behavior of automobile thermoelectric waste heat recovery under different driving cycles, *Applied Thermal Engineering*, 232, 2023, 121039.

[61] Luo, D., Yan, Y., Li, Y., Yang, X., Chen, H., Exhaust channel optimization of the automobile thermoelectric generator to produce the highest net power, *Energy*, 281, 2023, 128319.

[62] Abdelghany, E.S., Mohamed, E.S., Sarhan, H.H., Exhaust heat recovery performance analysis of a Bi-fuel engine utilizing a thermoelectric generation kit and fuel economy evaluation, *Case Studies in Thermal Engineering*, 49, 2023, 103288.

[63] Hong, T.D., Pham, M.Q., Nghiem, Q.T.P., Thermal uniformity enhancement of the motorcycle exhaust thermoelectric generator-Theory model for predicting heat exchanger fin profile, *Results in Engineering*, 19, 2023, 101324.

[64] Hong, T.D., Pham, M.Q., Huynh, K.Q., Tran, K.Q., Performance enhancement of the motorcycle exhaust thermoelectric generator-Optimization of

the hot-side heat exchanger configuration, *Case Studies in Thermal Engineering*, 51, 2023, 103616.

[65] Oh, S., Ko, K.H., Kim, J., Development of thermoelectric exhaust energy recovery system of a hydrogen internal combustion engine in a city bus using a Three-Dimensional multiphysics model, *Energy Conversion and Management*, 300, 2024, 118006.

[66] Khripach, N.A., Papkin, B.A., Korotkov, V.S., Zaletov, D.V., Study of the influence of heat exchanger body design parameters on the performance of a thermoelectric generator for automotive internal combustion engine, *Biosciences Biotechnology Research Asia*, 12(S2), 2015, 677-689.

[67] Meng, J.H., Wang, X.D., Chen, W.H., Performance investigation and design optimization of a thermoelectric generator applied in automobile exhaust waste heat recovery, *Energy Conversion and Management*, 120, 2016, 71-80.

[68] Kim, T.Y., Negash, A., Cho, G., Direct contact thermoelectric generator (DCTEG): A concept for removing the contact resistance between thermoelectric modules and heat source, *Energy Conversion and Management*, 142, 2017, 20-27.

[69] Luo, D., Wang, R., Yan, Y., Yu, W., Zhou, W., Transient numerical modeling of a thermoelectric generator system used for automotive exhaust waste heat recovery, *Applied Energy*, 297, 2021, 117151.

[70] Wang, Y.P., Chen, W., Huang, Y.Y., Liu, X., Su, C.Q., Performance study on a thermoelectric generator with exhaust-module-coolant direct contact, *Energy Reports*, 8, 2022, 729-738.

[71] Weng, C.C., Huang, M.J., A simulation study of automotive waste heat recovery using a thermoelectric power generator, *International Journal of Thermal Sciences*, 71, 2013, 302-309.

[72] Deng, Y.D., Chen, Y.L., Chen, S., Xianyu, W.D., Su, C.Q., Research on integration of an automotive exhaust-based thermoelectric generator and a three-way catalytic converter, *Journal of Electronic Materials*, 44, 2015, 1524-1530.

[73] Anand, P.N., Anshad, A., Joseph, A., James, G.E., Thomas, T., Development of Thermoelectric Generator, *International Journal for Innovative Research in Science & Technology*, 2(11), 2016, 2349-6010.

[74] Borcuch, M., Musiał, M., Gumuła, S., Sztekler, K., Wojciechowski, K., Analysis of the fins geometry of a hot-side heat exchanger on the performance parameters of a thermoelectric generation system, *Applied Thermal Engineering*, 127, 2017, 1355-1363.

[75] Gaurav, K., Sisodia, S., Pandey, S.K., Calculation of efficiency and power output by considering different realistic prospects for recovering heat from automobile using thermoelectric generator, *Journal of Renewable and Sustainable Energy*, 9(6), 2017, 064703.

[76] Shu, G., Ma, X., Tian, H., Yang, H., Chen, T., Li, X., Configuration optimization of the segmented modules in an exhaust-based thermoelectric generator for engine waste heat recovery, *Energy*, 160, 2018, 612-624.

[77] Shishov, K.A., Selection of the design of a hot heat exchanger of an automotive thermoelectric generator for an urban driving cycle, *Journal of Physics: Conference Series*, 1410, 2019, 012240.

[78] Quan, R., Li, T., Yue, Y., Chang, Y., Tan, B., Experimental study on a thermoelectric generator for industrial waste heat recovery based on a hexagonal heat exchanger, *Energies*, 13(12), 2020, 3137.

[79] ERDOGAN, B., DURAN, K., ZENGİN, İ., Experimental and Numerical Analysis of Using Thermoelectric Generator Modules on Hexagonal Exhaust Heat Exchanger, *Karaelmas Fen ve Mühendislik Dergisi*, 11(1), 2021, 54-60.

[80] Marana, A.L.O., Martin, C.A.G., Montes-Páez, E., Junior, O.H.A., Modeling and simulation of a thermoelectric waste heat recovery system–TWRHS, *Dyna*, 88(217), 2021, 265-272.

[81] Quan, R., Wang, J., Li, T., Compatibility optimization of a polyhedral-shape thermoelectric generator for automobile exhaust recovery considering backpressure effects, *Heliyon*, 8(12), 2022, e12348.

[82] Wojciechowski, K.T., Borcuch, M., Musial, M., Wyzga, P., A tested for performance studies of gas-liquid thermoelectric generators for waste heat harvesting, *Measurement*, 203, 2022, 111933.

[83] Zhao, X., Jiang, J., Zuo, H., Mao, Z., Performance analysis of diesel particulate filter thermoelectric conversion mobile energy storage system under engine conditions of low-speed and light-load, *Energy*, 282, 2023, 128411.

[84] Zhao, X., Jiang, J., Zuo, H., Mao, Z., Performance analysis of diesel particulate filter thermoelectric conversion mobile energy storage system under engine conditions of low-speed and light-load, *Energy*, 282, 2023, 128411.

[85] Lu, C., Wang, S., Chen, C., Li, Y., Effects of heat enhancement for exhaust heat exchanger on the performance of thermoelectric generator, *Applied Thermal Engineering*, 89, 2015, 270-279.

[86] Li, Y., Wang, S., Zhao, Y., Experimental study on the influence of the core flow heat transfer enhancement on the performance of thermoelectric generator, *Energy Procedia*, 105, 2017, 901-907.

[87] Nithyanandam, K., Mahajan, R.L., Evaluation of metal foam based thermoelectric generators for automobile waste heat recovery, *International Journal of Heat and Mass Transfer*, 122, 2018, 877-883.

[88] Li, Y., Wang, S., Zhao, Y., Yue, L., Effect of thermoelectric modules with different characteristics on the performance of thermoelectric generators inserted in the central flow region with porous foam copper, *Applied Energy*, 327, 2022, 120041.

[89] Buonomo, B., Cascetta, F., di Pasqua, A., Manca, O., Performance parameters enhancement of a thermoelectric generator by metal foam in exhaust automotive lines, *Thermal Science and Engineering Progress*, 38, 2023, 101684.

[90] Eldin, S.M., Alanazi, M., Alanazi, A., Alqahtani, S., Alshehery, S., Anqi, A.E., Economic and thermal analysis of a tubular thermoelectric power generator equipped with a novel fin-pin-porous based heat exchanger; comparative case study with conventional smooth channel, *Case Studies in Thermal Engineering*, 48, 2023, 103166.

[91] Orr, B., Akbarzadeh, A., Lappas, P., An exhaust heat recovery system utilizing thermoelectric generators and heat pipes, *Applied Thermal Engineering*, 126, 2017, 1185-1190.

[92] Li, B., Huang, K., Yan, Y., Li, Y., Twaha, S., Zhu, J., Heat transfer enhancement of a modularised thermoelectric power generator for passenger vehicles, *Applied Energy*, 205, 2017, 868-879.

[93] Cao, Q., Luan, W., Wang, T., Performance enhancement of heat pipes assisted thermoelectric generator for automobile exhaust heat recovery, *Applied Thermal Engineering*, 130, 2018, 1472-1479.

[94] Pacheco, N., Brito, F.P., Vieira, R., Martins, J., Barbosa, H., Goncalves, L.M., Compact automotive thermoelectric generator with embedded heat pipes for thermal control, *Energy*, 197, 2020, 117154.

[95] Högblom, O., Andersson, R., Multiphysics CFD simulation for design and analysis of thermoelectric power generation, *Energies*, 13(17), 2020, 4344.

[96] Carvalho, R., Martins, J., Pacheco, N., Puga, H., Costa, J., Vieira, R., Brito, F.P., Experimental validation and numerical assessment of a temperature-controlled thermoelectric generator concept aimed at maximizing performance under highly variable thermal load driving cycles, *Energy*, 280, 2023, 127979.

[97] Shen, Z.G., Huang, B., Liu, X., Effect of structure parameters on the performance of an annular thermoelectric generator for automobile exhaust heat recovery, *Energy Conversion and Management*, 256, 2022, 115381.

[98] Yang, W., Zhu, W., Yang, Y., Huang, L., Shi, Y., Xie, C., Thermoelectric performance evaluation and optimization in a concentric annular thermoelectric generator under different cooling methods, *Energies*, 15(6), 2022, 2231.

[99] Zhu, W., Yang, W., Yang, Y., Li, Y., Li, H., Shi, Y., Xie, C., Economic configuration optimization of onboard annual thermoelectric generators under multiple operating conditions, *Renewable Energy*, 197, 2022, 486-499.

[100] Yang, W., Zhu, W., Du, B., Wang, H., Xu, L., Xie, C., Shi, Y., Power generation of annular thermoelectric generator with silicone polymer thermal conductive oil applied in automotive waste heat recovery, *Energy*, 282, 2023, 128400.

[101] Yang, W., Jin, C., Zhu, W., Li, Y., Zhang, R., Huang, L., Shi, Y., Taguchi optimization and thermoelectrical analysis of a pin fin annular thermoelectric generator for automotive waste heat recovery, *Renewable Energy*, 220, 2024, 119628.

[102] Yang, W., Xu, A., Zhu, W., Li, Y., Shi, Y., Huang, L., Xie, C., Performance improvement and thermomechanical analysis of a novel asymmetrical annular thermoelectric generator, *Applied Thermal Engineering*, 237, 2024, 121804.

[103] Singh, B.S.B., Noh, N.A.S.M., Remeli, M.F., Oberoi, A., Experimental Study on Waste Heat Recovery from an Internal Combustion Engine Using Thermoelectric Generator, *Journal of Advanced Research in Applied Mechanics*, 72(1), 2020, 25-36.

[104] Deng, Y.D., Liu, X., Chen, S., Tong, N.Q., Thermal optimization of the heat exchanger in an automotive exhaust-based thermoelectric generator, *Journal of Electronic Materials*, 42, 2013, 1634-1640.

[105] Sukprapaporn, B., Maneechot, P., Ketjoy, N., Vaivudh, S., A suitable heat duct shape for a thermoelectric generator cooling system, *Journal of Renewable Energy and Smart Grid Technology*, 9(1), 2014, 19-30.

[105] Yuan, X., Bai, W., Deng, Y., Su, C., Liu, X., Liu, C., Wang, Y., Numerical investigation on the performance of an automotive thermoelectric

generator integrated with a three-way catalytic converter, *Journal of Renewable and Sustainable Energy*, 8(4), 2016, 044704.

[107] Yan, S.R., Moria, H., Asaadi, S., Dizaji, H.S., Khalilarya, S., Jermsittiparsert, K., Performance and profit analysis of thermoelectric power generators mounted on channels with different cross-sectional shapes, *Applied Thermal Engineering*, 176, 2020, 115455.

[108] Zhang, M., Wang, J., Tian, Y., Zhou, Y., Zhang, J., Xie, H., Wang, Y., Performance comparison of annular and flat-plate thermoelectric generators for cylindrical hot source, *Energy Reports*, 7, 2021, 413-420.

[109] Huang, B., Shen, Z.G., Performance assessment of annular thermoelectric generators for automobile exhaust waste heat recovery, *Energy*, 246, 2022, 123375.

[110] Asaduzzaman, M., Ali, M.H., Pratik, N.A., Lubaba, N., Exhaust Heat Harvesting of Automotive Engine Using Thermoelectric Generation Technology, *Energy Conversion and Management: X*, 19, 2023, 100398.

[111] Shu, G., Zhao, J., Tian, H., Liang, X., Wei, H., Parametric and exergetic analysis of waste heat recovery system based on thermoelectric generator and organic rankine cycle utilizing R123, *Energy*, 45(1), 2012, 806-816.

[112] Phillip, N., Maganga, O., Burnham, K.J., Dunn, J., Rouaud, C., Ellis, M.A., Robinson, S., Modelling and simulation of a thermoelectric generator for waste heat energy recovery in low carbon vehicles, *2nd International Symposium on Environment Friendly Energies And Applications*, (pp. 94-99), IEEE, 2012.

[113] Wang, Y., Dai, C., Wang, S., Theoretical analysis of a thermoelectric generator using exhaust gas of vehicles as heat source, *Applied Energy*, 112, 2013, 1171-1180.

[114] Zhang, Y., Cleary, M., Wang, X., Kempf, N., Schoensee, L., Yang, J., Meda, L., High-temperature and high-power-density nanostructured thermoelectric generator for automotive waste heat recovery, *Energy Conversion and Management*, 105, 2015, 946-950.

[115] Bhati, D.S., Baghel, A., Heat Harvester, *Journal of Electrical and Electronics Engineering*, 11(6), 2016, 120-125.

[116] Risseh, A.E., Nee, H.P., Goupil, C., Electrical power conditioning system for thermoelectric waste heat recovery in commercial vehicles, *IEEE Transactions on Transportation Electrification*, 4(2), 2018, 548-562.

[117] Zhao, Y., Wang, S., Ge, M., Liang, Z., Liang, Y., Li, Y., Performance investigation of an intermediate fluid thermoelectric generator for automobile exhaust waste heat recovery, *Applied Energy*, 239, 2019, 425-433.

[118] Hewawasam, L.S., Jayasena, A.S., Afnan, M.M.M., Ranasinghe, R.A.C.P., Wijewardane, M.A., Waste heat recovery from thermo-electric generators (TEGs), *Energy Reports*, 6, 2020, 474-479.

[119] Hassan, D.M., Mussa, M.A., Thermal Performance Analysis of Compact Heat Exchangers for Thermoelectric Generators, *Journal of Engineering*, 26(3), 2020, 33-45.

[120] Aljaghtham, M., Celik, E., Design optimization of oil pan thermoelectric generator to recover waste heat from internal combustion engines, *Energy*, 200, 2020, 117547.

[121] Karana, D.R., Sahoo, R.R., Thermal, environmental and economic analysis of a new thermoelectric cogeneration system coupled with a diesel electricity generator, *Sustainable Energy Technologies and Assessments*, 40, 2020, 100742.

[122] Zhao, Y., Fan, Y., Ge, M., Xie, L., Li, Z., Yan, X., Wang, S., Thermoelectric performance of an exhaust waste heat recovery system based on intermediate fluid under different cooling methods, *Case Studies in Thermal Engineering*, 23, 2021, 100811.

[123] Zhao, Y., Lu, M., Li, Y., Ge, M., Xie, L., Liu, L., Characteristics analysis of an exhaust thermoelectric generator system with heat transfer fluid circulation, *Applied Energy*, 304, 2021, 117896.

[124] Fernández-Yáñez, P., Fernández-López, A.J., Soriano, J.A., Armas, O., A computational method to study heat transfer in a helicopter turboshaft engine compartment for waste energy recovery purposes, *Applied Thermal Engineering*, 242, 2024, 122529.

[125] Yue, S., Shao, S., He, W., Li, Y., Liu, W., Liu, P., Ao, W., Pioneer exploration on the energy recovery technology for waste heat in solid rocket motors by utilizing thermoelectric materials, *Energy Conversion and Management*, 302, 2024, 118151.

[126] Demir, M. E., Dincer, I., Performance assessment of a thermoelectric generator applied to exhaust waste heat recovery, *Applied Thermal Engineering*, 120, 2017, 694-707.

[127] Arumugam, S., Ramakrishna, P., Sangavi, S., Sriram, G., Thermoelectric Analysis of Automobiles Exhaust Waste Heat Recovery Material–A Simulation Study, *Materials Today: Proceedings*, 16, 2019, 516-523.

[128] Asaadi, S., Khalilarya, S., Jafarmadar, S., A thermodynamic and exergoeconomic numerical study of two-stage annular thermoelectric generator, *Applied Thermal Engineering*, 156, 2019, 371-381.

[129] Tian, M.W., Mihardjo, L.W., Moria, H., Asaadi, S., Pourhedayat, S., Dizaji, H.S., Wae-hayee, M., Economy, energy, exergy and mechanical study of co-axial ring shape configuration of legs as a novel structure for cylindrical thermoelectric generator, *Applied Thermal Engineering*, 184, 2021, 116274.

[130] Yang, W., Zhu, W., Li, Y., Zhang, L., Zhao, B., Xie, C., Huang, L., Annular thermoelectric generator performance optimization analysis based on concentric annular heat exchanger, *Energy*, 239, 2022, 122127.

[131] Xu, Y., Xue, Y., Cai, W., Qi, H., Li, Q., Experimental study on performances of flat-plate pulsating heat pipes without and with thermoelectric generators for low-grade waste heat recovery, *Applied Thermal Engineering*, 225, 2023, 120156.

[132] Kim, D.H., Seo, S., Kim, S., Shin, S., Son, K., Jeon, S.J., Design and performance analyses of thermoelectric coolers and power generators for automobiles, *Sustainable Energy Technologies and Assessments*, 51, 2022, 101955.

[133] Kim, S., Park, S., Kim, S., Rhi, S.H., A thermoelectric generator using engine coolant for light-duty internal combustion engine-powered vehicles, *Journal of Electronic Materials*, 40, 2011, 812-816.

[134] Khripach, N.A., Korotkov, V.S., Papkin, I.A., Thermoelectric cooling system for internal combustion engine. Part 1: development of the technical aspects, *International Journal of Applied Engineering Research*, 11(15), 2016, 8547-8552.

[135] Baek, D., Ding, C., Lin, S., Shin, D., Kim, J., Lin, X., Chang, N., Reconfigurable thermoelectric generators for vehicle radiators energy harvesting, *IEEE/ACM International Symposium on Low Power Electronics and Design (ISLPED)*, (pp. 1-6), IEEE, 2017.

[136] Khripach, N.A., Korotkov, V.S., Papkin, I.A., Thermoelectric cooling radiator for internal combustion engine, *International Journal of Mechanical Engineering and Technology*, 8(11), 2017, 668-675.

[137] Kim, J., Baek, D., Ding, C., Lin, S., Shin, D., Lin, X., ..., Chang, N., Dynamic reconfiguration of thermoelectric generators for vehicle radiators energy harvesting under location-dependent temperature variations, *IEEE Transactions on Very Large Scale Integration (VLSI) Systems*, 26(7), 2018, 1241-1253.

[138] Awria, A., Albana, M.H., Hakim, R., Experimental study: design of Thermoelectric Generator (TEG) fixture for harvesting an automobile electricity, *International Conference on Applied Engineering (ICAE)*, (pp. 1-5), IEEE, 2018.

[139] Abderezzak, B., Randi, S., Experimental investigation of waste heat recovery potential from car radiator with thermoelectric generator, *Thermal Science and Engineering Progress*, 20, 2020, 100686.

[140] Ivanov, K., Aleksandrov, A., Design and Study of an Automotive Thermoelectric Generator, *7th International Conference on Energy Efficiency and Agricultural Engineering (EE&AE)*, (pp. 1-4). IEEE, 2020.

[141] Yu, J., Zhao, H., A numerical model for thermoelectric generator with the parallel-plate heat exchanger, *Journal of Power Sources*, 172(1), 2007, 428-434.

[142] Rezania, A., Rosendahl, L.A., Andreasen, S.J., Experimental investigation of thermoelectric power generation versus coolant pumping power in a microchannel heat sink, *International Communications in Heat and Mass Transfer*, 39(8), 2012, 1054-1058.

[143] Deng, Y.D., Liu, X., Chen, S., Xing, H.B., Su, C.Q., Research on the compatibility of the cooling unit in an automotive exhaust-based thermoelectric generator and engine cooling system, *Journal of Electronic Materials*, 43, 2014, 1815-1823.

[144] Su, C.Q., Xu, M., Wang, W.S., Deng, Y.D., Liu, X., Tang, Z.B., Optimization of cooling unit design for automotive exhaust-based thermoelectric generators, *Journal of Electronic Materials*, 44, 2015, 1876-1883.

[145] He, W., Wang, S., Lu, C., Zhang, X., Li, Y., Influence of different cooling methods on thermoelectric performance of an engine exhaust gas waste heat recovery system, *Applied Energy*, 162, 2016, 1251-1258.

[146] Aranguren, P., Astrain, D., Rodríguez, A., Martínez, A., Experimental investigation of the applicability of a thermoelectric generator to recover waste heat from a combustion chamber, *Applied Energy*, 152, 2015, 121-130.

[147] He, W., Wang, S., Zhang, X., Li, Y., Lu, C., Optimization design method of thermoelectric generator based on exhaust gas parameters for recovery of engine waste heat, *Energy*, 91, 2015, 1-9.

[148] Qiang, J.W., Yu, C.G., Deng, Y.D., Su, C.Q., Wang, Y.P., Yuan, X.H., Multi-objective optimization design for cooling unit of automotive exhaust-based thermoelectric generators, *Journal of Electronic Materials*, 45, 2016, 1679-1688.
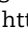
[149] Wang, L., Romagnoli, A., Cooling system investigation of thermoelectric generator used for marine waste heat recovery, *IEEE 2nd Annual Southern Power Electronics Conference (SPEC)*, (pp. 1-6), IEEE, 2016.

[150] Su, C.Q., Zhu, D.C., Deng, Y.D., Wang, Y.P., Liu, X., Effect of cooling units on the performance of an automotive exhaust-based thermoelectric generator, *Journal of Electronic Materials*, 46, 2017 2822-2831.

[151] Deasy, M.J., Baudin, N., O'Shaughnessy, S.M., Robinson, A.J., Simulation-driven design of a passive liquid cooling system for a thermoelectric generator, *Applied Energy*, 205, 2017, 499-510.

[152] Kunt, M.A., Gunes, H., Experimental Investigation of the Performance of Different Heat Exchanger Profiles in the Waste Heat Recovery System with Thermoelectric Generator for Automobile Exhaust Systems, *SSRG Journal*, 4(8), 2017, 1-5.

[153] Lei, X., Wang, Y., Deng, Y., Su, C., Liu, X., Chen, G., Combined numerical and experimental investigation on the optimum coolant flow rate for automotive thermoelectric generators, *Journal of Electronic Materials*, 48, 2019, 1981-1990.

[154] He, W., Guo, R., Takasu, H., Kato, Y., Wang, S., Performance optimization of common plate-type thermoelectric generator in vehicle exhaust power generation systems, *Energy*, 175, 2019, 1153-1163.

[155] Hilmin, M.N.H.M., Remeli, M.F., Singh, B., Affandi, N.D.N., Thermoelectric power generations from vehicle exhaust gas with TiO_2 nanofluid cooling, *Thermal Science and Engineering Progress*, 18, 2020, 100558.

[156] Poornima, D., Vivekanandan, C., Performance of Water Cooled Thermoelectric Generator System for Petrol Engines Using Cuk Converter, *5th International Conference on Computing Methodologies and Communication (ICCMC)*, (pp. 653-659), IEEE, 2021.

[157] Nazarieh, M., Kariman, H., Hoseinzadeh, S., Numerical simulation of fluid dynamic performance of turbulent flow over Hunter turbine with variable angle of blades, *International Journal of Numerical Methods for Heat & Fluid Flow*, 33(1), 2023, 153-173.

ORCID iD

Mohammed Y. Jabbar https://orcid.org/0000-0003-0975-6587
Saba Y. Ahmed https://orcid.org/0000-0002-5440-4292
Salwan Obaid Waheed Khafaji https://orcid.org/0000-0001-5144-6895

Publisher's Note Shahid Chamran University of Ahvaz remains neutral with regard to jurisdictional claims in published maps and institutional affiliations.